

# Sediment delivery to the seabed on continental margins

PAUL S. HILL\*, JASON M. FOX\*, JOHN S. CROCKETT†, KRISTIAN J. CURRAN\*,  
CARL T. FRIEDRICHS‡, W. ROCKWELL GEYER§, TIMOTHY G. MILLIGAN¶,  
ANDREA S. OGSTON†, PERE PUIG\*\*, MALCOLM E. SCULLY‡,  
PETER A. TRAYKOVSKI§ and ROBERT A. WHEATCROFT††

\*Department of Oceanography, Dalhousie University, Halifax, Nova Scotia B3H 4J1, Canada (Email: paul.hill@dal.ca)

†School of Oceanography, University of Washington, Seattle, WA 98195, USA

‡Virginia Institute of Marine Science, College of William and Mary, Gloucester Point, VA 23062-1346, USA

§Department of Applied Physics and Engineering, Woods Hole Oceanographic Institution, Woods Hole, MA 02543, USA

¶Habitat Ecology Division, Fisheries and Oceans Canada, Bedford Institute of Oceanography, Dartmouth, Nova Scotia B2Y 4A2, Canada

\*\*Department of Marine Geology and Physical Oceanography, Institut de Ciències del Mar (CSIC), Barcelona E-08003, Spain

††College of Oceanic and Atmospheric Sciences, Oregon State University, Corvallis, OR 97331-5503, USA

## ABSTRACT

On river-influenced continental margins, terrigenous muds tend to accumulate in the middle of the continental shelf. The common occurrence of mid-shelf mud belts has been attributed to three basic across-margin transport mechanisms. Muds either diffuse to the mid-shelf under the influence of storms, or they are advected there by oceanographic currents, or they arrive at the mid-shelf in dense suspensions that flow across the margin under the influence of gravity. Until recently, observations generally favoured the hypothesis that ocean currents are responsible for advecting dilute suspensions of mud to the mid-shelf. Transport by dense gravity flows was widely rejected, based primarily on the arguments that the bathymetric gradients of continental shelves are too small to sustain gravity flows, and that sediment concentrations cannot grow large enough to cause suspensions to flow down gradient. Observations conducted on the Eel River continental shelf off northern California, however, demonstrate that cross-margin transport by dense suspensions can be an important mechanism for the emplacement of muds on the mid-shelf. Dense suspensions form near the seabed when sediment in the wave boundary layer cannot deposit because of stress exerted on the bottom by waves, and when sediment does not diffuse out of the wave boundary layer because of relatively weak current-induced turbulence. In the future, the importance of these flows on other margins needs to be assessed.

**Keywords** Flocculation, particle settling velocity, bottom boundary layer, sediment transport, plumes, fluid mud, gravity flows, mid-shelf mud deposit, nepheloid layer.

## INTRODUCTION

During the 1960s research on the sedimentology of continental shelves underwent dramatic transformation. The complexity of spatial patterns of sediment composition and size made it clear that purely descriptive studies and simple conceptual models (Fig. 1) were inadequate because they failed to probe systematically or treat adequately

the mechanisms and rates of **sediment transport**. Without a comprehensive knowledge of sediment transport, formation of the veneer of sediments on continental shelves was impossible to explain mechanistically. This lack of understanding was a fundamental concern to sedimentologists and sedimentary geologists, because sedimentary rocks formed on shelves and other nearshore areas represent a major portion of the stratigraphic record.

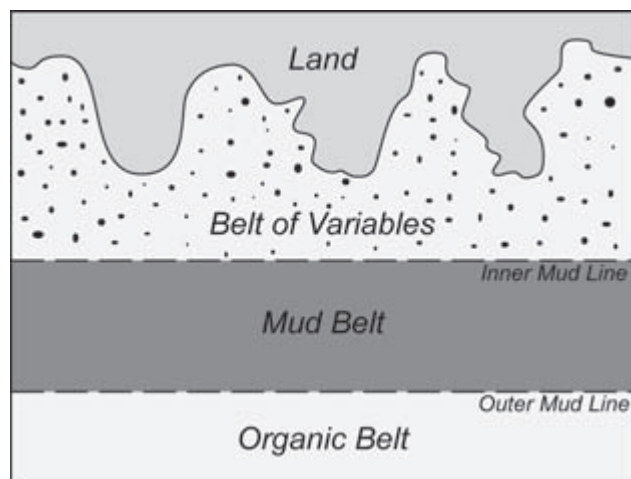


**Fig. 1** An early conceptual model of sediment distribution on continental shelves. An inshore region called the 'Belt of Variables' is characterized by variable but generally coarse ( $> 63 \mu\text{m}$ ) sediment sizes. This region gives way at the inner mud line to a mid-shelf 'Mud Belt' with mean sediment  $< 63 \mu\text{m}$  because of decreasing energy offshore. At the outer mud line, terrigenous mud gives way to pelagic biogenic deposits in the 'Organic Belt'. This outer transition is caused by the depletion of suspended terrigenous sediment due to its deposition shoreward of the transition. (Redrawn from Marr, 1929.)

An inability to explain the present was leaving geologists ill-equipped to unlock the secrets of the past stored in the stratigraphic record.

Two new general methodologies supplanted traditional descriptive sedimentology on continental shelves during the 1960s. First, models were developed that cast continental-shelf sediment transport in quantifiable, mechanistically based terms. Second, instrumentation was developed that made it possible to monitor sediment concentrations, waves and currents near the seabed over long time periods, thus enabling systematic characterization of the mechanisms, pathways and rates of sediment movement on continental shelves. An emerging philosophy among marine geologists was that progress in understanding the stratigraphic record depended on building an understanding of the formation of bedding at the scale of individual events such as storms, floods, debris flows and turbidity currents. Knowledge gained through event-scale studies would be applied to the sweeping time-scales of the rock record by judicious use

of emerging models of shelf sediment transport. This philosophy was summarized in the preface to Swift *et al.*'s 1972 monograph on shelf sediment transport which stated 'Geological oceanographers and marine geologists will hopefully never lose their unique sense of the vastness of geological time, which gives them a special insight into their studies, but they stand to gain much from the increased sensitivity to short-term processes which when integrated through geological time and preserved, yield the stratigraphic record.'

The decades following the 1960s witnessed dramatic advances in measurements and models of shelf sediment transport (e.g. Grant & Madsen, 1986) and continental-margin stratigraphy (e.g. Mitchum *et al.*, 1977). These efforts, in large part, however, evolved separately, and the fundamentally different time-scales considered by process sedimentologists and stratigraphers posed considerable challenges to building an integrated understanding of strata formation, from the event scales considered by sedimentologists, to the million-year time-scales considered by stratigraphers.

With the goal of meeting these challenges, the US Office of Naval Research developed and funded the programme entitled *Strata Formation on Continental Margins* (STRATAFORM). STRATAFORM brought together sedimentologists, stratigraphers and modellers with the explicit goal of using investigations of short-term ( $< 100$  yr) sedimentary processes to place better constraint on longer time-scale ( $10^4$ – $10^6$  yr) stratigraphic interpretations (Nittrouer, 1999). The overall approach encompassed detailed event-scale observations of sediment delivery and deposition, investigations of longer-term sediment accumulation, seismic imaging of strata, and extensive coring of recent and ancient (Ma) deposits (Nittrouer, 1999). Vital to the integration of these various efforts into a coherent framework were modelling studies designed to bridge the gap between the time-scales of sedimentary processes and sequence stratigraphy.

The Eel River margin on the coast of northern California (Fig. 2) was one of two study sites in STRATAFORM and was the exclusive site for studying short-term sedimentary processes, which are the focus of this paper. The margin is tectonically active and prone to seismically triggered mass wasting (Lee *et al.*, this volume, pp. 213–274). Intense winter storms batter the coast, generat-

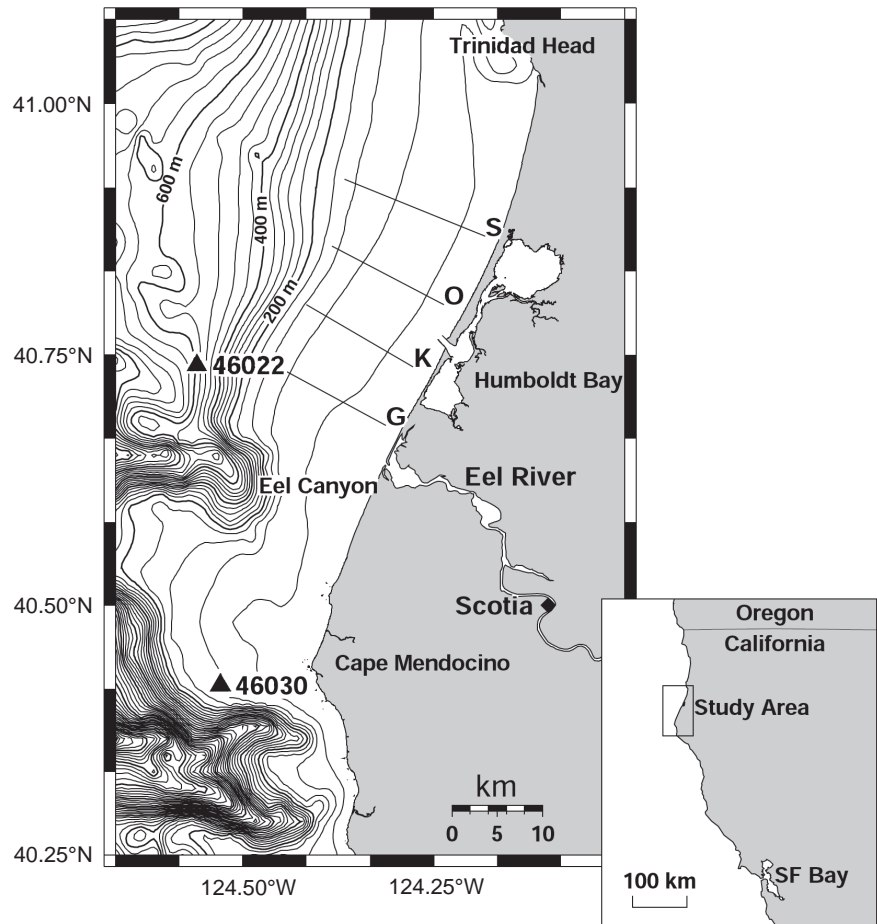


**Fig. 2** Location map for the Eel River margin. Lines G, K, O and S indicate positions of a subset of cross-shelf transects that extend from the Eel Canyon (just south of the river mouth) to Trinidad Head (at the northern limit of the Eel margin). Triangles marked with numbers identify the positions of NOAA's National Data Buoy Center (NDBC) oceanographic buoys. The diamond labelled 'Scotia' marks the position of the Scotia River monitoring station. Contour interval is 40 m.

ing large waves at sea and episodic flooding on land. The active processes on the margin enhance the possibility of observing significant sediment-transporting events.

In 1995 a series of storms resulted in prolonged and intense rainfall over the entire Eel River basin. The ensuing flood was one of the largest recorded in the 85 yr of hydrographic monitoring on the river, and it delivered an estimated  $25 \times 10^6$  t of fine-grained ( $< 63 \mu\text{m}$ ) sediment to the coastal ocean (Wheatcroft *et al.*, 1997). A month after the flood, extensive coring revealed a distinct layer of flood-derived mud on the shelf. The oblong deposit was up to 8.5 cm thick, 30 km long in an along-shelf direction, 8 km wide across-shelf, and centred on the 70-m isobath north of the river mouth (Wheatcroft *et al.*, 1997). Thus, the STRATAFORM programme was initiated by the formation of a distinct event bed that could be probed and whose fate could be tracked.

The goal of this paper is to evaluate mechanisms that deliver sediment to continental margins by focusing on the Eel dispersal system, which received substantial input during the 1995 flood, during an ensuing larger flood in 1997, and during a series of smaller floods in 1998. An essential aspect of this synthesis is to place results from the Eel margin firmly into context with the large body of work that preceded them.

The paper begins with a review that is guided by the question of how well the fate of Eel River flood sediment could have been predicted given the state of knowledge in the early 1990s. Next, the observations are presented, with particular attention being paid to where these results support or refute reigning continental-shelf sediment-transport paradigms. Finally, the paper summarizes current understanding of sediment delivery to the seabed and provides new insight into which processes deserve greater attention in the future.

## REVIEW OF PREVIOUS WORK

### Early conceptual models

Interest in the physical environment of continental shelves flourished early for economic and strategic reasons (Emery, 1969). Ninety per cent of the world's marine food resources and nearly 20% of the world's petroleum and natural gas were being extracted from continental shelves. Shelves also promised to fill rapidly growing demand for sand and gravel and to provide a rich source of minerals. Strategically, shelves were key to the operation of submarines because the complex acoustic environment made it easy to conceal underwater objects. This upsurge of interest in continental shelves motivated several seminal papers that laid the conceptual foundations for the next three decades of research on continental-shelf sedimentology (Curry, 1965; Moore, 1969; Swift, 1970; McCave, 1972).

The most fundamental challenge for researchers of the time was developing sound physical models to explain the distribution of various grain sizes on the continental shelf. Geologists for some time had realized that simple equilibrium models (e.g. Fig. 1) failed to explain the offshore progression of grain sizes commonly observed on the Pacific Coast of North America. On the west coast, sands typically blanket inner shelves, muds occupy the middle shelves, and sand covers the outer shelves (Shepard, 1932; Emery, 1952). Emery (1952) proposed that inner-shelf sands and mid-shelf muds were currently being supplied from the continent and that outer-shelf sands were **relict** in the sense that they were not connected to modern supply and dispersal systems. More specifically, relict sands on the outer shelf were deposited when sea level was lower during the last ice age. The rapidity of sea-level rise inhibited adjustment of underlying sediment texture to rising waters.

The notion of **modern** and **relict** sediments took hold (Curry, 1965). Attention turned to explaining why modern sands were retained nearshore, why muds bypassed the inner shelf to form a mid-shelf Holocene mud blanket, and why relict sands on the outer shelf had not been covered by muds as well. Curry (1965) developed a simple model for sedimentation of river-derived sediments that divided the total sediment load into two parts. The

sand, or **bedload**, is carried close to the seabed and parallel to shore, where it deposits in a linear wedge. He proposed that, in general, wave action is too weak to transport significant quantities of sand in water depths greater than 10 m. The mud, or **suspended load**, is carried continuously or intermittently in suspension farther seaward but also parallel to shore, where it deposits in a mid-shelf mud blanket. The mud blankets typically lie in water depths deeper than 10 m. Curry (1965) suggested that when mid-shelf mud deposits are significantly deeper than 10 m, relict sands separate the modern sands and muds.

Curry's admittedly simple model left some key gaps that others proceeded to fill. In particular, Swift (1970) explicitly addressed the mechanisms by which mud bypassed the inner shelf and emphasized the importance of storm sediment transport. Swift (1970) viewed the shoreline as a sediment source, and because of the non-linear increase in sediment-transport rate with stress on the seabed, he identified storms as the key agent for moving sediment seaward. This focus on storms produced the realization that sand movement in water depths greater than 10 m is achieved easily. Swift (1970) drew on the work of Dunbar & Rodgers (1957) to hypothesize that sediment moves offshore by **diffusion**. In essence, these workers felt that currents and waves associated with storms are not organized enough to produce a strong directionality in transport. Instead, sediment moves short distances during storms, first in one direction, then in another. With the shoreline acting as a sediment source and the shelf break acting as a sediment sink, cross-shelf gradients of sediment concentration form during storms. These gradients produce a diffusive flux of sediment, especially fine sediment, across the shelf. The appearance of muds on the mid-shelf arises from preferential deposition of the coarse fraction during the intermittent transport events (Fig. 3a).

McCave (1972) focused more closely on the mechanisms by which fine sediment deposits form. He defined the issue as one of supply versus removal. Muds accumulate where supply overwhelms the ability of waves and currents to resuspend and remove them. Mid-shelf mud belts form because suspended fine sediment supplied from the coast has concentrations high enough over the mid-shelf to allow depositional flux to exceed

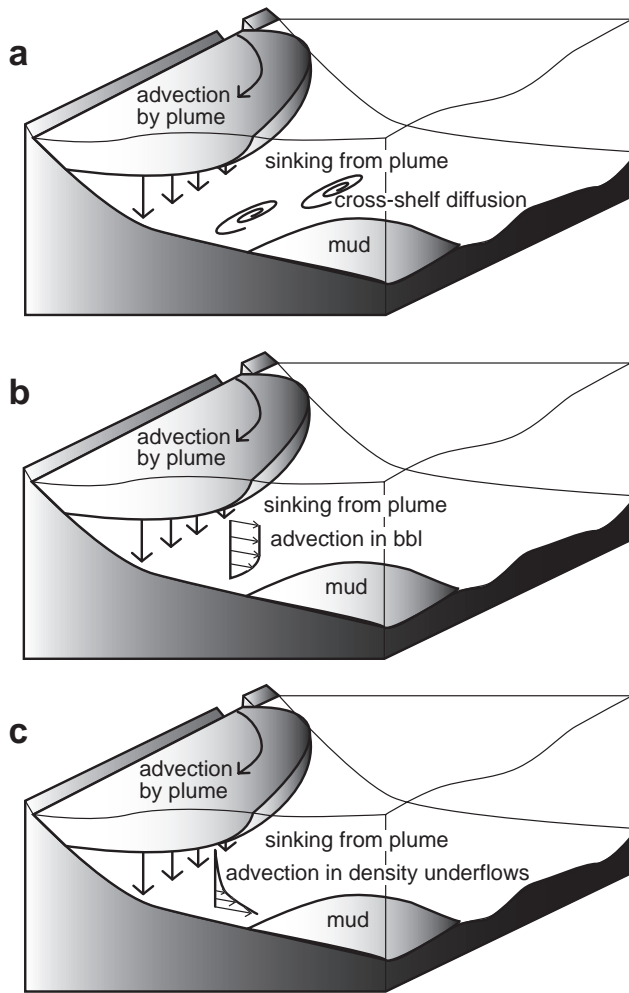


**Fig. 3** Three conceptual models for formation of mid-shelf mud belts. All three assume that the removal of mud from advective buoyant plumes occurs rapidly. They differ in proposed mechanisms for seaward transport of muds that have sunk from the plume: (a) wave-generated diffusion (Swift, 1970); (b) advection in oceanographic currents (McCave, 1972) – bbl, bottom boundary layer; (c) seaward transport occurs in wave-supported, gravity-driven underflows (Moore, 1969).

erosional flux, which can be relatively small in mid-shelf water depths. The small erosional flux is mostly due to diminishing wave stress with increasing water depth.

McCave (1972) favoured advective rather than diffusive transport of fine sediment across the inner shelf. He surmised that if sediment is diffusing away from the coast to the shelf break, as proposed by Swift (1970), then most of the sediment escaping coastal seas should be accumulating on

the continental slope and rise and in the abyss. Sediment budgets, however, show that most sediment escaping the shelves ends up in the great fans and cones of sediment at the bases of submarine canyons and other major supply points. He concluded that **advection** transports mud from major supply points to the canyons, and then off the shelf. Semi-permanent currents caused by wind, density and inertia were identified as the dominant means of advective transport of muds (Fig. 3b).

McCave's (1972) case was compelling for advection to dominate diffusion as the mechanism for moving fine sediments across shelf. His proposed mechanisms, however, did little to explain why sediment deposition was focused at the base of canyons. Instead, his mechanisms produce broadly distributed loss of sediment from the shelf at points downstream of major supply. Several years before McCave's work, Moore (1969) confronted the same issue of sediment focusing addressed by McCave. Working in California's Borderland Basins, Moore noticed on seismic-reflection profiles that sediments tended to dip away from submarine canyons, gullies and channels rather than away from centres of coastal drainage. He observed that sills within a basin commonly separate thick deposits near a canyon mouth from thin deposits farther away, that some nearshore basins nearly devoid of sediment are bordered seaward by basins with thick deposits, and that typically the only basins with thick sedimentary fill are integrated into a distributary system of canyons, valleys and channels. These patterns of sediment thickness led Moore (1969) to reject the concept of broadly distributed sediment loss from continental shelves. Moore offered an alternative model for how fine sediments migrate across continental shelves into submarine canyons.

Moore (1969) considered the fate of riverine sediments from their point of entry into the coastal ocean to their point of exit from the shelf at the heads of submarine canyons. At river mouths, sand and mud embark on different transport pathways. Sand sinks from buoyant riverine plumes rapidly, and is entrained by coast-parallel longshore transport in the surf zone and on the inner shelf. Where this transport system intersects canyons, sand is introduced directly into canyon heads. Mud at the river mouth remains temporarily in suspension as lower-density river water flows over basin waters.

The bulk of this mud settles rapidly from buoyant plumes, often advecting only several kilometres from the river mouth. Subsequently, or contemporaneously, during periods of energetic wave activity, mud is resuspended, and turbid layers develop over the seafloor. Under the influence of coastal currents and downslope gravity, these wave-supported layers then move across the seafloor as wide, relatively thin sheets. Muds accumulate where they escape wave stresses large enough to resuspend them, either in canyon heads or in water deep enough to inhibit large, wave-induced bed stresses (Fig. 3c).

In the late 1960s, then, several competing conceptual models of continental-shelf sediment transport emerged to guide subsequent decades of research. All essentially agreed that sand deposits rapidly at river mouths and moves alongshore in the surf zone and inner shelf. All envisioned mud residing temporarily within buoyant riverine discharge plumes. The models diverged in their proposed rates and mechanisms of transport once sediments reach the seafloor. Swift (1970) proposed that fine sediment diffuses seaward in a series of storm-generated events. McCave (1972) proposed that advection in inertially, buoyantly or atmospherically driven currents moves sediment seaward. Moore (1969) argued wave-driven erosion produces near-bottom suspensions dense enough to flow across shelf under the influence of gravity (Fig. 3).

Two key questions emerged from these competing conceptual models. Where on the shelf does fine sediment separate from buoyant discharge plumes via sedimentation, and how does fine sediment move across shelf to modern mid-shelf mud deposits?

#### Sediment loss from discharge plumes

Observations of suspended-sediment concentration collected near the mouths of rivers around the globe provide clear support for the hypothesis that mud and sand both sink rapidly from discharge plumes. As summarized by Drake (1976), studies around the Mississippi (Wright & Coleman, 1974), the Po (Nelson, 1970), and the Santa Barbara and Santa Clara Rivers (Drake, 1972) all showed that fine silt and clay disappear from surface waters and appear in **bottom nepheloid layers** within kilometres of river mouths. Later studies produced

similar results in, for example, the dispersal systems of the Zaire, Columbia and Ebro rivers (Nittrouer & Sternberg, 1981; Eisma & Kalf, 1984; Palanques & Drake, 1990).

The rapid removal of fine sediment from discharge plumes on continental shelves requires some form of particle repackaging into larger aggregate particles, because fine silts and clays simply sink too slowly to account for observed loss rates. To demonstrate this, consider the arguments of Drake (1976) regarding the 1969 flood deposit near the mouths of the Santa Barbara and Santa Clara Rivers. Just after a large flood, more than 80% of the discharged sediment could be accounted for in water depths of less than 50 m, at distances < 20 km from the river mouths (Drake *et al.*, 1972). Given that shelf currents typically fall in the range of 10–20 cm s<sup>-1</sup> (~10–20 km day<sup>-1</sup>), these observations suggested that particles must have been sinking at speeds of approximately 25–50 m day<sup>-1</sup>. These speeds translate to tenths of 1 mm s<sup>-1</sup>, which are typical of medium silts but exceed settling velocities of clay particles by several orders of magnitude. Similar results have been found in other environments, including tropical rivers and fjords (Eisma & Kalf, 1984; Syvitski *et al.*, 1985).

The hypothesis that particle repackaging causes rapid loss of fine sediment from river plumes was widely proposed and generally accepted. Mechanisms and rates of particle repackaging became a topic of research, and two mechanisms were proposed (e.g. Stumm & Morgan, 1981; McCave, 1984). The increasing ionic strength of water caused by the addition of salt compresses the **ion clouds** that surround charged particles, like fine-sediment grains, in water. In freshwater, ion clouds are thick, so when particles approach one another, their clouds cause repulsion at relatively large separation distances. In seawater, the ion clouds are compressed to such an extent that particles can approach one another quite closely before their ion clouds repel. At small separation distances the powerful yet distance-limited **van der Waals' force** of attraction can overwhelm the repulsive force between ion clouds, causing particles to cohere in a process called **electrochemical coagulation** (e.g. Stumm & Morgan, 1981). Pioneering experiments demonstrated that coagulation occurs at low salinities (Whitehouse *et al.*, 1960; Krone, 1962), a fact that was used to explain the trapping of sediment in

estuaries (e.g. Postma, 1967; Kranck, 1973, 1981; Edzwald *et al.*, 1974). Similar processes were invoked to explain rapid disappearance of sediment from river plumes on the continental shelf (McCave, 1972; Drake, 1976; Boldrin *et al.*, 1988).

**Biogenic aggregation** refers to the agglomeration by organisms of mineral matter into faecal pellets (Drake, 1976; McCave, 1984). In some environments it probably plays an important role in speeding removal of sediment from plumes (e.g. Schubel *et al.*, 1978). The remarkable consistency of sediment removal rates in a variety of settings, however, suggests that biogenic aggregation alone cannot explain rapid particle sinking.

Demonstration of coagulation in the laboratory paired with its hypothesized role in nearshore sedimentation of muds sparked efforts to measure the size and settling velocity of particle aggregates. Rather quickly the tendency of invasive sampling methods to disrupt fragile aggregates was documented (Gibbs, 1982a,b; Gibbs & Konwar, 1983), leading to the development of non-invasive methods for measuring aggregate properties *in situ*. Photography proved most effective (Syvitski & Murray, 1981; Eisma *et al.*, 1983, 1991, 1996; Kranck, 1984; Johnson & Wangersky, 1985; Syvitski *et al.*, 1991; Kranck & Milligan, 1992). Other methods also emerged, such as gentle capture paired with microscopy (Kranck *et al.*, 1992; Droppo & Ongley, 1994) and instruments that link the angular distribution of scattered laser light to particle-size distribution (Bale & Morris, 1987; Agrawal & Pottsmith, 1994).

These studies yielded apparently conflicting results regarding the importance of coagulation as a particle repackaging mechanism. According to the coagulation hypothesis, particles in freshwater are dispersed. Upon entering the sea, river waters mix with salty ocean water. A small rise in salinity to a few parts per thousand induces enough compression of ion clouds to allow aggregates to form. Maximal aggregate size then is set either by sedimentation or by disaggregation resulting from turbulence (Kranck, 1973). In estuaries, however, the expected increase in aggregate size at the interface between fresh and salt water failed to materialize. Instead, aggregate sizes showed no dependence on salinity, with typical diameters of several hundred micrometres in river and seawater alike (Eisma, 1986; Eisma *et al.*, 1991; Kranck *et al.*, 1992). In fjords, however, observations of aggregates did indicate

rapid formation when freshwater suspensions met the sea (Hoskin & Burrell, 1972; Syvitski & Murray, 1981; Cowan & Powell, 1990; Cowan, 1993).

The contrasting results from fjords and estuaries can be reconciled by considering the role of organic matter in aggregation. In a process called **flocculation**, organic molecules can bridge the gap between two particles by bonding to both surfaces. Aggregates produced in this manner are known as **flocs**. The efficacy of organic matter as a bonding agent depends on the composition, configuration and concentration of organic matter, all of which vary with environment and salinity (Eisma *et al.*, 1991; O'Melia & Tiller, 1993). Rivers discharging into temperate estuaries are likely to contain higher concentrations of large organic molecules than glacial meltwaters flowing into fjords, so flocculation predominates in estuaries, whereas coagulation controls particle packaging in the headwaters of fjords.

Scant observations exist of aggregate size in plumes extending from river mouths to the continental shelf, so it remains unclear how much aggregation modifies the *in situ* size distribution of plume sediments. Berhane *et al.* (1997) observed no dependence of aggregate size on salinity in the Amazon plume, but it was admitted that a lack of low-salinity observations may have masked evolution of aggregate size near the river mouth. Prior to the mid-1990s, then, repackaging of sediment was viewed widely as critical to producing rapid removal of fine sediment from surface plumes on the continental shelf. A dominant mechanism for repackaging could not be identified, however. The contribution of coagulation, biogenic aggregation and flocculation mediated by organic matter varied among environments (e.g. Syvitski & Murray, 1981; Berhane *et al.*, 1997).

For determining sediment fluxes, aggregate size is important insofar as it affects sediment settling velocity. Early laboratory work demonstrated clearly the significant enhancement to mud settling velocity caused by aggregation (Krone, 1962; Kranck, 1980), so attention turned to characterizing settling velocity *in situ*. Two main approaches were developed. **Owen tubes** and related devices (Burt, 1986; Dyer *et al.*, 1996) monitor concentration through time in a tube. The tube is lowered to a desired depth in a horizontal position with its ends open. Upon retrieval, the tube closes and flips into a vertical

position, thus presumably capturing without severe disturbance a sample of suspension. Bulk clearance rate of the suspension is used to calculate a representative settling velocity. No direct observations of particle sinking are made. The other approach is to observe directly and *in situ* the descent of particles in an enclosure that prevents horizontal advection of particles through the viewing volume. Vertical displacements over set time intervals are used to calculate particle settling velocities (Fennessy *et al.*, 1994; ten Brinke, 1994; Syvitiski *et al.*, 1995; Dyer *et al.*, 1996; Hill *et al.*, 1998).

These two different approaches yielded distinctly different results. In Owen tubes clearance rate increases with increasing concentration (Burt, 1986; Dyer *et al.*, 1996). The explanation given for this result was that aggregation is faster at higher concentrations. Faster aggregation arguably begets larger aggregates, producing the observed increases in clearance rates. Direct observations failed to support this explanation. Across a range of environments and sediment concentrations, aggregate settling velocities are typically in the range of  $1 \text{ mm s}^{-1}$  (ten Brinke, 1994; Hill *et al.*, 1998).

The observed increase in clearance rate with sediment concentration in Owen tubes has been linked conceptually and through direct and indirect observations to aggregation within the tubes (Milligan, 1995; Dearnaley, 1996; Milligan & Hill, 1998). These workers proposed that removal of sediment from a settling tube proceeds in several steps. First, *in situ* aggregates are disrupted to an unknown degree during sampling. Second, large aggregates form in the quiescent environment of the tube at a rate dependent on concentration. Last, aggregates sink out of suspension at approximately  $1 \text{ mm s}^{-1}$ . Concentration dependence of removal rate arises due to the concentration dependence of re-aggregation rate, not because aggregates become larger and sink faster at higher concentrations.

Turbulence probably influences aggregate size and settling velocity (Milligan & Hill, 1998), yet observations leave its role unclear. Theory suggests that aggregate size varies with an inverse power of the **turbulent-kinetic-energy dissipation rate** (e.g. Hunt, 1986). Limited experimentation with natural aggregates, however, showed that dependence of size on turbulent-kinetic-energy dissipation rate is either not significant or weaker than predicted (Alldredge *et al.*, 1990).

Time can also influence aggregate size and, by implication, aggregate settling velocity. If sediment grains are dispersed as they enter the sea, then a finite amount of time is required for aggregates to grow to an equilibrium size. If sediment concentration is high, then less time is required for aggregates to form (e.g. McCave, 1984; Hill, 1992). It is difficult to specify an actual time required for aggregation due to uncertainties regarding particle contact, adhesion and break-up rate (Hill, 1992, 1996; Hill & Nowell, 1995).

Prior to the mid-1990s, then, the variables controlling aggregate size and settling velocity were not clear. The most robust result of *in situ* studies was that settling velocities of  $1 \text{ mm s}^{-1}$  are typical of many marine environments. Therefore, settling velocities of this magnitude could be expected in the Eel River plume, as long as turbulence or lack of time did not prevent aggregates from attaining sizes large enough to sink at this rate.

#### **Advective transport in river plumes**

Plume direction, speed, thickness and width are the hydrographic parameters that, along with sediment settling velocity, determine where sediment discharged by a river will reach the seafloor. Research into the dynamics of plumes blossomed in the 1970s, with investigations framed increasingly in quantitative terms. Two subdisciplines were at the forefront of plume research at the time: marine sedimentology and physical oceanography. These disciplines focused their investigations somewhat differently, with the sedimentologists naturally more interested in processes close to river mouths where the bulk of fluvial sediment deposits, and the physical oceanographers more concerned with transport and mixing of river waters that occur both near to and far from river mouths. The work of these groups was complementary and, taken as a whole, provides both solid theoretical and observational frameworks on which to build a conceptual model of plume hydrography on the Eel shelf.

An issue recognized early as important to the direction followed by plumes is **plume buoyancy** (Bates, 1953; Wright, 1977). When the density of inflowing, sediment-laden water is much less than the basin water, the plume rides over the seawater and spreads under the influence of gravity. These plumes are called **hypopycnal**. When inflowing

suspensions have approximately the same density as basin water, the plume behaves much like a turbulent inertial jet. These plumes are called **homopycnal**. Under these two scenarios the steering of the plume is dominated either by Earth's rotation or by oceanographic and atmospheric forcing such as winds, currents and tides (Bates, 1953; Scrutton & Moore, 1953; Wright & Coleman, 1974; Wright, 1977; Eisma & Kalf, 1984; Garvine, 1987; Palanques & Drake, 1990; Geyer *et al.*, 1996). In contrast, when river waters are so laden with sediment that the inflowing plume exceeds the density of basin water, a gravity current forms and flows along the seafloor in the direction of maximal gradient (Bates, 1953; Mulder & Syvitski, 1995; Parsons *et al.*, this volume, pp. 275–337). The course of such **hyperpycnal** plumes also is affected by Earth's rotation and oceanographic forcing by tides and currents.

For many years, hyperpycnal plumes were not thought to be possible in marine settings, because the sediment concentrations required to make river water denser than seawater were too high to ever be realized under natural conditions (Bates, 1953; Drake, 1976). A systematic analysis of 150 rivers by Mulder & Syvitski (1995), however, indicated that some rivers do indeed carry sediment concentrations  $\geq 40 \text{ kg m}^{-3}$  required to overcome typical seawater densities. The conditions for such high concentrations are most common in small- and medium-sized mountainous drainage basins. Mulder & Syvitski (1995) suggested that during major floods, the Eel may reach high enough density to form hyperpycnal underflows. If so, then shelf topography would be important in determining the dispersal pathway of plume sediment. Unfortunately, the uncommon and unpredictable nature of hyperpycnal plumes makes them difficult to observe directly.

Proceeding under the assumption that the Eel plume is less dense than the receiving waters on the shelf leads to the prediction that the plume is steered up the coast to the right as it leaves the mouth. This prediction is relatively safe because both Earth's rotation and oceanographic processes during floods of the Eel force the plume northward along the coast. In the northern hemisphere, currents veer to the right under the influence of the **Coriolis force**, which is towards the north for the westward-discharging Eel (e.g. Garvine, 1987). The Eel discharges 90% of its sediment during

and immediately following winter storms (Brown & Ritter, 1971). The cyclonic circulation of the storms produces strong winds blowing from the south during peak discharge. The attendant wind stress on the ocean's surface, combined with the Coriolis force, pushes water to the right, or shoreward in the case of the Eel margin. In response, the sea surface develops a seaward slope that in turn produces a **barotropic flow**. This flow is deflected to the right, again by the effect of the Earth's rotation. In short, winds blowing from the south during storms force a northward flow along the coast (Smith & Hopkins, 1972). Finally, reworking of river-mouth sands by waves associated with winter storms produces a northward littoral drift that has formed an oblique entry of the Eel into the Pacific. This mouth geometry also favours northward transport (Wright, 1977; Garvine, 1987).

The speed of the plume is not as easy to predict as the direction. The deceleration of a plume upon entering the sea depends on the inertia of the outflow, the density contrast between the river and basin waters, and the degree to which plume interaction with the seabed extracts momentum from the flow (Wright, 1977). Inertia dominates plume behaviour when outflow velocity is large, and the density contrast between river and basin waters is small. Buoyancy dominates plume behaviour when outflow velocity is small and the density contrast is large. **Inertia-dominated plumes** decelerate due to turbulent mixing with ambient fluid along the plume's edges and base, but **buoyancy-dominated plumes** decelerate due to spreading and thinning of plume waters as they flow over basin waters. These mechanisms of deceleration differ fundamentally, so it is essential to identify which one dominates in a particular plume.

The **densimetric Froude number** ( $Fr$ ) characterizes the importance of inertia relative to buoyancy. It is dimensionless and defined by the equation

$$Fr = \frac{u}{(g'h_p)^{1/2}} \quad (1)$$

where  $u$  ( $\text{m s}^{-1}$ ) is the mean outflow speed,  $h_p$  (m) is plume thickness and  $g'$  ( $\text{m s}^{-2}$ ) is modified gravity, which is defined by

$$g' = \frac{\Delta\rho}{\rho} g \quad (2)$$

In Eq. 2,  $\Delta\rho$  ( $\text{kg m}^{-3}$ ) represents the density contrast between plume and basin water,  $\rho$  ( $\text{kg m}^{-3}$ ) is the density of basin water, and  $g$  ( $\text{m s}^{-2}$ ) is gravitational acceleration. If the Froude number is much greater than unity, then inertial forces dominate plume dynamics. If it is much less than unity, then buoyancy dominates plume dynamics (e.g. Wright, 1977).

Before the mid-1990s, the variables required to calculate  $Fr$  had not been measured explicitly on the Eel River margin, but data that made it possible to estimate them were available. Turning first to outflow speed, it is approximately equal to river discharge,  $Q$  ( $\text{m}^3 \text{s}^{-1}$ ), divided by channel depth  $h_c$  (m) and channel width  $W_c$  (m). During typical, annual floods, Eel discharge is  $\sim 5000 \text{ m}^3 \text{ s}^{-1}$  (Brown & Ritter, 1971). Channel width is approximately 1000 m and channel depth is approximately 5 m. The outflow speed during floods, therefore, is  $\sim 1 \text{ m s}^{-1}$ . The density contrast between the plume and basin water, based on observations elsewhere (e.g. Wright & Coleman, 1974), is probably  $\sim 10 \text{ kg m}^{-3}$ , and density of basin water is  $\sim 1025 \text{ kg m}^{-3}$ . With these inputs,  $(g'h_p)^{1/2}$  is approximately equal to  $0.7 \text{ m s}^{-1}$ . The outflow Froude number is therefore larger than unity, so plume dynamics at the mouth are dominated by inertia.

Inertia-dominated plumes do not ride up over basin water to the extent that buoyancy-dominated plumes do, so they can be slowed by frictional interaction with the seabed. Wright (1977) noted that small bottom gradients and depths less than or equal to channel depth seaward of the mouth produce conditions for which bottom friction plays a key role in plume deceleration and spreading. Bottom gradient on the Eel shelf is relatively steep ( $0.007 \text{ m m}^{-1}$  or  $0.4^\circ$ ; Leithold, 1989), and the mouth

region has not formed a significant subaqueous delta because of vigorous wave reworking of river-mouth deposits. Bed friction probably does not alter plume dynamics markedly.

Based on this information, it is possible to surmise that the Eel plume during floods is inertia-dominated and not affected strongly by bottom friction. It discharges into the Pacific where oceanographic conditions force a general northward transport. In addition, mouth geometry tends to direct the river outflow northward and along the coast. Interestingly, these general conditions resemble those assumed by Garvine (1987) in a numerical model of plume dynamics. The results of that model can be of use in elucidating plume structure and geometry in the vicinity of the Eel.

Garvine's (1987) model produces a plume with a distinct anticyclonic turning region near the mouth (Fig. 4). The dimensions of this gyre are set by the internal **Rossby radius of deformation**, defined as

$$Li = \frac{u}{f} \quad (3)$$

where  $Li$  is the Rossby radius (m),  $u$  is outflow speed ( $\text{m s}^{-1}$ ) and  $f$  is the Coriolis frequency ( $\text{s}^{-1}$ ). Assuming that outflow speed is approximately equal to  $1 \text{ m s}^{-1}$  and that the Coriolis frequency is  $10^{-4} \text{ s}^{-1}$  yields a Rossby radius of approximately 10 km. Garvine's model predicts that downstream of this bulge there is a sharp transition to cyclonic turning into a coastal current. This turning is forced by locally high pressure gradients created by water being forced against the coast. The coastal current that forms is in approximate geostrophic balance for the cross-shelf component.

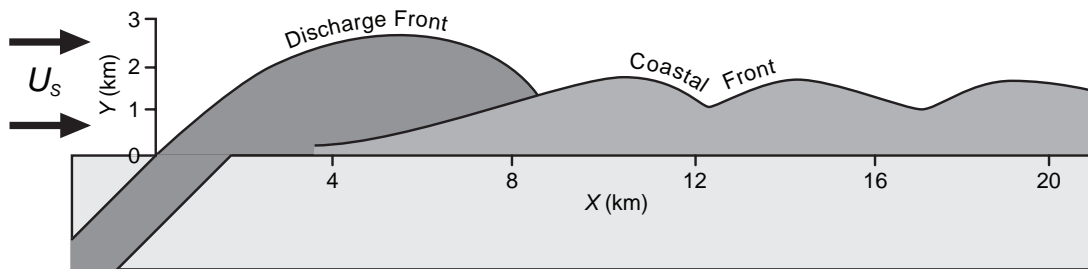


**Fig. 4** Schematic of a numerical model for evolution of a buoyant discharge plume. The variable  $U_s$  represents the velocity of a poleward-directed ambient current. (Redrawn from Garvine, 1987.)

If the Eel plume behaves like Garvine's model plume, then the fine sediment delivered by the Eel should deposit primarily under the anticyclonic turning region at the mouth. To demonstrate this, consider a simple calculation of the **residence time** of water in the gyre by approximating its volume as a half cylinder with radius  $Li$  ( $10^4$  m) and depth  $h_c$  (5 m). This volume equals  $\sim 10^9$  m<sup>3</sup>. Assuming an inflow to this volume equal to the Eel discharge during annual floods ( $5000$  m<sup>3</sup> s<sup>-1</sup>), the residence time of a water parcel is  $\sim 2 \times 10^5$  s, which is just over 2 days. Given typical bulk settling rates of 25–50 m day<sup>-1</sup> observed in a variety of environments (Drake, 1976; Eisma & Kalf, 1984; Syvitski *et al.*, 1985) and individual aggregate settling velocities of 100 m day<sup>-1</sup> (ten Brinke, 1994; Hill *et al.*, 1998), fine sediment has ample time to sink out of the plume and reach the seabed before being carried beyond the anticyclonic gyre at the mouth. Sediment therefore should reach the seabed within approximately 10 km of the river mouth and several kilometres from shore.

This simple prediction does not address explicitly the existence of mudstreams extending hundreds to thousands of kilometres downstream of some river mouths (McCave, 1972). Observations of rapid sinking and laterally extensive mudstreams can be reconciled by considering the role of resuspension. Near the coast, turbulence and downwelling can destroy water-column stratification and exert considerable stress on the seabed. In combination, these effects can prevent the deposition of plume sediment and lead to its retention in the plume and associated coastal current (Smith & Hopkins, 1972). The Eel margin typically experiences large waves and downwelling during floods, so a significant amount of fine sediment may be forced northward in nearshore regions. This nearshore flux is difficult to constrain because it depends on the fraction of the plume width under which resuspension occurs, and on northward flow speeds.

Despite uncertainty over how much sediment moves north on the Eel margin in a shore-attached mudstream, the alongshore position of the Eel mud deposit on the shelf indicates that a substantial fraction of Eel mud separates from the plume and its associated coastal current within the  $\sim 10$ -km distance suggested by the previous calculations. Decadal accumulation rates based on vertical profiles of <sup>210</sup>Pb in the seabed show that maximal accumulation rates occur 15 km north of the river

mouth (Leithold, 1989). In fact, Leithold (1989) used the distribution of accumulation rates to suggest that the plume flows directly over the mid-shelf mud deposit and loses sediment due to deposition directly to the seabed. The region of maximum accumulation measured by Leithold (1989) is centred 15–20 km offshore, yet the anticyclonic bulge at the mouth should extend to less than 10 km offshore and the associated coastal current should be even thinner (Garvine, 1987; Fig. 4). Therefore, sediment sinking from the plume must move across shelf either by diffusion during storms (Swift, 1970), by advection in coastal currents (McCave, 1972), or by advection in wave-supported, gravity-driven undercurrents (Moore, 1969).

#### **Bottom-boundary-layer transport of flood sediment**

Driven by competing hypotheses and rapid technological advances, understanding of benthic-boundary-layer sediment transport advanced dramatically during the 1970s and 1980s. The earliest deployments of current meters in continental-shelf bottom boundary layers documented quite clearly the dominant role of storms in sediment transport (Smith & Hopkins, 1972; Sternberg & McManus, 1972; Sternberg & Larsen, 1976). These measurements supported Swift's (1970) hypothesis that storms dominated transport, but they failed to support the hypothesis that storm-driven transport was diffusive and produced no net along-shelf transport. Instead, correlations were observed between storm resuspension and the direction and strength of near-bottom currents.

On the Washington shelf, storms cause significant across-shelf and along-shelf transport of fine sediment. This advection produces northward dispersal due to the prevalence of northward-flowing near-bed currents during storms (Smith & Hopkins, 1972; Sternberg & McManus, 1972; Sternberg & Larsen, 1976). Similar results were obtained in Norton Sound, Alaska, where wave-induced bottom currents associated with local storms were seen as critical to the northward dispersal of the fine sediment emanating from the Yukon River (Drake *et al.*, 1980). On the Russian River shelf just south of the Eel margin, sediment transport throughout a year is dominated by a few storms that generate strong northward currents with a substantial seaward component (Drake & Cacchione, 1985;

Sherwood *et al.*, 1994). On the Ebro margin in Spain, oceanographic currents push storm-resuspended sediment southward and seaward (Cacchione *et al.*, 1990). These studies and others favour the hypothesis that advection in bottom currents dominates the transport of fine sediment once it sinks from surface plumes. The generally similar forcing on the Russian River margin, the Columbia River margin and the Eel margin suggested that advective transport in the bottom boundary layer would occur primarily during winter storms and would on average be directed northward and seaward. This prediction is consistent with the position of maximum accumulation on the Eel shelf just north and seaward of where sediment would be likely to sink from the plume.

The clear documentation of advective transport by storm- and wave-generated near-bed flows diverted attention away from wave-supported, gravity-driven underflows as a plausible mechanism for across-shelf transport of muds. Furthermore, such underflows were deemed unlikely due to the extraordinarily large sediment concentrations required to overcome typical ocean stratification (Drake *et al.*, 1972). Nonetheless, observations accumulated slowly suggesting that density underflows remained a viable transport mechanism in shelf settings.

Density underflows were first recognized in the form of **turbidity currents** flowing down slopes that were steep compared with the gradients found in nearshore and continental-shelf settings (see Walker, 1973, for review). These steeper slopes allowed turbidity currents to flow rapidly enough to erode sediment from the seabed, thereby maintaining or enhancing their motive force (Bagnold, 1962). The maintenance of a dense suspension capable of flowing downslope seemed unlikely on low gradients until **fluid muds** were observed in estuaries such as the Gironde and Severn (Migniot, 1968; Kirby & Parker, 1977). These dense suspensions were the product of sediment trapping by estuarine flow that produced locally high fluxes of sediment to the seabed. The high fluxes overwhelmed local removal rates and produced concentrations of sediment great enough to hinder particle settling. These highly concentrated layers of mud are mobile and can move under the influence of gravity or currents (Migniot, 1968; Kirby & Parker, 1977).

Fluid muds were considered a unique byproduct of the circulation within estuaries until research in

the Amazon and Huanghe rivers demonstrated that they can form at density fronts on the continental shelf. Flow convergence at fronts leads to sediment trapping akin to that observed in estuaries. Sediment trapping produces high concentrations and hindered settling, and it can lead to downslope advection under the influence of gravity (Wright *et al.*, 1988; Kineke *et al.*, 1996). These observations suggested that strong density fronts are a key factor in the formation of gravity-driven flows, and, in a sense, they refuted implicitly Moore's (1969) hypothesis that waves alone can produce concentrations high enough to generate fluid muds.

Seymour (1986) addressed explicitly the possibility that concentrations of sediment great enough to flow downslope under the influence of gravity can form under waves. Taking a theoretical approach, he concluded that velocities, sediment size and supply, and bottom gradients on a typical inner continental shelf are more than adequate to produce wave-supported, gravity-driven underflows. He went on to explain some anomalous observations of other studies in the context of his proposed mechanism.

Sedimentary geologists also struggled to define the mechanisms underlying the formation of **tempestites**, which are sedimentary layers deposited during storms. These storm layers are common in the geological record of past continental-shelf sedimentation. They are curious in that they often show evidence of strong, seaward-directed, near-bottom flow. This evidence led to ongoing support for the hypothesis that wave-supported, dense, near-bed suspensions flowed downslope under the influence of gravity, much as Moore (1969) envisioned (e.g. Hamblin & Walker, 1979; Myrow & Southard, 1996).

By the mid-1990s, therefore, Moore's (1969) hypothesis that sediment moves across shelf under the influence of gravity was not widely recognized in the oceanographic and marine-geology communities. It could not be rejected, however, based on available theory and data. Furthermore, the geological record of storm sedimentation was difficult to explain without it.

#### Summary of past research

Based on past research, a coherent conceptual model for sedimentation on the Eel River shelf can be

constructed. The river plume enters the coastal ocean dominated by inertia. An anticyclonic bulge with radius of 10 km forms at the mouth. This bulge transforms into a northward flowing coastal current with a width of order 10 km or less. Much of the fine sediment in the plume, under the influence of aggregation, sinks from the plume at rates of 25–100 m day<sup>-1</sup>. This sediment leaves the plume primarily beneath the anticyclonic bulge. Upon leaving the plume, near-bed currents advect sediment northward and seaward in dilute suspensions. This near-bed advection explains qualitatively the location of maximum sediment accumulation on the shelf 15 km north of the river mouth and 15–20 km from shore. The remainder of this paper describes how recent observations of sediment delivery during floods on the Eel margin support or refute elements of this simple conceptual model.

## SEDIMENT DELIVERY TO THE EEL MARGIN

### Site description

The Eel shelf extends from Cape Mendocino in the south to Trinidad Head in the north (Fig. 2). The shelf is relatively narrow and steep. The shelf break occurs in water depths of 150 m, and it is located approximately 20 km from shore, indicating a slope of slightly greater than 0.4°. In addition to this relatively steep bathymetric gradient, two other physiographical features may play important roles in processing Eel River sediment on the shelf. The Eel Canyon incises the shelf just south of the river mouth. Its proximity to the mouth makes it a potentially important sink for sediment discharged by the Eel River. Humboldt Bay is a long, broad bay with a narrow inlet 15 km north of the river mouth. It, too, may affect sediment dynamics because of significant tidal exchange between the bay and the shelf (Geyer *et al.*, 2000).

The Coast Range rises to elevations > 2000 m over distances of 80 km in the Eel watershed. This steep topography leads to large erosion rates in the Eel basin. Large erosion rates also are favoured by the erodibility of the underlying Mesozoic Franciscan Complex, a *mélange* of intensely deformed sedimentary, low-grade metamorphic and igneous rocks. Much of the Franciscan is so highly sheared that it cannot maintain a slope of greater than

10–15°, commonly failing by shallow landslides following periods of heavy rainfall (Brown & Ritter, 1971; Nolan *et al.*, 1995). The topography also forces intense orographic precipitation as moist ocean air flows in from the west.

After trending inland perpendicular to the shore for 10 km, the main stem of the Eel River turns roughly shore-parallel, draining the heart of the Coast Range south of the river mouth. This interesting morphology arises in part due to uplift in the vicinity of the Mendocino Triple Junction to the south. The result is that the entire watershed often receives intense precipitation contemporaneously during storms, producing rapid and large increases in streamflow.

The regional-scale climate produces essentially two seasons. In the summer a broad area of high pressure is located over the ocean, with its centre well to the west of the California coast. From April to November, clockwise circulation around the high causes winds to blow from the north, and precipitation is minimal. During winter, the Aleutian Low develops in the north Pacific and pushes the high-pressure centre to the east. This shift exposes northern California to intense low-pressure systems moving onshore from the Pacific (Nunn, 1999). These lows have counter-clockwise circulation, and their approach is heralded by strong winds blowing from the south. After the passage of the lows, winds often shift to blow from the north. This stormy, wet period typically extends from November through March.

The average annual precipitation in the Eel basin is 1.26 m. The drainage area of the river is ~8000 km<sup>2</sup>, so the mean annual discharge of the river is ~10 km<sup>3</sup> of water (Morehead & Syvitski, 1999). This figure translates to a mean annual discharge of approximately 300 m<sup>3</sup> s<sup>-1</sup>. The episodicity of precipitation, however, leads to peak discharges well in excess of this value. A typical large annual flood can last about a week and produce peak discharges of 5000 m<sup>3</sup> s<sup>-1</sup>. Larger, rare flood events produce peak discharges in excess of 8000 m<sup>3</sup> s<sup>-1</sup> (Morehead & Syvitski, 1999; Sommerfield *et al.*, this volume, pp. 157–212).

### Observational programme

The field efforts for the sediment-transport-and-accumulation component of STRATAFORM

extended primarily over four flood seasons between 1994 and 1998. The observations can be grouped broadly into seabed observations, plume observations and bottom-boundary-layer observations.

#### *Seabed observations*

Seabed sampling was carried out primarily with a 20 × 30 cm box corer (e.g. Wheatcroft & Borgeld, 2000). In 1997–98 a hydraulically damped piston corer was used to collect cores in inner shelf sandy sediments. Coring took place on nine cruises: February, May and September 1995; March and July 1996; January and May 1997; and March and July 1998. In general, during a cruise, 40–70 stations were sampled, extending along-shelf from just south of the river mouth to just south of Trinidad Head 50 km to the north. Stations extended across-shelf to the upper slope (Wheatcroft & Borgeld, 2000).

Sediments within cores were characterized with a variety of techniques. To assess and quantify sediment layering within the seabed, sediment slabs were X-rayed onboard, generally within 30 min of collection, thus limiting the effects of subsequent compaction or bioturbation on internal bedding. Vertical distribution of grain size within cores was characterized in several ways. Sediment was wet-sieved, then size distribution was measured with a Coulter Multisizer (Drake, 1999). In other analyses, discrete organic matter was separated from the sediment. The remaining inorganic sediment was disaggregated, and the size distribution was measured with a Multisizer (e.g. Milligan & Kranck, 1991). Grain size also was characterized with sieve-and-pipette analysis (e.g. Folk, 1977). Resistivity as a function of depth in core was measured as a proxy for sediment porosity (Wheatcroft & Borgeld, 2000). Organic geochemical characterization of the shelf sediments was also undertaken (Leithold & Hope, 1999). Carbon-to-nitrogen ratios and the isotopic ratios of  $^{13}\text{C}$  to  $^{12}\text{C}$  were used to identify sediment containing terrestrial organic matter introduced by the river onto the continental shelf.

Accumulation rates in sediment cores were measured over a range of time-scales by using a suite of radioisotopes (Sommerfield *et al.*, this volume, pp. 157–212). Most relevant to the short-term, event-scale focus of this paper is  $^7\text{Be}$  (e.g. Sommerfield

*et al.*, 1999). This isotope is formed by cosmic-ray spallation of nitrogen and oxygen in the Earth's atmosphere, where it adsorbs onto aerosols and then can reach the Earth's surface by wet or dry deposition. In the vicinity of turbid rivers, virtually all  $^7\text{Be}$  remains adsorbed to particle surfaces. It is, therefore, an excellent tracer of particles recently supplied to the ocean. Its utility in constraining short-term deposition rates derives from the facts that  $^7\text{Be}$  is concentrated in the surface of sub-aerially exposed soils and that  $^7\text{Be}$  has a half-life of only 53.3 days. The appearance of  $^7\text{Be}$  in the seafloor therefore indicates that those sediments have resided in the coastal ocean < 8 months. The Eel River dominates sediment discharge onto the shelf and most of that discharge occurs during 4 months in late autumn and winter, so sediments with measurable  $^7\text{Be}$  can be linked unambiguously to discharge events during the preceding year (Sommerfield *et al.*, 1999).

#### *Plume observations*

Plume observations can be divided into two categories. Between 1996 and 2000, rapid-response helicopter surveys were conducted in association with floods of the Eel River. In 1996–97 and 1997–98 these helicopter observations were paired with time series collected from moorings placed on the G and K transects (see Fig. 2; Geyer *et al.*, 2000).

A helicopter-based sampling programme was developed for STRATAFORM because of the typically extreme sea conditions that accompany floods. By monitoring the discharge of the Eel River via the internet, it was possible to deploy equipment and scientific personnel to sample the plume within 24 h of a discharge threshold on the Eel River. With support and assistance of US Coast Guard Group Humboldt Bay, a profiling instrument package was lowered from a search-and-rescue helicopter through the water column on a grid of 12 stations that extended from the river mouth northward 30 km along the shelf. Sampling generally was shoreward of the 40-m isobath, because the sediment plume did not extend farther seaward than this. The instrument package comprised a CTD (conductivity, temperature, depth device), a camera for observing *in situ* aggregate size, two pressure-actuated Niskin bottles designed to collect sediment

suspensions at 2 m and 10 m below the sea surface, and an optical backscatter sensor (OBS) to monitor the vertical distribution of sediment concentration (Hill *et al.*, 2000; Curran *et al.*, 2002a).

In the first deployment, moorings were located in 30 m and 60 m of water on the G line just north of the river mouth. The path followed by the plume was generally shoreward of these positions so, in the following year, moorings were located on the K line, which is 10 km up-coast from the river mouth. Moorings in 20 m, 40 m and 60 m of water on the K line carried temperature, salinity and OBS sensors at 0.5-m and 4.5-m water depths on the moorings. Current meters were placed at 2 m and 6 m below the surface (Geyer *et al.*, 2000).

#### *Bottom-boundary-layer observations*

Bottom tripods and quadrapods, hereafter referred to generically as tripods, were used to monitor waves, currents and suspended-sediment concentration in the bottom boundary layer. Throughout the programme, a tripod was maintained on the S line at 60-m water depth (S60) (Ogston & Sternberg, 1999; Ogston *et al.*, 2000). The configuration of the deployment arrays changed from year to year. Tripods were deployed across the shelf on the S line, extending from 55 m to 70 m, to investigate the role of cross-shelf flux convergence in determining the cross-shelf position of the mud deposit (Cacchione *et al.*, 1999; Ogston & Sternberg, 1999; Wright *et al.*, 1999). Tripods were placed at G65, K63 and S60 to investigate along-shelf flux convergence in determining the along-shelf position of the mud deposit (Cacchione *et al.*, 1999; Ogston & Sternberg, 1999; Wright *et al.*, 1999). An array of tripods was emplaced on the K line with instruments located at 20-, 40- and 60-m water depths to gain more information about the cross-shelf sediment flux in the bottom boundary layer at the along-shelf position where loss of sediment from the plume was maximal (Traykovski *et al.*, 2000; Wheatcroft & Borgeld, 2000).

In general, tripods were equipped with vertical arrays of OBS sensors and electromagnetic current meters. These arrays characterized flow velocity and sediment concentration from heights of 10–30 cm above bottom (cmab) to 1–2 m above bottom (mab) (e.g. Ogston *et al.*, 2000). The tripods also

generally had upward-looking acoustic Doppler current profilers (ADCP) to characterize flow above the tripods. Important additions to this general suite of sensors were acoustic backscatter sensors (ABS) mounted on two tripods along the K line. These downward-looking sensors were deployed to measure profiles of acoustic-backscatter intensity between the seabed and 1.28 mab. The data from these sensors can be used as a proxy for suspended-sediment concentration. These sensors provide observations below the lowermost OBSs (Traykovski *et al.*, 2000).

## **Results**

### *Environmental conditions during study period*

Large floods with peak discharges in excess of  $10,000 \text{ m}^3 \text{ s}^{-1}$  occurred on the Eel River in January 1995 and January 1997 (Figs 5–8). In terms of peak discharge observed since the 1930s, the 1997 and 1995 floods rank second and third behind the remarkable event of 1964, which produced a peak discharge of  $21,000 \text{ m}^3 \text{ s}^{-1}$  (Wheatcroft & Borgeld, 2000). A moderate flood with a peak discharge of  $\sim 5000 \text{ m}^3 \text{ s}^{-1}$  occurred in March 1995, and a series of moderate floods marked the La Niña winter of 1997–98 (Geyer *et al.*, 2000; Wheatcroft & Borgeld, 2000). The winter of 1995–96 was relatively dry.

During the peak discharge months, winds typically blow out of the south, with brief periods out of the north. The same pattern holds true during flood events. As intense low-pressure systems move onshore, winds blow strongly from the south, with typical wind speeds of  $20 \text{ m s}^{-1}$ . After the fronts move onshore, winds during flood events decrease and switch to blow from the north.

Large waves are typical of the Eel shelf during winter. Mean wave height is 2.4 m, and 1% of the time wave heights exceed 5.5 m. Waves as high as 12 m have been observed (Ogston & Sternberg, 1999). The largest waves tend to occur in winter. During flood events, the margin typically is exposed to large waves due to the association of high winds and precipitation with low-pressure systems (Cacchione *et al.*, 1999; Ogston & Sternberg, 1999; Geyer *et al.*, 2000; Traykovski *et al.*, 2000). Not all periods of large waves, however, occur during flood events.

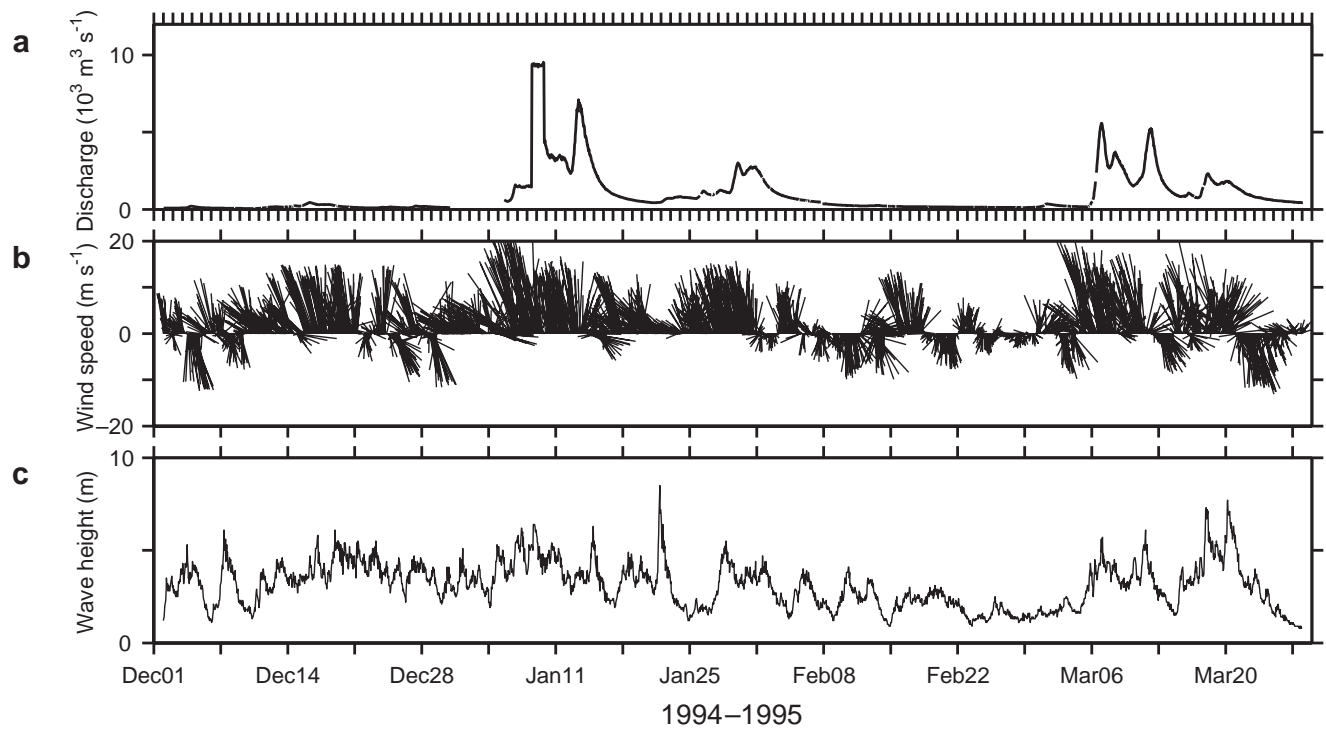


**Fig. 5** Environmental conditions on the Eel margin during winter 1994–95. (a) Hourly mean discharge at the Scotia station on the Eel River. (b) Wind velocity vectors, with positive indicating winds blowing toward the north. Winds were measured at NOAA’s National Data Buoy Center (NDBC) buoy 46022. (c) Wave heights measured at the same buoy. Note the large flood in January 1995, and the moderate flood in March 1995. The greatest peak in January is truncated in the graph, because the monitoring equipment failed at the highest turbidity levels.

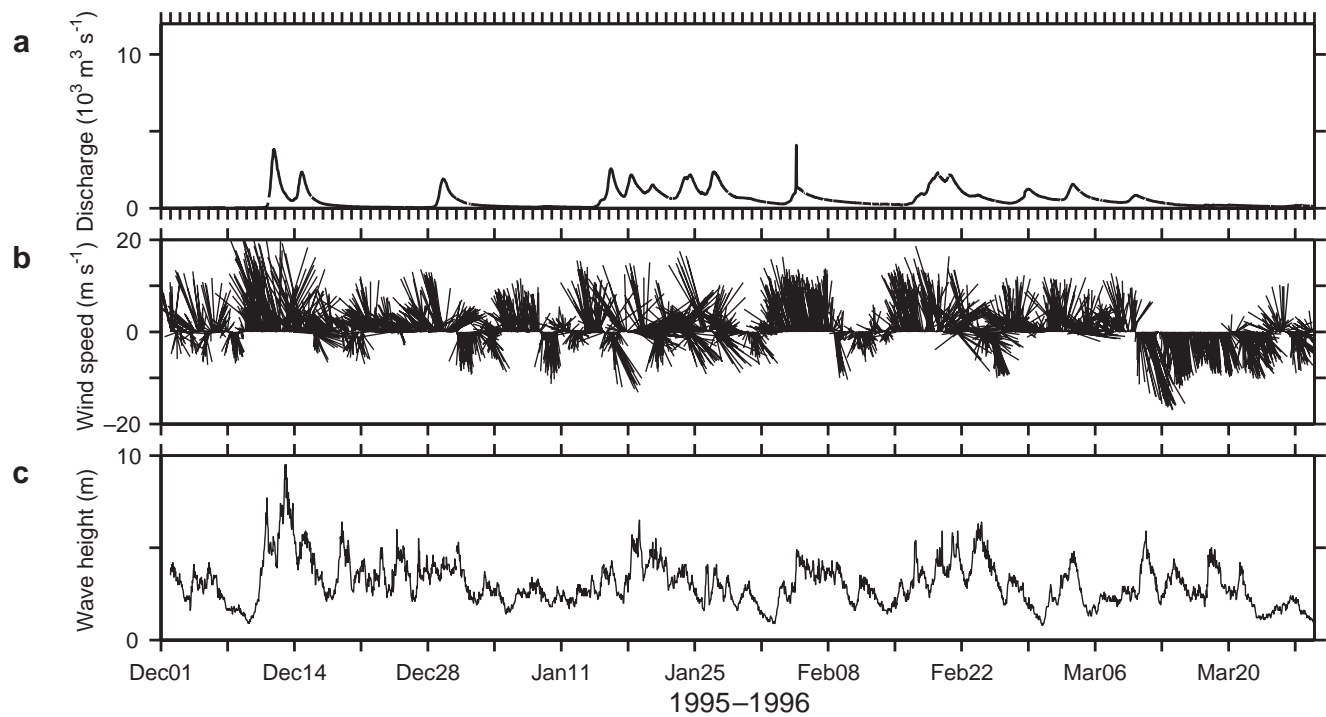


**Fig. 6** Environmental conditions on the Eel margin during winter 1995–96. See Fig. 5 for details. Note the lack of significant discharge events during this flood season.

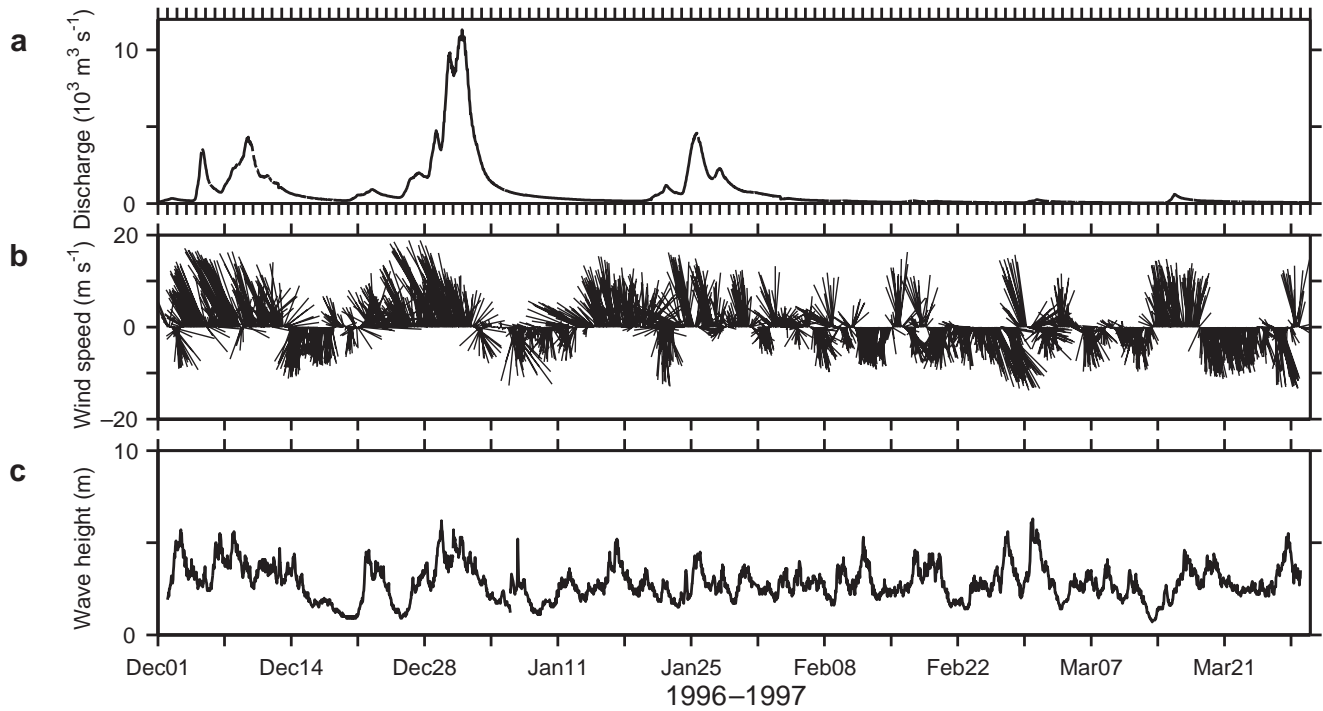


**Fig. 7** Environmental conditions on the Eel margin in winter 1996–97. See Fig. 5 for details. Data in the middle and bottom panels from December 1996 were measured by NOAA’s National Data Buoy Center (NDBC) buoy 46030. These data were used when buoy 46022 was not functioning. Note the large discharge event in January 1997.

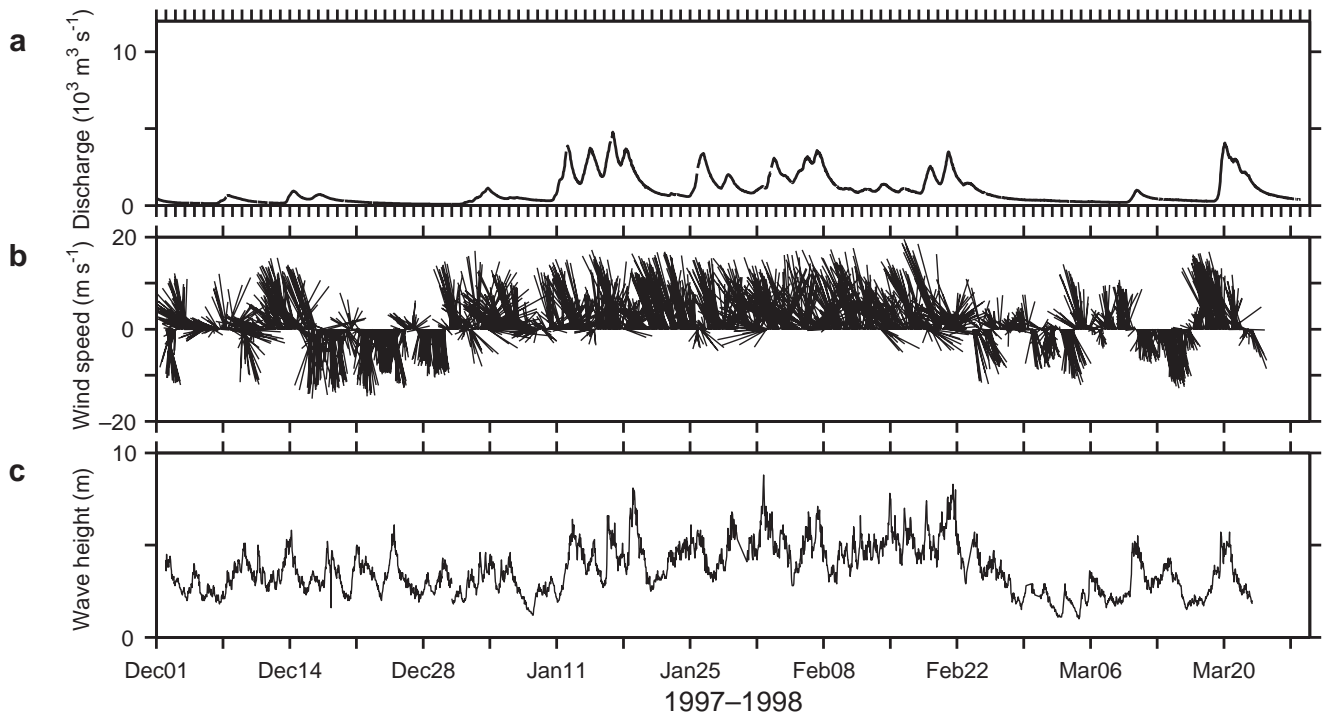


**Fig. 8** Environmental conditions on the Eel margin during the winter of 1997–98. See Fig. 5 for details. Note the series of moderate discharge events starting in mid-January.

Description of the flood deposits

Floods of the Eel produce mud deposits that differ physically and chemically from the ambient shelf sediments (Fig. 9). In X-radiographs, sharp wavy contacts separate flood layers from underlying sediment. The flood layers tend to be relatively X-ray

transparent and rich in physical structure, including laminations and cross-bedding (see also Nittrouer *et al.*, this volume, pp. 1–48; Wheatcroft *et al.*, this volume, pp. 101–155; Sommerfield *et al.*, this volume, pp. 157–212; Wheatcroft & Borgeld, 2000). In 1995, the flood layer possessed two to six alternating X-ray transparent and X-ray opaque layers.

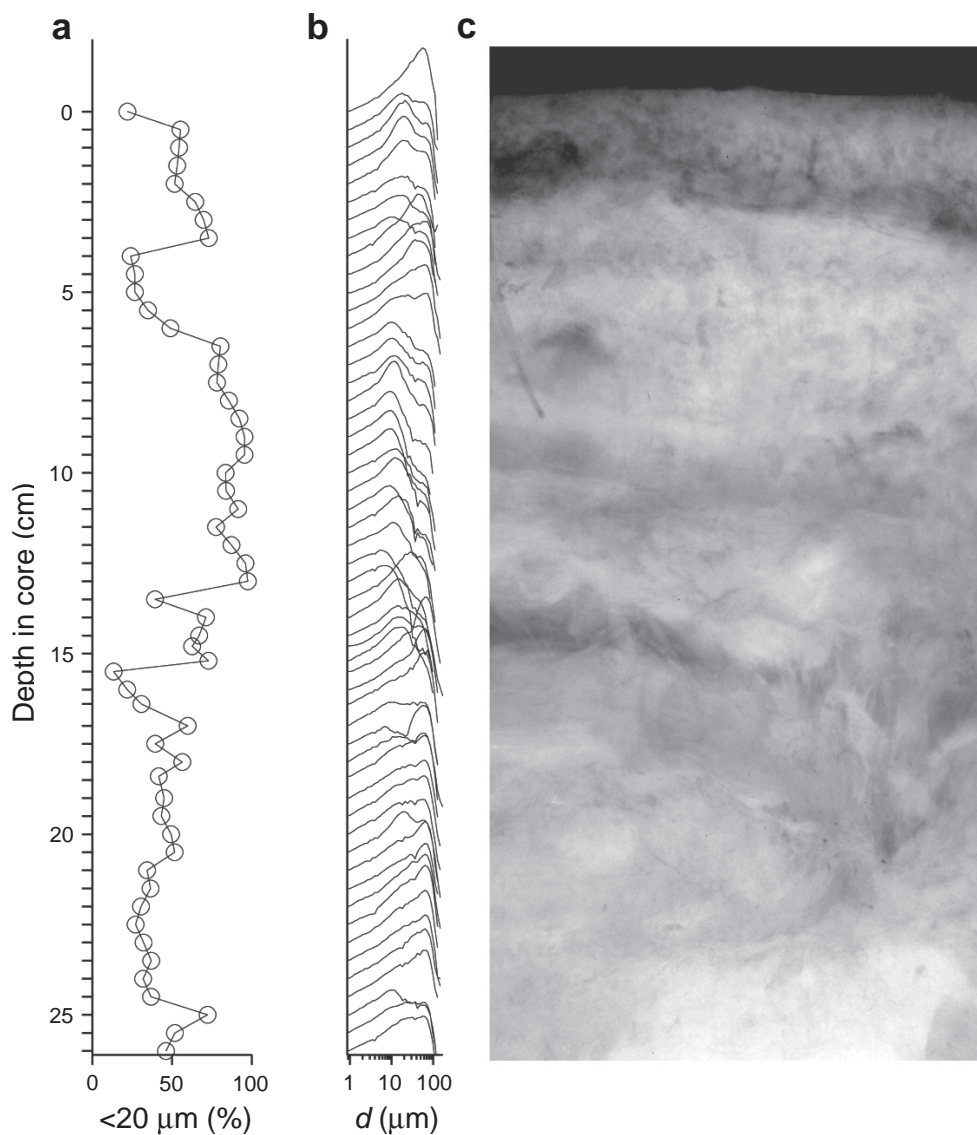


**Fig. 9** Vertical distribution of grain size in an X-rayed slab from a box core collected at site S60 in 1997 (also see Nittrouer *et al.*, this volume, pp. 1–48; Wheatcroft *et al.*, this volume, pp. 101–155; Sommerfield *et al.*, this volume, pp. 157–212). (a) Disaggregated inorganic grain-size distributions plotted as a percentage volume  $< 20 \mu\text{m}$  equivalent spherical diameter. (b) Fully disaggregated inorganic grain-size distributions are plotted. The data are relative volume versus equivalent spherical diameter plotted on logarithmic axes. Individual sample plots are displaced by amounts proportional to depths in core, which are shown in centimetres along the vertical axis. (c) X-ray negative of the slab. Bright areas correlate generally with coarser sediment. The 1997 flood layer appears at the top of the core (top  $\sim 3$  cm), and the January 1995 flood layer sits between 7 and 13 cm depth in core.

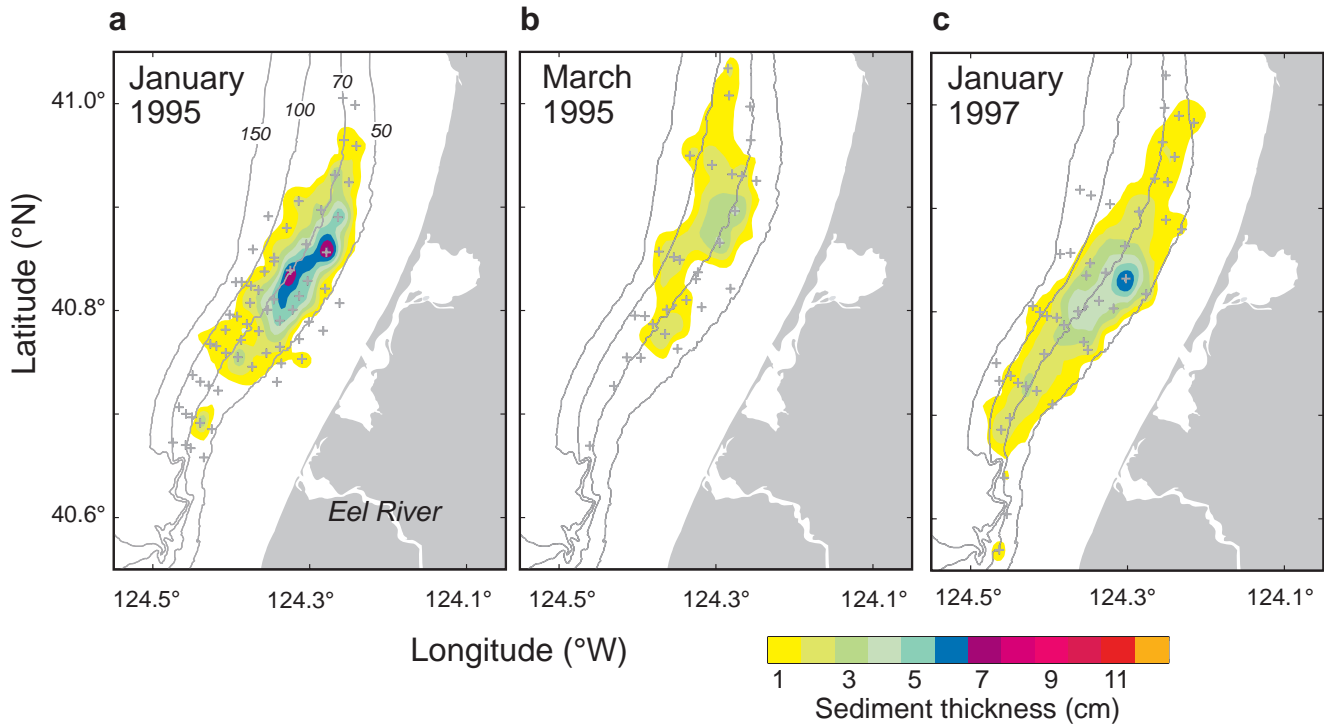


**Fig. 10** Isopach maps from three flood deposits: (a) January 1995; (b) March 1995; (c) January 1997. Station locations are indicated. (Redrawn from Wheatcroft & Borgeld, 2000.)

Laminations appeared at some sites in the flood layer produced in January 1997, but at other sites the layer was massive and X-ray transparent. The cores with massively bedded flood layers were located nearer to the river mouth than the cores with laminated flood layers. The spatial differences in bedding within the 1997 flood layer presumably reflect differences in near-bed depositional dynamics (Wheatcroft & Borgeld, 2000).

The differences in X-ray density are tied closely to changes in grain size (Fig. 9). Sediment delivered to the mid-shelf region by floods tends to be finer than the ambient shelf sediment. The flood layers have > 90% of their mass in particles smaller than 20  $\mu\text{m}$ , while ambient sediment contains < 50% mass in the < 20- $\mu\text{m}$  fraction (Drake, 1999). In the January 1995 and January 1997 flood layers,  $^7\text{Be}$  was detected uniformly throughout the layers in water depths greater than 50 m. Below the layers, no  $^7\text{Be}$  was detected (Sommerfield *et al.*, 1999). The presence of  $^7\text{Be}$  in the layers attests to their rapid emplacement and terrestrial source. Flood layers tended to have higher carbon to nitrogen ratios and more negative  $\delta^{13}\text{C}$  values than ambient sediment,

again indicating a terrestrial source (Leithold & Hope, 1999).

The various distinct physical and chemical signatures of the flood layers made it possible to identify them and map their spatial extent (Fig. 10). Interestingly, the large and moderate floods of 1995 generated distinct flood layers, as did the large flood of 1997, but the series of moderate floods in 1998 produced none (Wheatcroft & Borgeld, 2000). The floods of 1998 poured large volumes of water and sediment into the coastal ocean over the course of the flood season, but none of the events was particularly large. Furthermore, 1998 experienced a generally more energetic wave climate than other years (Fig. 8), suggesting that sediment dispersal and reworking by waves made flood layers indistinguishable from surrounding shelf sediments.

The areal distributions of the flood layers formed during the January and March 1995 and January 1997 floods were ellipsoidal (Wheatcroft & Borgeld, 2000; Fig. 10). Their major axes extended along shelf and were approximately 35–50 km long. Minor axes were 10 km wide and oriented across shelf. Deposits thinned away from central loci of maximal thickness.

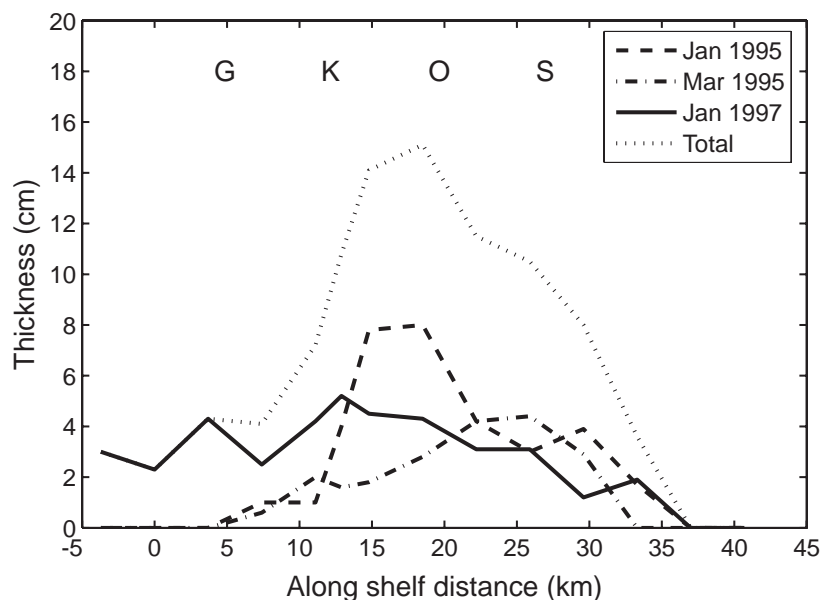


**Fig. 11** Flood-layer thickness versus along-shelf distance from the river mouth for three flood deposits. The letters at the top of the panel denote positions of cross-shelf transects (Fig. 2). (Redrawn from Wheatcroft & Borgeld, 2000.)

The centres of mass of the various flood deposits were centred on the 70-m isobath, 15 km north-east of the river mouth. Recognizable flood layers were found in water depths as shallow as 50 m and as deep as 110 m (Fig. 10). In terms of maximal thickness, the layer associated with the January 1995 flood was thickest (8 cm), followed by the January 1997 and March 1995 layers (~5 cm) (Fig. 11). This thickness ranking differs from a ranking based on integrated flood-sediment discharge, for which the 1997 flood ranks first and the January 1995 event ranks second. This reversed ranking emphasizes the importance of both sediment delivery and sediment dispersal in determining the thickness of mid-shelf flood deposits (Wheatcroft & Borgeld, 2000).

The extensive coring of flood layers combined with their distinctiveness made it possible to estimate the total mass of sediment in each layer. Wheatcroft & Borgeld (2000) applied moving-average least-squares and inverse-distance algorithms to calculate the thickness and the volume of the flood layers. Then, using an average porosity based on resistivity measurements and an assumed quartz density for the sediments, they estimated the total mass of each layer. The January 1995 layer holds  $6.2 \times 10^9$  kg of sediment, the March 1995 layer holds  $2.5 \times 10^9$  kg and the 1997 layer contains  $6.7 \times 10^9$  kg of sediment. The larger mass of the 1997 layer is consistent with its ranking as a larger discharge event.

The mid-shelf flood layers account for a relatively small fraction of the total sediment amount delivered to the coastal ocean by the river during floods. The Eel has a long record of measurements of suspended-sediment concentration as a function of water discharge (Brown & Ritter, 1971; Fig. 12). These data have been used to link concentration to discharge mathematically, either through empirical relationships (Wheatcroft *et al.*, 1997) or through process-based mechanistic models that address the stochastic behaviour of hydrological systems (Syvitski *et al.*, 2000; Morehead *et al.*, 2003). The empirical approach indicates that sediment discharge on the Eel, which is the product of water discharge and suspended-sediment concentration, varies approximately with the square of water discharge, thus highlighting the importance of floods to sediment accumulation on the Eel margin.

Wheatcroft & Borgeld (2000) used an empirical relationship between discharge and suspended-sediment concentration and the record of discharge for each flood event (Figs 5, 7 & 12) to estimate the total mass of sediment discharged during the course of the event. Estimates for the mass of sediment delivered to the ocean during the 17-day January 1995 event range from  $\sim 22$  to  $\sim 29 \times 10^9$  kg. Estimates for the March 1995 flood range from  $\sim 10$  to  $\sim 15 \times 10^9$  kg, and for the 1997 event from  $\sim 29$  to  $\sim 45 \times 10^9$  kg. These predictions are imprecise, in large part because natural variability produces

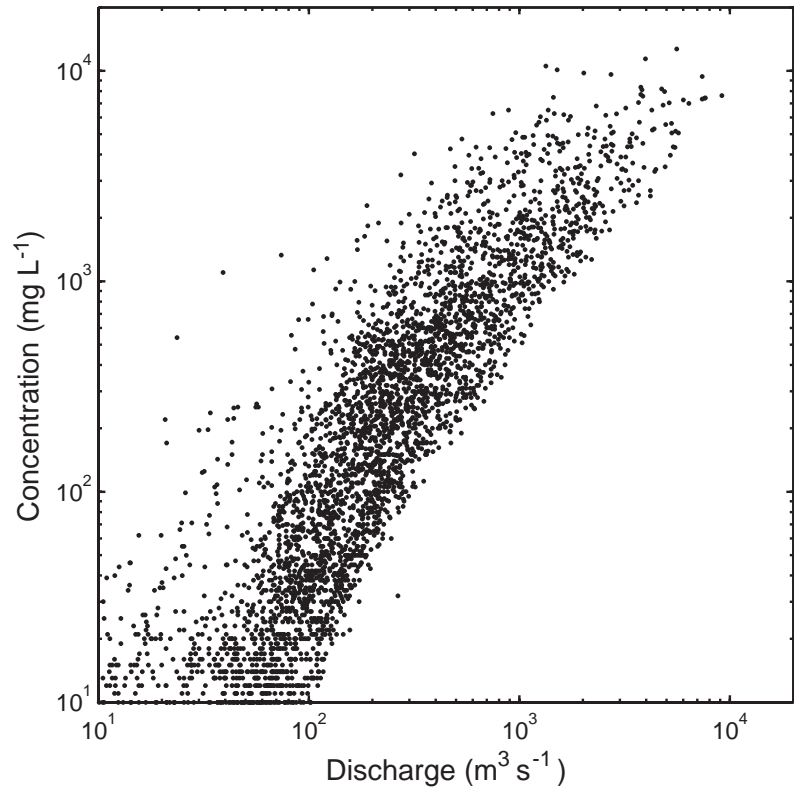


**Fig. 12** Suspended-sediment concentration versus river discharge for the Eel River.

a wide range of possible concentrations for a given discharge, and because data during large discharges are scant.

The percentages of the total flood sediment contained within the flood layers average about 25% (Wheatcroft & Borgeld, 2000). The ranges for each flood are 22–31% for January 1995, 17–24% for March 1995 and 15–30% for January 1997. These percentages indicate that the Eel margin is dispersive, retaining only a fraction of the total sediment in mid-shelf, muddy flood deposits. The remainder of the flood sediment must be either stored somewhere on the inner shelf, transported off-shelf, or carried along-shelf beyond the study area.

#### Plume hydrography

During floods, the Eel plume was observed to flow northward, as expected (Geyer *et al.*, 2000; Fig. 13). Near-surface speeds averaged  $0.5 \text{ m s}^{-1}$  during periods of elevated discharge. During low discharge, along-shelf flow to the north was weaker, averaging only  $0.1 \text{ m s}^{-1}$ . Plume speeds as high as  $1.3 \text{ m s}^{-1}$  were associated with the January 1997

flood. In 1998, maximum plume speeds of up to  $0.8 \text{ m s}^{-1}$  were observed. Plume speeds often fell markedly during the waning stages of flood events. For example, on 3 January 1997, at the end of the flood, plume speeds fell to  $0.2 \text{ m s}^{-1}$ .

Flood plumes typically did not extend beyond the 40-m isobath in a seaward direction. When the speed of the plume was large, salinity at the 40-m isobath on the K line was similar to seawater. When plumes slowed at the end of some high-discharge events, salinity decreased at K40 to below 20. The spread of low-salinity plume water to the 40-m isobath was not accompanied by an increase in sediment concentration, however. These observations of plume velocity and extent led Geyer *et al.* (2000) to propose a division of plumes into 'fast and narrow', 'slow and wide' or 'rough' (Fig. 14).

Wind forcing played a dominant role in determining the velocity and cross-shelf extent of Eel flood plumes. Strong winds from the south accompanied precipitation in the Eel basin, and these winds exerted northward-directed stress on the sea surface, thus contributing to the large, northward plume velocities during floods. When winds

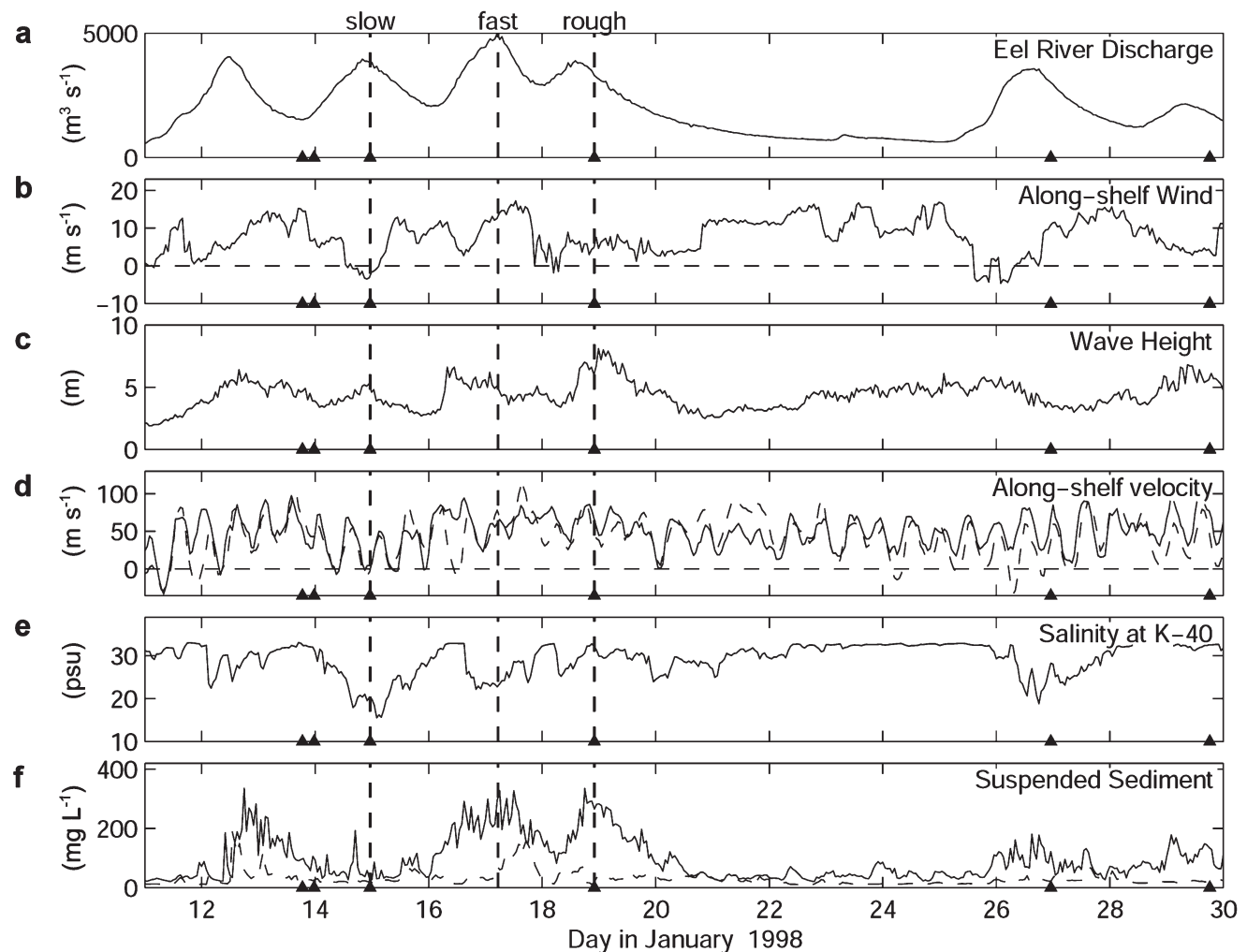


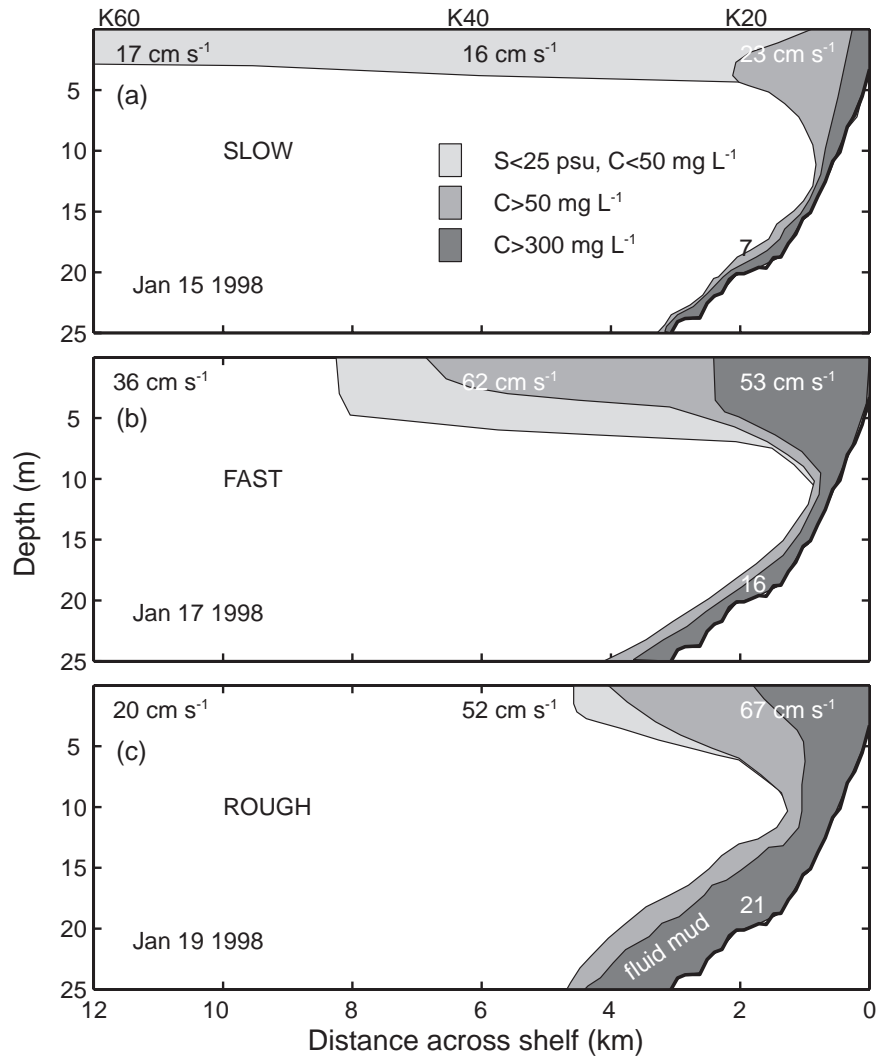
**Fig. 13** Time series of forcing variables and conditions at the K line during winter 1997–98. (a) Eel River discharge. (b & c) Along-shelf wind speed (+ northward) and wave height at buoy 46022. (d) Plume velocity along-shelf (+ northward) 2 m below the surface at K20 (solid line) and K40 (dashed line). (e) Salinity at K40 0.5 m below the surface. (f) Estimated suspended-sediment concentration 0.5 m below the surface at K20 (solid line) and at K40 (dashed line). The lines labelled ‘slow’, ‘fast’ and ‘rough’ mark the times represented by plume cross-sections plotted in Fig. 14. Times of helicopter surveys are marked by triangles. (Redrawn from Geyer *et al.*, 2000.)

blew from the north at the close of some events, the sign of the wind stress on the sea surface changed, thereby slowing but not halting the northward flow of the plume. Based on observations of winds at NOAA buoy 46022 and plume velocities at the moorings on the K line in 1998, Geyer *et al.* (2000) proposed that along-shelf currents had a response of  $1 \text{ m s}^{-1} \text{ Pa}^{-1}$  of along-shelf wind stress. During winter 1998 the average northward wind stress when Eel discharge exceeded  $800 \text{ m}^3 \text{ s}^{-1}$  was  $0.15 \text{ Pa}$ , yielding an average of  $0.15 \text{ m s}^{-1}$  of wind-induced, along-shelf flow at the sea surface. During periods

of low discharge, wind direction was variable and wind speed was less than during periods of high discharge. As a result, average wind stress was not significantly different from zero, so winds during these times exerted no net effect on along-shelf transport.

The cross-shelf extent of the plume also was affected strongly by the wind (Geyer *et al.*, 2000; Fig. 14). Winds from the south produced a landward flow of surface waters due to Ekman transport. The landward flow caused a build up of surface waters against the coast, which deepened

**Fig. 14** Cross-sections of suspended-sediment and salinity structure for the plume at the K line during the three times indicated in Fig. 13. The light shading shows where the low-salinity plume has less than  $50 \text{ mg L}^{-1}$  suspended-sediment concentration. Darker shading corresponds to higher concentrations of suspended sediment. Numbers represent along-shelf plume speeds ( $\text{cm s}^{-1}$ ) 2 m below the surface or speed in the bottom boundary layer. (a) A plume that moves slowly and spreads offshore under the influence of northerly winds. (b) Plume structure when downwelling-favourable winds blowing from south to north pushed surface waters along-margin and constrained the plume to shallower water. (c) Rough plumes occur when large waves resuspend sediment lost from the plume, forming dense near-bed fluid-mud suspensions. Note that fluid-mud layers occupy only the lower  $\sim 10 \text{ cm}$  of the dark-shaded region in panel c. (Redrawn from Geyer *et al.*, 2000.)



the pycnocline there. The build up produced geostrophic flow that drove surface water along margin to the north. The aggregate effect of these processes was to keep the surface plume confined to relatively shallow water, inshore of the 40-m isobath, during periods when the wind blew strongly from the south. Fast plumes thus were narrow as well. Winds blowing from the north generated seaward flow in surface waters and shoaling of the pycnocline at the coast. Under these conditions, the plume thinned as it spread seaward. Weak wind forcing from the north associated with the trailing edges of low-pressure systems thereby produced slow, wide plumes.

Tides introduced significant variability into plume velocities. When diurnal and semi-diurnal tides

were in phase, variations in along-shelf velocity of up to  $0.5 \text{ m s}^{-1}$  were observed (Geyer *et al.*, 2000; Fig. 13). This variability equalled the along-shelf average plume speed in 1998. Tidal flow in and out of Humboldt Bay probably also caused variability in along-shelf flow. On an ebb tide, flow out of Humboldt Bay introduced an offshore-directed source of momentum into the coastal ocean that was equivalent to the momentum associated with the Eel River when it discharges  $10^4 \text{ m}^3 \text{ s}^{-1}$  (Geyer *et al.*, 2000). This large momentum source potentially could have distorted and slowed the plume, as well as provided energy for plume mixing and sediment resuspension. Unfortunately, the measurement programme was not designed in a way that allowed any systematic quantification for the

effect of Humboldt Bay tidal exchange on plume structure and velocity.

Observations of plume density and velocity are consistent with the hypothesis that the Eel's dynamics are governed by inertia at the river mouth (Geyer *et al.*, 2000). Using mouth geometry, discharge and salinity during floods, Geyer *et al.* (2000) calculated that Froude numbers at the mouth exceeded unity. Using measured velocities at the K line and estimated mouth velocities to constrain the size of the anticyclonic bulge at the mouth, they calculated that the inertial radius for the Eel in 1998 was  $\sim 10$  km. Inertia could have pushed the plume seaward to approximately the 50-m isobath, and it could have influenced plume dynamics to the K line. Mouth geometry, however, affected the extent of inertial influence. The river mouth directed flow northward into the coastal ocean at an angle of  $20^\circ$  from the coast. Such an angle of entry probably reduced the seaward extent of the inertial bulge and increased the along-shelf distance over which inertial effects influenced the plume (Garvine, 1987; Geyer *et al.*, 2000).

Theoretically, a buoyant river plume evolves along-shelf into a coastal current with a cross-shelf width determined by a geostrophic force balance. Buoyant water near the coast spreads seaward over more saline, denser basin water. As it spreads, it is deflected to the right in the northern hemisphere by the effect of Earth's rotation. In the limit of a current flowing along a vertical wall and therefore not experiencing any frictional drag from the seabed, the width,  $W_p$  (m), of a coastal current in semi-geostrophic balance is defined by (Lentz & Helfrich, 2002)

$$W_p = \frac{(g'h_p)^{1/2}}{f} \quad (4)$$

where, as before (Eqs 2 & 3),  $g'$  and  $f$  are modified gravity and the Coriolis frequency, respectively, and  $h_p$  is plume thickness (m). Assuming that the plume density during floods was  $1012 \text{ kg m}^{-3}$  and that the density of basin water was  $1023 \text{ kg m}^{-3}$  (Geyer *et al.*, 2000), modified gravity equalled 0.11. Assuming that a plume thickness of 5 m was typical during floods (Geyer *et al.*, 2000) yields a plume width of  $\sim 7$  km. Given the regional bathymetric gradient of  $0.4^\circ$ , this width suggests that the plume remained inshore of the 50-m isobath

in 1998 due to the effects of Earth's rotation on the northward-flowing coastal current.

The final factor that can affect plume width and speed is bottom friction. Lentz & Helfrich (2002) proposed a complete expression for plume width that includes the effect of bottom friction:

$$W_p = \frac{(g'h_p)^{1/2}}{f} \left[ 1 + \frac{(2Qg'f)^{1/4}}{\alpha g'/f} \right] \quad (5)$$

Assuming a discharge of  $5000 \text{ m}^3 \text{ s}^{-1}$  and a bottom gradient  $\alpha$  of  $0.007 \text{ m m}^{-1}$  yields a value for the second term inside the brackets of  $\sim 0.1$ . This result indicates that during floods the plume was perhaps only 10% wider than it would have been in the absence of bottom friction. Given the idealizing assumptions that underlie Eqs 4 and 5, this difference is not significant.

In summary, a variety of forces acted to confine the Eel plume landward of the 40-m isobath during floods. The flood deposits were found seaward of the 40-m isobath, so subplume transport in the bottom boundary layer must have transported flood sediment seaward. Understanding of the cross-shelf position of the flood deposits therefore requires an understanding of boundary-layer transport; understanding of the along-shelf position of the flood deposits requires an understanding of the rate at which sediment sank out of the northward-advecting surface plumes during floods.

#### *Sediment loss from the plume*

Helicopter-based observations of sediment in the Eel plume indicate that sediment removal occurred more rapidly than by single-grain sinking alone, yet not as rapidly as has been observed in other, less energetic systems (Hill *et al.*, 2000; Curran *et al.*, 2002a). In general, 40–75% of the sediment delivered to the ocean by the river during floods sank from the plume between the river mouth and the K line 10 km to the north (Geyer *et al.*, 2000; Hill *et al.*, 2000). Therefore, sediment sank rapidly enough from the plume to account for the position and mass of flood deposits.

Helicopter- and mooring-based observations revealed that sediment sank from surface waters inshore of the 40-m isobath (Geyer *et al.*, 2000; Hill *et al.*, 2000). When winds blew strongly from the

south, the brackish waters of the plume did not extend beyond the 40-m isobath at the surface, so naturally sediment from the river did not extend beyond this either. When winds shifted to northerly at the end of some storms, the salinity signature of river water did appear as far offshore as the 40-m isobath, yet sediment was not associated with the lower salinity water (Geyer *et al.*, 2000; Figs 13 & 14). Sediment did not make it far seaward during northerly winds because the plume slowed and thinned under such forcing. Slower plumes took longer to reach the K line, and thinner plumes reduced the residence time of particles within them. These factors combined to cause removal of sediment from the plume landward of the 40-m isobath, even when upwelling-favourable winds allowed the plume to spread farther offshore (Geyer *et al.*, 2000).

Sediment clearance rates from the Eel plume exceeded single-grain clearance rates, yet they were not as large as observed in other environments. Clearance rates can be parameterized with an **effective settling velocity**. The effective settling velocity is the term  $w_e$  ( $\text{m s}^{-1}$ ) in the equation

$$C_s(x) = C_s(0) \exp\left(-\frac{w_e}{h_p u} x\right) \quad (6)$$

which is a representation of the one-dimensional spatial decay of sediment concentration with distance from the river mouth. The term  $C_s(x)$  ( $\text{kg m}^{-3}$ ) is sediment mass concentration at along-shelf position  $x$  (m), and  $C_s(0)$  is sediment mass concentration at the river mouth. The terms  $h_p$  (m) and  $u$  ( $\text{m s}^{-1}$ ), as before, represent plume thickness and velocity, respectively (Hill *et al.*, 2000).

A regression of the logarithm of  $C_s(x)/C_s(0)$  on the logarithm of  $x$  from various helicopter surveys in 1998 provided estimates of  $w_e/h_p u$ . By inserting values for  $h_p$  and  $u$  into this estimate, effective settling velocities were calculated. For five flood events in 1998, values for  $w_e$  ranged from 0.06 to 0.1  $\text{mm s}^{-1}$  (Hill *et al.*, 2000). These values exceed the value of 0.04  $\text{mm s}^{-1}$  that would have resulted if particles sank as single grains, but they are well below the  $\sim 1 \text{ mm s}^{-1}$  settling velocity of individual aggregates and the 0.3–0.6  $\text{mm s}^{-1}$  effective settling velocities observed elsewhere (Drake, 1972; Syvitski *et al.*, 1985).

The observed clearance rates probably exceeded single-grain clearance rates due to aggregation. Aggregates were observed in the plume on all surveys. Median aggregate equivalent circular diameter, averaged over all surveys, was 232  $\mu\text{m}$  and varied from 125  $\mu\text{m}$  to as high as 405  $\mu\text{m}$  (Curran *et al.*, 2002a; Fig. 15). Large aggregate size was described with the parameter  $d_{25}$ , which is the equivalent circular diameter at the lower boundary of the upper quartile of particle areas in an image (Curran *et al.*, 2002a). The mean value of  $d_{25}$  was 280  $\mu\text{m}$  among all surveys. Although aggregate settling velocities were not measured directly, Sternberg *et al.* (1999) did measure them in the bottom boundary layer on the Eel shelf (Fig. 16). Using the relationship from that study for aggregates in the plume yields a settling velocity of 1  $\text{mm s}^{-1}$  for the median aggregate diameter, which is a value consistent with other observations of aggregate settling velocity in a wide range of environments (Hill *et al.*, 1998, 2000; Curran *et al.*, 2002a). Interestingly, aggregate size and inferred aggregate settling velocity showed no systematic variation with discharge, concentration, winds, waves, turbulent-kinetic-energy dissipation rate, or time from river mouth (Hill *et al.*, 2000; Curran *et al.*, 2002a; Fig. 15).

The observation that values for effective settling velocity fell between single-grain values and values for individual aggregates arguably indicated that sediment in the plumes was partially aggregated. Hill *et al.* (2000) calculated that observed clearance rates could be reproduced by packaging 75% of the sediment mass at the river mouth in aggregates, and assigning the remaining 25% to single grains. This calculation assumed that dilution of the plume with seawater at the river mouth effectively stopped any subsequent aggregation down-current of the river mouth, by reducing the sediment concentration to the point where interparticle collisions became too rare to affect particle packaging significantly. This extent of particle packaging in suspension is consistent with other studies (Syvitski *et al.*, 1995; Dyer & Manning, 1999).

Curran *et al.* (2002a) examined the above hypothesis regarding particle packaging in two ways. First, they examined along-shelf evolution of the **aggregate fraction**, defined as the proportion of the total suspended mass that is packaged within

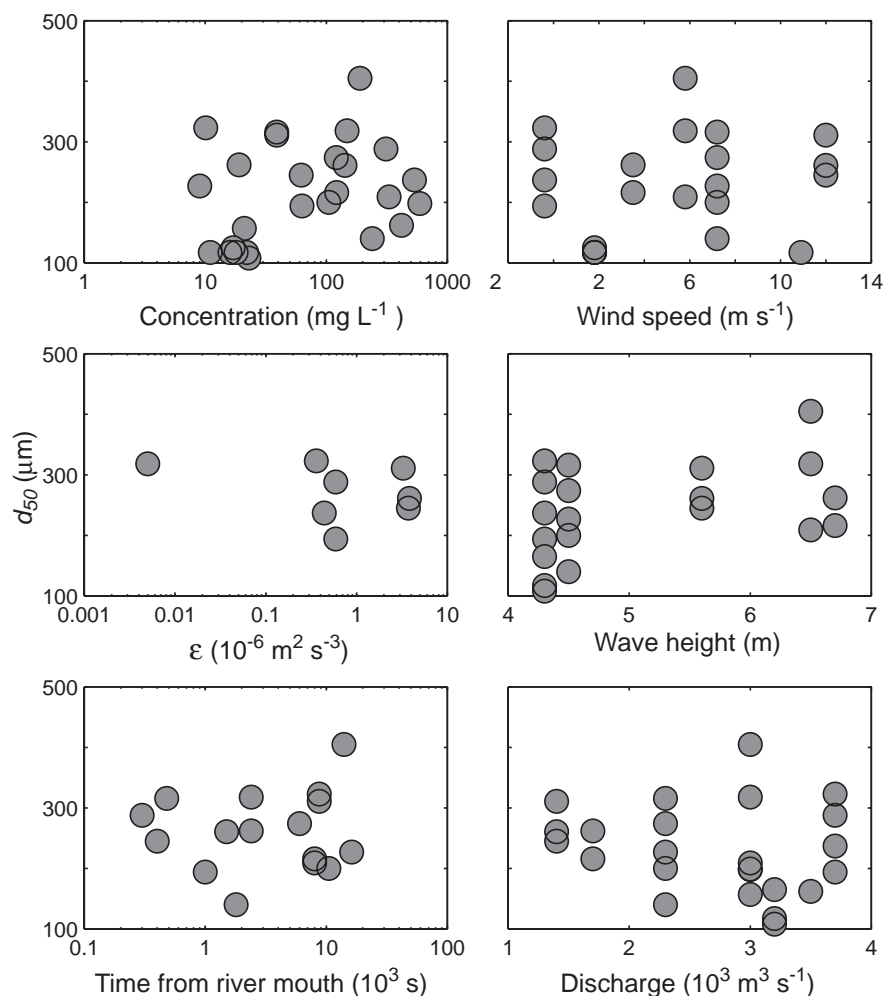


**Fig. 15** Aggregate size in the Eel plume versus various environmental variables. Aggregate size is represented by  $d_{50}$ , which is the equivalent circular diameter of the median aggregate area in an image. Variable  $\epsilon$  is turbulent-kinetic-energy dissipation rate at the depth of an image. Systematic variation is not observed. (Redrawn from Curran *et al.*, 2002a.)

aggregates. They calculated this fraction by estimating the mass concentration of aggregates in plume photographs, and dividing it by the total suspended-sediment mass in suspension. To estimate aggregate mass concentration from photographs, they used aggregate settling velocity versus size data from the Eel shelf (Sternberg *et al.*, 1999) and Stokes Law to estimate aggregate mass as a function of diameter (Fig. 16). This relationship was applied to each aggregate in an image to generate an estimate of total aggregate mass concentration.

If the plume was partially aggregated and too dilute to allow any subsequent aggregation down-current of the river mouth, then the aggregate fraction would have decreased along-shelf because aggregates sink faster than the single grains found in the Eel plume (Curran *et al.*, 2002a). Along-shelf

evolution of the aggregate fraction, however, was not observed, thus refuting the Hill *et al.* (2000) hypothesis (Fig. 17). Like aggregate size, aggregate fraction showed no dependence on sediment concentration, wave height, river discharge, winds, turbulent-kinetic-energy dissipation rate, or time from the river mouth. The variability of aggregate properties across a wide range of environmental conditions indicated that some other factor determined aggregate size and the aggregate fraction in the Eel plume.

The second method used by Curran *et al.* (2002a) to examine the Hill *et al.* (2000) hypothesis regarding packaging was analysis of the differential sedimentation of individual grain sizes. In a fully aggregated suspension, all particle sizes should be removed from the plume at the same rate.

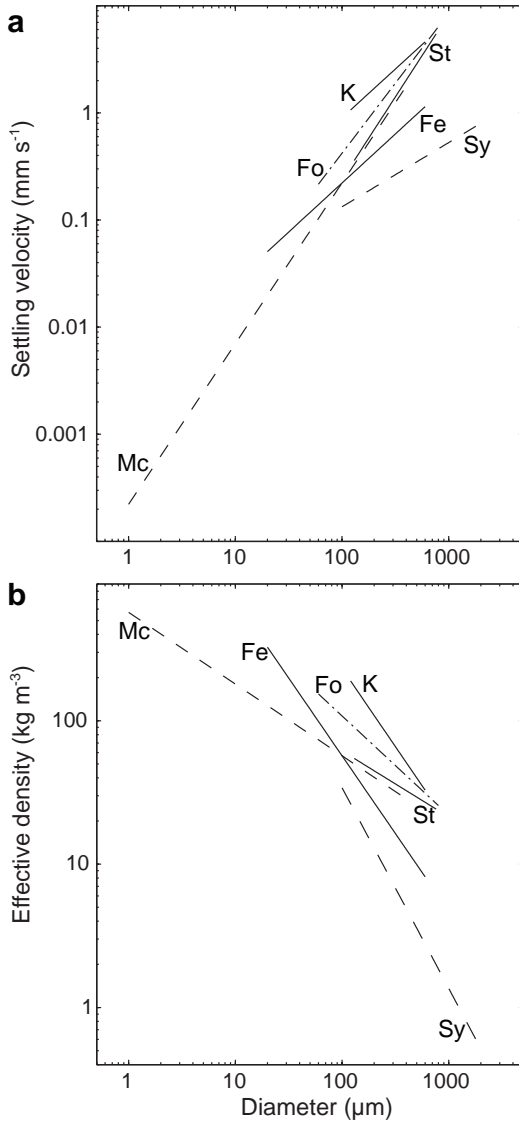


**Fig. 16** Relationships between aggregate properties and aggregate size from six different studies: Mc (McCave, 1975); K (Kranck *et al.*, 1992); Fe (Fennessy *et al.*, 1994); Sy (Syvitski *et al.*, 1995); St (Sternberg *et al.*, 1999); Fo (Fox *et al.*, 2004). (a) Settling velocity versus size. (b) Estimated effective density versus size. (Redrawn from Fox, 2003.)

In a disaggregated suspension, effective settling velocity would scale with the square of particle diameter. For partially aggregated suspensions, size-dependent effective settling velocities would vary in a way that is predictable and bracketed by the end-member values for the disaggregated and fully aggregated cases. Curran *et al.* (2002a) found that size-dependent effective settling velocities

did not conform to a relationship derived under the assumptions that the aggregate fraction at the river mouth was 0.75 and no further aggregation took place beyond the river mouth. Instead, the size-dependent values of  $w_e$  indicated that aggregate fractions in the plume were higher.

Curran *et al.* (2002a) reconciled the observations of high and non-evolving aggregate fractions with low removal rates by invoking sediment resuspension in the surf zone. Helicopter observations demonstrated that sediment did not enter the plume by resuspension in water depths of 20 m or greater, but the same could not be said of shallower waters. During surveys, wave breaking occurred out to water depths as great as 15 m. During floods, the surf zone was grey with suspended mud. Breaking waves offer substantial energy for resuspension. Therefore, Curran *et al.* (2002a) argued that sediment that sank to the seabed in waters shallower than 15 m was re-entrained into the plume. This resuspension reduced effective settling velocities. Furthermore, horizontal diffusion of sediment-laden surface waters supplied the plume seaward of the 15-m isobath with aggregated sediment that had been resuspended in the surf zone.

In summary, sediment separation from the plume in the cross-shelf direction occurred between approximately 15 m and 40 m water depths. Inshore of the 15-m isobath, wave breaking re-entrained sediment into the plume. Sediment did not sink from the plume seaward of the 40-m isobath primarily because inertial dynamics, Ekman transport and geostrophy all conspired to limit the spread of the plume to no more than 10 km from shore.

The along-shelf position of sediment loss agrees well with the along-shelf location of the flood deposits. The **e-folding distance** for sediment loss is the distance over which sediment concentration in the plume falls to  $1/e$  of its initial value (Hill *et al.*, 2000). It is calculated for the Eel plume with the equation

$$x_e = \frac{h_p u}{w_e} \quad (7)$$

Assuming, as before, that plume thickness was approximately 5 m, plume velocity was  $0.5 \text{ m s}^{-1}$  and that effective settling velocity was  $10^{-4} \text{ m s}^{-1}$ , the e-folding distance of sediment in the plume

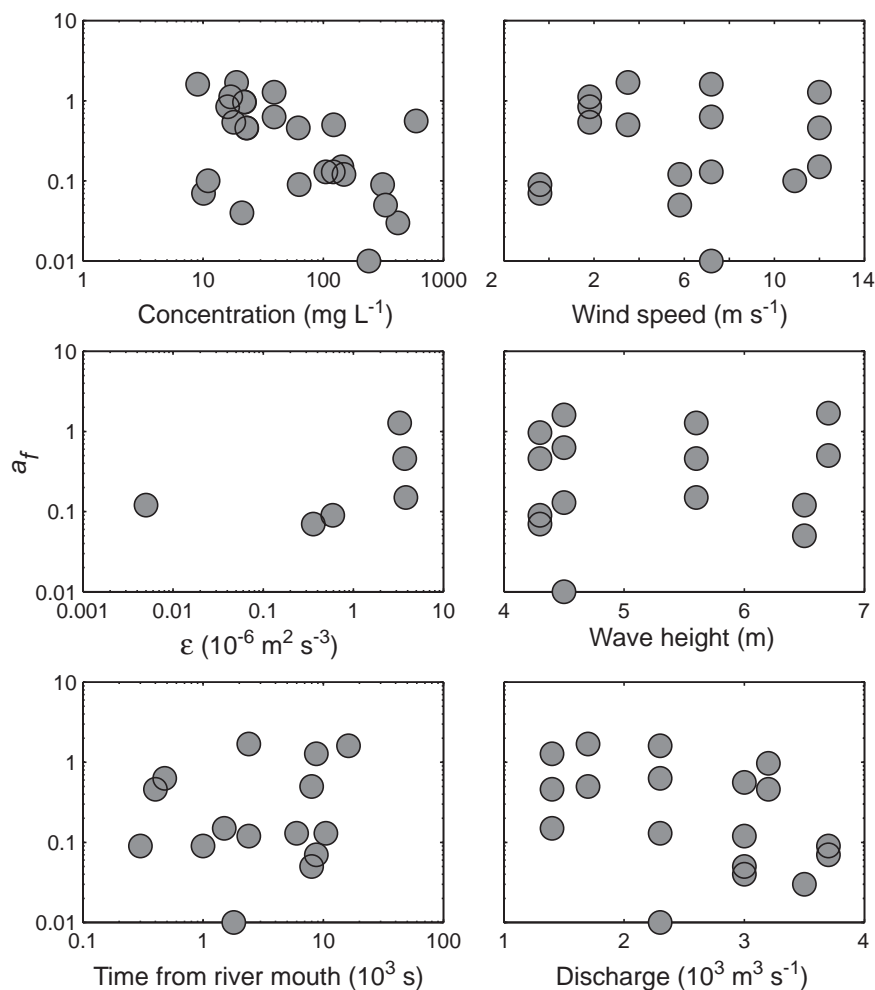


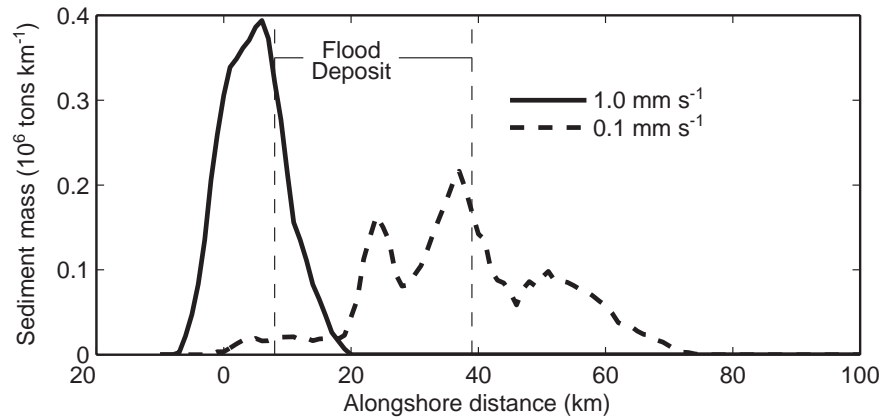
**Fig. 17** Aggregate fraction ( $a_f$ ) in the Eel plume versus various environmental variables. Variable  $\epsilon$  is turbulent-kinetic-energy dissipation rate at the depth of an image. Systematic variation is not observed. Fractions exceed unity in some cases, indicating that the drag law used to calculate aggregate mass overestimates drag for permeable aggregates. (Redrawn from Curran *et al.*, 2002a.)

was approximately 25 km. This distance exceeds somewhat the 15-km along-shelf position of the centres of mass of the flood layers, but this is to be expected because the e-folding distance describes the distance required for almost two-thirds of the sediment to fall from the plume. In general, this calculation indicates that sediment did not move much farther along-shelf after leaving the surface plume.

This relatively crude calculation for the along-shelf loss of sediment agrees with calculations for along-shelf distribution of sediment loss from the plume that were based on moored velocity measurements at K20 (Geyer *et al.*, 2000; Fig. 18). These authors modelled advection of sediment away from the river mouth for 10 days (10–20 January 1998) during a period of elevated discharge (Fig. 18). Along-shelf velocity as a function of depth below

the sea surface was based on ADCP measurements of water-column velocity profiles. The advective flux was assumed to be distributed evenly between the shore and the 40-m isobath. In one set of calculations, sediment was assigned a settling velocity of  $1 \text{ mm s}^{-1}$ , typical of aggregates. In another set, sediment was assigned a settling velocity of  $0.1 \text{ mm s}^{-1}$ , approximately equal to the observed effective settling velocity. In the model runs with settling velocity equal to  $1 \text{ mm s}^{-1}$ , sediment arrived at the seabed close to the river mouth. The position of maximum deposition was  $< 5 \text{ km}$  from the mouth (Fig. 18). In the calculations with settling velocity equal to  $0.1 \text{ mm s}^{-1}$ , sediment arrived at the seabed  $< 80 \text{ km}$  from the river mouth, with maximum flux at  $\sim 40 \text{ km}$  (Fig. 18). The flood deposits, interestingly, extended from  $\sim 5 \text{ km}$  to  $40 \text{ km}$  from the river mouth (Figs 10 & 11). Plume velocity, plume

**Fig. 18** Model estimates for along-shelf distribution of sediment leaving the Eel plume between 10 January and 20 January 1998. Calculations were carried out with two settling velocities:  $1 \text{ mm s}^{-1}$  (solid line) and  $0.1 \text{ mm s}^{-1}$  (dashed line). The peaks in the  $0.1 \text{ mm s}^{-1}$  curve record pulses in river discharge. (Redrawn from Geyer *et al.*, 2000.)



thickness and aggregation-influenced settling velocities therefore combined to deliver sediment to the seabed at an along-shelf position similar to the flood deposits. The subsequent bottom-boundary-layer processes that transported sediment from the nearshore region beneath the plume to the mid-shelf, where the deposits were found, probably did not produce substantial along-shelf advection of sediment.

Several processes that potentially affect plume transport of sediment were not well documented in the field. As already discussed, resuspension of plume-derived sediment in the surf zone probably retarded the removal rate of sediment from the plume. Data to support or refute this hypothesis directly were not available, however. The surf zone on the Eel margin during winter storms is wide and extremely energetic, making measurements of suspended-sediment concentration and vertical distribution nearly impossible. Tidal exchange with Humboldt Bay was not well documented either. As noted previously, enormous quantities of water flow in and out of Humboldt Bay with the tide. Given the position of the flood deposits directly offshore of the Bay mouth, it is possible that deceleration and deflection of the plume by waters flowing out of the Bay affected the fate of plume sediment during the floods. Unfortunately, measurements were not available to explore the effect of the Bay in any systematic fashion. Finally, laboratory experiments indicate that **convection** can speed the removal of sediment from hypopycnal plumes. In short, sediment concentration can build at the interface between the sediment-laden, relatively fresh fluid on the surface and the salty basin waters below. The build-up occurs because the density

gradient slows sediment sinking. If concentration grows large enough, then convection ensues, leaking sediment into the lower layer (Parsons *et al.*, 2001). This intriguing mechanism may speed the loss of fine sediment from river plumes, but observations did not resolve it in the field.

#### *Transport in the bottom boundary layer*

Boundary-layer measurements of velocity and sediment concentration collected with vertical arrays of current meters and optical backscatter sensors supported the conceptual model of transport proposed many years ago by McCave (1972). This view states that sediment is maintained in the bottom boundary layers by waves and that the sediment is advected by near-bottom currents.

Observations from the tripod at S60 clearly demonstrated the importance of waves (Ogston *et al.*, 2000; Fig. 19). Whenever concentration 30 cmab was elevated, wave orbital velocities were also large. A correlation between sediment concentration and current speed was not evident (Fig. 19). Waves, therefore, were the primary supplier of suspended sediment to the bottom boundary layer.

As on other margins, the importance of waves for supplying sediment to the bottom boundary layer gave storms overriding importance in determining sediment transport rates and pathways. The importance of storms was amplified by the common co-occurrence of elevated discharge and large waves (Figs 5–8). For example, in 1995–96, virtually all transport occurred during a 20-day period in winter. Almost three-quarters of the net along-shelf transport took place during just three storms (Ogston & Sternberg, 1999).

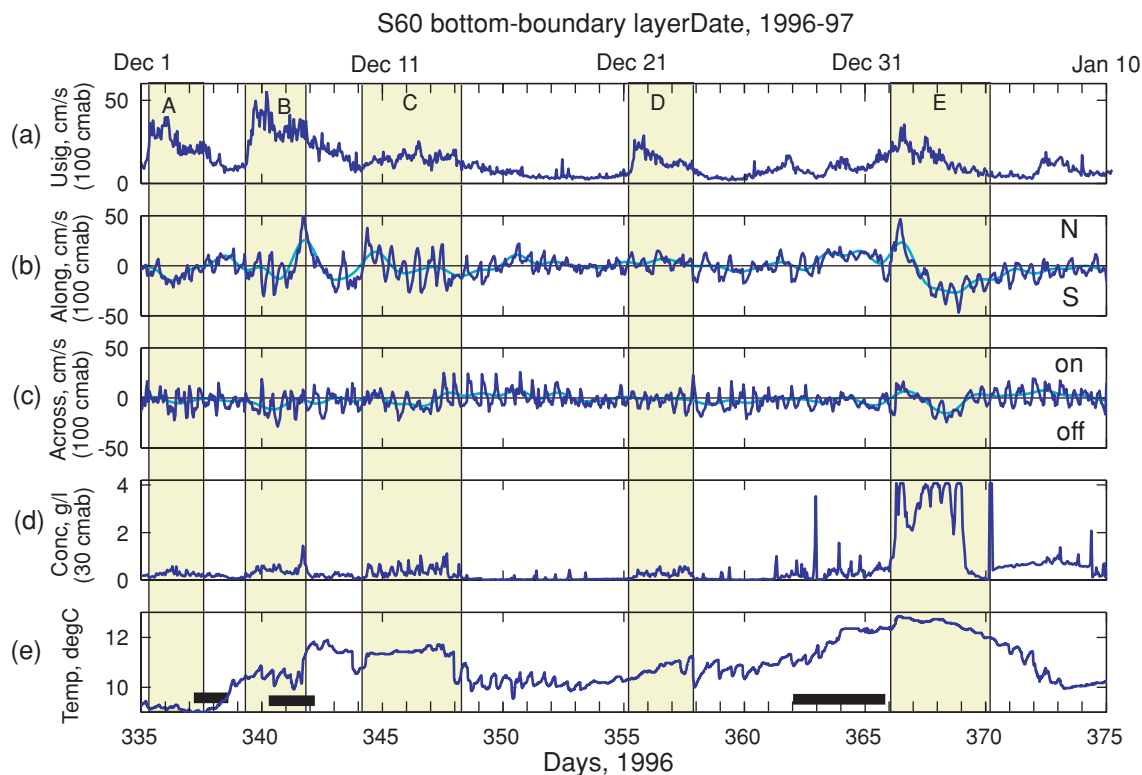


**Fig. 19** Time-series, bottom-boundary-layer data from a tripod at location S60. The hourly averaged data shown are: (a) significant wave orbital velocity; (b) mean along-shelf currents, with the blue line depicting mean current (positive to the north and along bathymetry) and the cyan line showing the low-frequency component; (c) mean across-shelf currents, with the blue line representing mean current (positive landward across bathymetry) and the cyan line representing the low-frequency component; (d) suspended-sediment concentration; (e) temperature. All instruments were located 100 cmab except for the suspended-sediment sensor (d), which was 30 cmab. Pale yellow bands (A, B, C, D, E) bracket periods of elevated suspended-sediment concentration. Black bars indicate periods of downwelling-favourable winds. (Redrawn from Ogston *et al.*, 2000.)

Waves alone generate little net transport because they are oscillatory; bottom currents fill that role. Bottom currents on the Eel followed a regular pattern during storms. At the beginning of storms, currents near the seabed in the vicinity of the flood deposit flowed north. After passage of the lows, along-shelf currents switched direction and flowed to the south (Cacchione *et al.*, 1999; Wright *et al.*, 1999; Fig. 19). This pattern of current reversal inhibited along-shelf dispersal during storms, helping to explain why the along-shelf positions of sediment loss from the plume and the flood layers were similar.

**Flow convergence** in the bottom boundary layer helps to explain the cross-shelf location of the flood deposits. In winter 1995–96, mean cross-shelf current velocity at S60 was seaward at  $2.5 \text{ cm s}^{-1}$ , but at S70 it was landward at  $0.5 \text{ cm s}^{-1}$  (Wright *et al.*, 1999). This near-bed convergence of flow presumably produced a net cross-shelf influx of

sediment to the boundary layer above the deposit, which in turn increased deposition rates there. Similarly, Ogston & Sternberg (1999) demonstrated that along-shelf velocity and suspended-sediment concentration in 1996–97 were correlated at low frequency, and they argued that large-scale oceanographic forcing contributes to accumulation of sediment in the flood deposits.

In summary, early tripod observations supported the generally accepted view of boundary-layer transport on wave-dominated margins. The comfortable fit between these observations and the accepted paradigm of shelf sediment transport was shaken profoundly by tripod observations made in the winter of 1997–98.

In winter 1997–98, the tripods at K60 and K20 collected data indicating that thin layers with high sediment concentrations occasionally appeared just above the seabed (Fig. 20). Furthermore, these layers apparently accounted for significant sea-

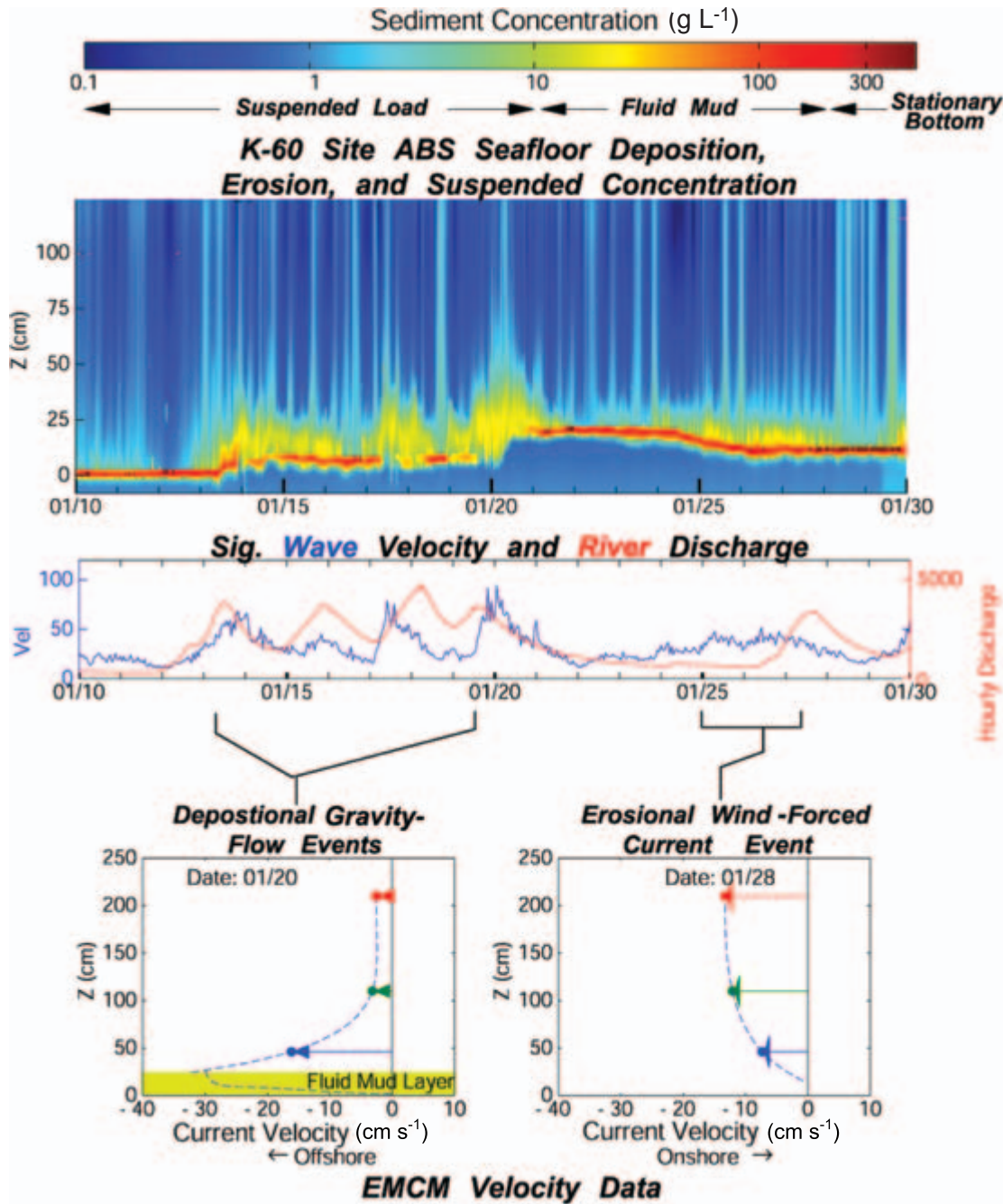


**Fig. 20** Data from a tripod at the K60 site that show an acoustic-backscatter record of deposition associated with gravity-flow events that occur during periods of high energy with sediment input from the Eel River. Velocity profiles clearly show the difference between gravity-flow events and events forced by mean currents. (From Traykovski *et al.*, 2000.)

ward transport as well as observed rapid changes in seabed elevation (Traykovski *et al.*, 2000). Close scrutiny of these occasional events at the K line in 1997–98, and at K63 and S60 in 1996–97 (Ogston *et al.*, 2000), led to the surprising conclusion that the near-bed layers were actually wave-supported

fluid muds that flowed cross-shelf under the influence of gravity.

The first observation that failed to conform to the conventional shelf sediment-transport paradigm was a rapid drop in the intensity of acoustic backscatter from an upward-looking ADCP deployed

50 cmab at K20 (Traykovski *et al.*, 2000). After the intensity drop, the instrument continued to collect data that looked reasonable. It appeared simply as if outgoing and returning acoustic pulses suffered significantly greater attenuation after the drop in acoustic intensity than before. This curious result led Traykovski *et al.* (2000) to consider the possibility that the instrument had been buried by fine sediment. Assuming relatively high porosities consistent with recently deposited muds, Traykovski *et al.* (2000) estimated that burial of the tripod by 2 m of mud was consistent with the observed decrease in acoustic backscatter intensity.

The burial hypothesis received support from acoustic-backscatter observations at K60 (Traykovski *et al.*, 2000; Fig. 20). Acoustic-backscatter sensors transmit sound pulses toward the seabed, and the intensity of return as a function of time is used to construct vertical profiles for sediment concentration down to the sediment–water interface. During periods of high wave energy, layers appeared that were ~10–15 cm thick. Concentrations within these layers were so high that normally strong acoustic returns from the seabed were obscured, indicating sediment concentrations in excess of  $10 \text{ kg m}^{-3}$ . These values are large enough to qualify the layers as fluid muds, that is, they were dense enough to flow downslope under the influence of gravity. Above these layers, estimated sediment concentrations decreased abruptly with height to values  $\sim 0.1 \text{ kg m}^{-3}$ . The steep concentration gradients at the top of the layers suggested that turbulence was suppressed by suspended-sediment stratification (Trowbridge & Kineke, 1994; Traykovski *et al.*, 2000).

Large changes in bed elevation accompanied the periods of elevated near-bed concentration (Traykovski *et al.*, 2000). During two events at K60 in 1998, the bed level increased by a total of 19 cm (Fig. 20). These depositional events occurred during periods of elevated wave orbital velocities, which was inconsistent with conventional transport models that predict net erosion when wave energy increases and net deposition when wave energy decays. Changes in bed height therefore also implicated alternative transport mechanisms in deposition of sediment on the Eel shelf.

The fingerprints of fluid muds were found at S60 and K63 as well (Ogston *et al.*, 2000). Following the January 1997 flood, an OBS located 30 cmab at S60 experienced sediment concentrations that

exceeded the maximum for which the instrument was designed (Fig. 19). The OBSs at 10 cmab and 23 cmab on the tripod at K63 also went off scale following the January 1997 flood. Ogston *et al.* (2000) estimated that near-bed sediment concentrations may have reached  $> 100 \text{ kg m}^{-3}$  at K63, and were  $\sim 10 \text{ kg m}^{-3}$  at S60. At K63, the elevated sediment concentrations led to a rapid 10–15 cm increase in bed elevation. Fluid muds, therefore, apparently formed near the seabed at several different times during the study period, and these times were associated with large waves and elevated river discharge.

Perhaps the most compelling evidence for fundamentally different transport dynamics during periods of elevated near-bed sediment concentration on the Eel shelf came from near-bed velocity profiles. When near-bed, high concentration layers were absent, velocity increased with distance above the seabed, as predicted by conventional wave-current boundary-layer theory (Fig. 20). When near-bed, high-concentration layers were present, however, velocity very close to the seabed was directed seaward, while higher in the water column velocities were smaller and at times even directed onshore (Traykovski *et al.*, 2000; Fig. 20). These inverted velocity profiles could not be explained with conventional boundary-layer theory. They could be explained by invoking gravity-driven seaward flow of sediment-laden layers (Ogston *et al.*, 2000; Traykovski *et al.*, 2000).

The final pieces of evidence implicating fluid muds in transport of sediment on the Eel shelf were Richardson numbers with near critical values. The **Richardson number**,  $Ri$ , is a dimensionless number equal to the ratio of stabilizing force of density stratification to the mixing force induced by velocity shear. In a sediment-stratified boundary layer, the Richardson number is defined by the equation

$$Ri = g' \frac{\partial C / \partial z}{(\partial u / \partial z)^2} \quad (8)$$

in which  $g'$  is modified gravity ( $\text{m s}^{-2}$ ),  $C$  is sediment volume concentration ( $\text{m}^3 \text{ m}^{-3}$ ) and  $u$  is fluid velocity ( $\text{m s}^{-1}$ ). When  $Ri$  is small, shear is sufficient to overcome the stabilizing effects of suspended-sediment stratification, so sediment diffuses upward under the influence of turbulent eddies. As  $Ri$  grows,

eventually shear cannot overcome suspended-sediment stratification, and upward diffusion of suspended sediment is hindered because of suppressed turbulence. The critical value of the Richardson number at which the transition occurs is 0.25 (e.g. Trowbridge & Kineke, 1994; Friedrichs *et al.*, 2000; Wright *et al.*, 2001).

Friedrichs *et al.* (2000) estimated  $Ri$  by using simultaneous measurements of velocity and suspended-sediment concentration. Calculations were made for a range of heights above bottom at S60 from January to March 1996 and at G65 from November 1996 to January 1997. They observed that whenever waves and suspended-sediment concentrations were large, the Richardson number equalled approximately 0.25. When waves were small,  $Ri$  was less than 0.25 (Friedrichs *et al.*, 2000). Based on these results, the authors argued that large waves provided enough sediment to the near-bed region via resuspension that Richardson numbers reached critical values. As the flow stratified, sediment became trapped near the bed in the wave boundary layer, unable to diffuse upward due to the suppression of turbulence. Limited upward diffusion allowed sediment concentrations to increase enough to induce downslope transport as gravity flows.

The bottom-boundary-layer observational programme provided clear evidence that dense fluid-mud suspensions can form and flow downslope on an open continental shelf, even in the absence of convergent flow at strong density fronts. This evidence supported directly the mechanism for across-shelf sediment transport hypothesized decades earlier (Moore, 1969). The surprising findings led to two lines of further investigation. First, the quantitative importance of gravity-driven near-bed transport was explored. Next, the mechanisms of formation, flow and deposition of near-bed dense suspensions were investigated, with an eye toward answering the question of why, for so long, this mode of transport had been discounted as not viable on open continental shelves.

In winter 1996–97 cross-shelf flux of sediment was dominated by the near-bed high concentration events following the January 1997 flood (Ogston *et al.*, 2000; Fig. 21). At S60, sediment flux 30 cmab exceeded the average annual flux by two orders of magnitude. Net sediment transport during the 3-day flood equalled 75% of the total annual transport

from the previous year. These calculations underestimated the total flux because they did not include the near-bed region where concentrations would have been highest but were not measured. Nonetheless, they clearly documented the dominance of high-concentration events in cross-shelf transport on the Eel margin (Ogston *et al.*, 2000).

Wright *et al.* (2001) indicated that the sediment concentration within a dense layer could be described adequately based on the critical Richardson number criterion (Parsons *et al.*, this volume, pp. 275–337). Using linear wave theory, the thickness of the layer and concentration within the layer were predicted as functions of water depth and wave properties. The gravitational downslope velocity was estimated by balancing frictional drag at the seabed against the gravitational force on the excess density of the high-concentration suspension. This balance was able to model the observed downslope velocities of 10–30 cm s<sup>-1</sup> at K60 in January 1998 (Fig. 20).

To predict the cross-shelf flux for a 2-week period of elevated discharge in January 1998, sediment was input to the K line based on an analysis of plume sedimentation (Geyer *et al.*, 2000). Sediment lost from the plume was placed in the inner-shelf wave boundary layer. It was then allowed to flow downslope with velocities predicted by the frictional/gravitational balance. For 10–24 January 1998 the model transported  $8 \times 10^4$  kg m<sup>-1</sup> of sediment past K60 (Traykovski *et al.*, 2000). Transport of this magnitude accounted for a large fraction of the sediment delivered to the shelf by the river and exceeded transport by the more conventional pathway of advection by near-bed currents. These results argue strongly that Moore's mechanism of cross-shelf transport of sediment by density underflows is not only viable but is also the dominant pathway for seaward transport on the Eel shelf. The dominance of gravity-driven near-bed transport on the Eel shelf raises the question of why Moore's hypothesis remained dormant for so long. This question can be reduced to two pertinent questions that have long been considered by sedimentary geologists in attempting to explain tempestites in the geological record (e.g. Myrow & Southard, 1996).

1 How can sediment concentrations grow large enough to induce downslope, gravity-driven transport

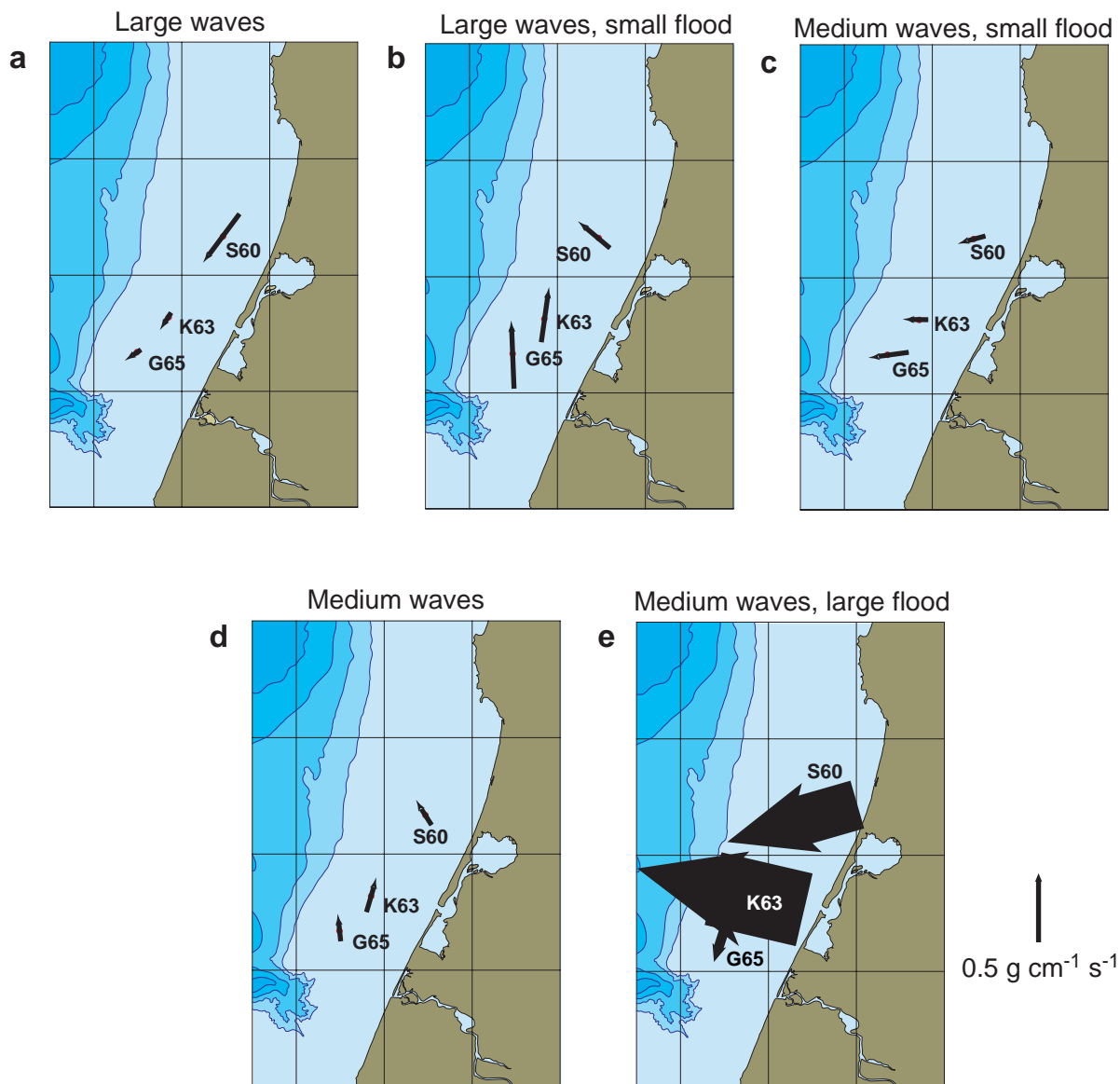


**Fig. 21** Vectors of time-averaged, vertically integrated sediment flux in the lower 120 cm of the water column during five transport events (a–e) in 1996–97 (shaded areas in Fig. 19). Vectors are scaled in length and width by the magnitude of the flux. (Redrawn from Ogston *et al.*, 2000.)

in the highly dispersive environment of a storm-wracked open continental shelf?

2 How can gravity-driven flows persist on the low gradients typical of continental shelves?

#### *Modelling of wave-supported fluid muds*

To produce large near-bed sediment concentrations on open continental shelves, there must be a large supply of easily resuspended sediment. In

the absence of strong density fronts, there also must be wave energy to resuspend that sediment. Under these conditions, especially in the absence of strong currents that cause sediment to diffuse out of the wave boundary layer, sediment concentration within the wave boundary layer can grow large enough to induce suspended-sediment stratification (Friedrichs *et al.*, 2000). Stratification retards upward turbulent diffusion of sediment, but it also reduces the transmission of turbulent,

wave-induced stress to the seabed. As a result, suspended sediment starts to deposit. Deposition reduces stratification, increases stress and leads to resuspension. This negative feedback is responsible for keeping Richardson numbers near critical when waves are large and sediment is available (Friedrichs *et al.*, 2000). These conditions apparently occurred frequently on the Eel shelf due to the co-occurrence of precipitation, high discharge and large waves. Plume-derived sediment loaded the wave boundary layer either by direct sedimentation or by storm resuspension after temporary deposition on the seabed.

The earlier failure of continental shelf sedimentologists to recognize fluid muds in open shelf settings is attributable to the fact that the layers are thin, generally residing below the lower-most sediment sensors on tripods. Without data from downward-looking ABSs, the gravity-driven flows arguably would have been missed on the Eel shelf. Perhaps such flows exist elsewhere and simply have not been observed due to limits of instrumentation. Counter to this hypothesis is the argument that the Eel shelf is at present particularly well suited to producing gravity-driven flows, because of simultaneous production of large sediment discharge by a river and large waves by storms (Wheatcroft & Borgeld, 2000). High-resolution boundary-layer observations on other river-influenced shelves will help to resolve this issue.

Another issue that caused Moore's (1969) hypothesis to languish was concern over how gravity currents were maintained on continental shelves, which have small bathymetric gradients. A source of stress at the seabed is required to maintain the suspended sediment in a gravity-driven flow. A suspension flowing downslope under the influence of gravity generates stress on the seabed, and if the flow is fast enough, stress imparted to the seabed is large enough to maintain sediment in suspension (Bagnold, 1962). The small gradients typical of continental shelves cannot support this so-called **autosuspension** because bathymetric gradient affects the magnitude of downslope-directed gravitational force on a dense suspension.

Wright *et al.* (2001) demonstrated this argument quantitatively by making use of the critical Richardson number concept. They reformulated the Richardson number into a bulk parameter ( $Ri_B$ )

defined by the equation (Trowbridge & Kineke, 1994)

$$Ri_B = \frac{(B/\ell^2)}{(U_{\max}/\ell)^2} \quad (9)$$

In Eq. 9,  $B$  is the vertically integrated buoyancy anomaly ( $\text{m}^2 \text{s}^{-2}$ ), and  $U_{\max}$  is the maximum near-bed velocity ( $\text{m s}^{-1}$ ). The buoyancy anomaly,  $B$ , is defined by

$$B = \int_0^\ell g' C dz \quad (10)$$

and  $\ell$  is the height of the top of the dense layer. The term  $U_{\max}$  is defined by

$$U_{\max} = (U_w^2 + U_g^2 + V_c^2)^{1/2} \quad (11)$$

where  $U_w$  is the near-bed velocity associated with waves,  $U_g$  is the near-bed velocity associated with the gravity current itself and  $V_c$  is the near-bed along-shelf current velocity. Under the condition of  $U_g \gg U_w, V_c$ , Eq. 9 reduces to

$$Ri_B = \frac{B}{U_g^2} \quad (12)$$

Invoking a balance between frictional drag at the seabed and the gravitational force on the dense suspension,  $U_g$  can be written

$$U_g = \sqrt{B \sin \theta / C_D} \quad (13)$$

where  $\theta$  is the angle between the seabed and a horizontal line, and  $C_D$  is a dimensionless drag coefficient with a typical value  $\sim 0.003$ . Substituting Eq. 13 into Eq. 9 arrives at an expression for the bulk Richardson number of

$$Ri_B = \frac{C_D}{\sin \theta} \quad (14)$$

When ample sediment is available for resuspension, the bulk Richardson number takes a value of 0.25, and Eq. 14 can be solved for critical angle. The value is  $0.7^\circ$ . On seabeds with smaller bathymetric gradients, gravity currents flow too slowly to maintain sediment in suspension, deposition

occurs, and the current stops. Larger gradients allow gravity flows to maintain sediment in suspension and flow indefinitely (Wright *et al.*, 2001).

The gradient of the Eel shelf apparently precludes gravity-driven transport, if the role of waves and currents in resuspending sediment is neglected. Wright *et al.* (2001) pointed out that when  $U_{\max}$  is enhanced by waves or currents, gravity-driven currents can be maintained on lower gradients. So, the ideal conditions for gravity-driven sediment transport on open shelves are strong waves and/or currents with a large supply of easily resuspended sediment.

The concepts of critical Richardson number and wave-supported near-bed dense suspensions can be extended to a consideration of depositional dynamics. Maximal cross-shelf flux according to this conceptual model can be expressed as (Wright *et al.*, 2001; Scully *et al.*, 2002)

$$Q_{\text{gmax}} = \frac{\alpha \rho_s U_{\max}^3}{4C_D g'} \quad (15)$$

where  $Q_{\text{gmax}}$  is the maximal gravity-induced cross-shelf flux ( $\text{kg m}^{-1} \text{s}^{-1}$ ),  $\alpha$  is the bathymetric gradient, and other variables are as defined previously. The flux of sediment to the seafloor is defined by the cross-shelf gradient in  $Q_{\text{gmax}}$ :

$$-\frac{\partial Q_{\text{gmax}}}{\partial x} = -\frac{\rho_s}{16C_D g'} \frac{\partial \alpha U_{\max}^3}{\partial x} \quad (16)$$

Under the simplifying assumption that  $U_{\max}$  is set entirely by monochromatic waves impinging on the shelf, Eq. 16 can be solved:

$$J_g = \frac{\rho_s}{16C_D g'} \frac{\alpha^2 U_{\max}^3}{h} \left[ \frac{3kh}{\tanh kh} - \frac{h}{\alpha^2} \frac{\partial \alpha}{\partial x} \frac{(2\beta^2 + 1)}{(1 - \beta^2)} \right] \quad (17)$$

In Eq. 17,  $J_g$  is sediment flux to the seabed from the gravity current,  $k$  is wave number ( $\text{m}^{-1}$ ),  $h$  is water depth and  $\beta$  equals  $\alpha/16C_D$  (Scully *et al.*, 2002).

Equation 17 indicates that the sediment flux to the seafloor under wave-supported gravity-driven flows depends strongly on wave energy. Furthermore, it demonstrates the importance of water depth and bathymetric gradient. The first term inside the brackets originates from the seaward

decay in wave orbital velocity near the seabed. It always favours deposition. It also indicates that, at some water depth, the flux becomes insignificant. The second term inside the brackets characterizes the effect of bathymetric gradient. It favours deposition when the gradient decreases in the seaward direction, and erosion when the gradient increases seaward. In other words, concave slopes are depositional and convex slopes are erosional (Scully *et al.*, 2002).

Scully *et al.* (2002) evaluated the predictive capabilities of the above model by comparison with data from the tripods. First, they compared predicted and observed cross-shelf velocities at S60 for January 1997 and at K60 for January 1998. The predictions assumed that all cross-shelf transport was by wave-supported, gravity-driven flows. During periods of low discharge, predictions failed to match observations. During periods of elevated discharge from the river, however, predicted and observed velocities were well correlated. These results suggest that the wave-supported, gravity-driven model of cross-shelf flow captures the underlying physics, but only when enough sediment is available to stratify flow within the wave boundary layer. During low discharge periods, conventional boundary-layer transport by the combined effects of waves and currents dominates.

Scully *et al.* (2002) also compared predicted deposition with mid-shelf cores collected after the floods in January and March 1995 and January 1997, as well as with the observed timing and magnitude of changes in bed elevation observed with the ABS at K60 in 1998. The model was successful in this test as well, and highlighted an important behaviour of wave-supported, gravity-driven flows: rapid deposition coincides with short periods of highest wave energy associated with storms, because deposition depends on the cube of  $U_{\max}$ . As a result, even though the January 1997 flood had the highest estimated sediment discharge, the January 1995 flood had the thickest mid-shelf deposit because it had the greatest associated wave energy. This counter-intuitive result was further highlighted in 1998, when, in spite of large wave orbital velocities, no erosion was observed or predicted at K60, and significant deposition occurred.

Scully *et al.* (2003) created a numerical model of wave-supported, gravity-driven flows on the Eel shelf in order to compare observed and pre-

dicted spatial distribution of flood deposits for the various years of observation. The conversion to a numerical model made it possible to include realistic shelf geometry and along-shelf variation in sediment supply in the analysis. The numerical model produced thicknesses and along- and across-

shelf distributions of flood sediment that agree in general with observed deposit geometries (Fig. 22). Maximal mid-shelf deposition was predicted between 10 km and 30 km north of the river mouth in water depths of ~50–70 m. The predicted deposits extended along-shore for ~40 km and seaward to

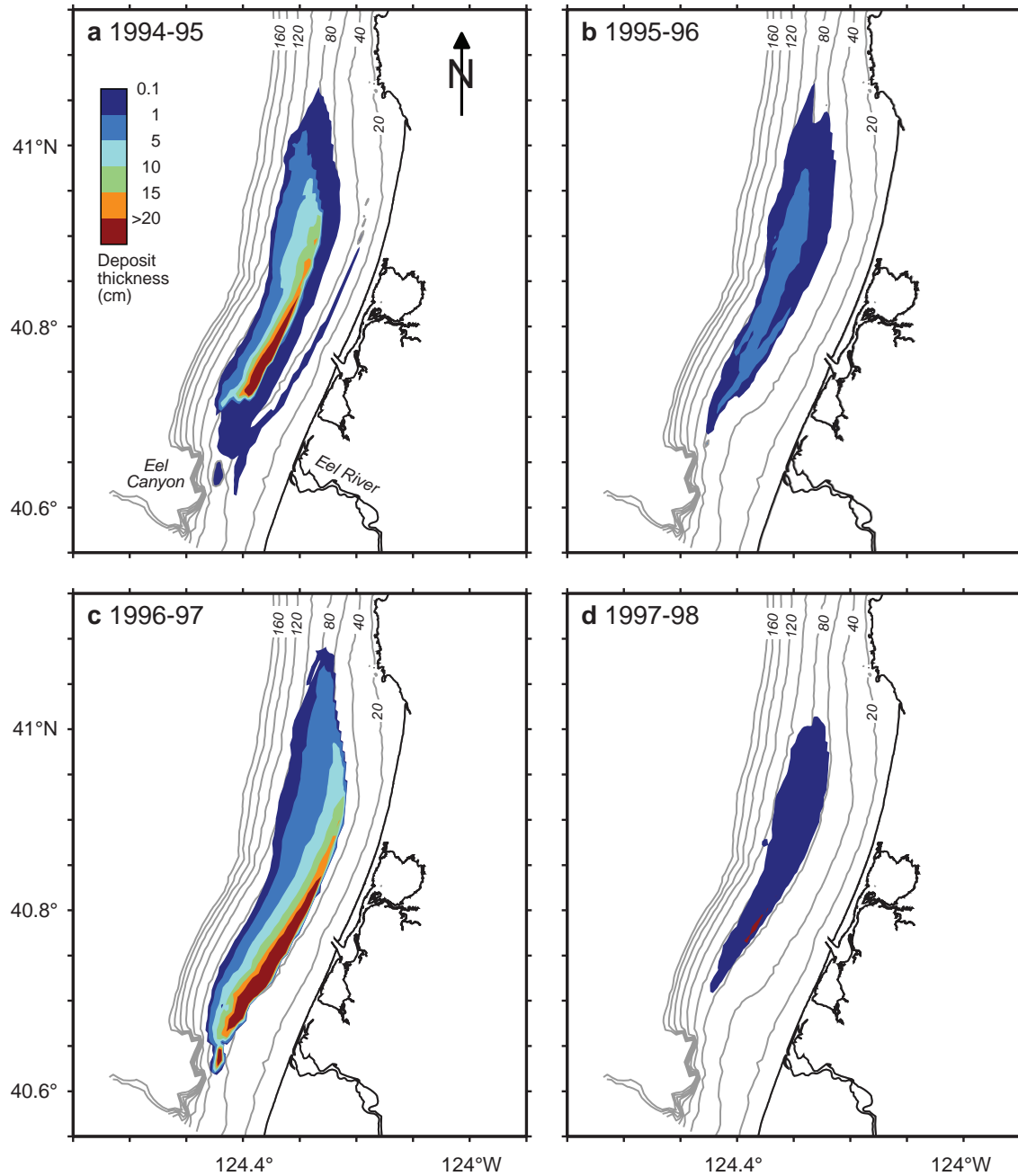


**Fig. 22** Predicted wave-supported, gravity-driven deposit thicknesses for four winters. Thicknesses are based on an assumed porosity of 0.75. (Redrawn from Scully *et al.*, 2003.)

the 100-m isobath. Following the floods of 1995 and 1997, predicted mid-shelf deposition agreed favourably with observations, accounting for roughly 29% and 39% of the sediment discharge, respectively. The model predicted significantly less mid-shelf deposition during 1995–96 and 1997–98 when only 16% and 3% of the sediment load, respectively, was predicted to deposit on the mid-shelf. The agreement between the model's predictions and observations is encouraging, and suggests that the physics of wave-supported, gravity-driven flows underlie observed patterns of flood sediment deposition on the Eel shelf.

The results of Scully *et al.* (2003) suggest that the along- and across-shelf position of the flood deposits was controlled both by the across-shelf morphology and by sediment delivery rate to the wave boundary layer. Across-shelf position was determined by water depth, wave energy and bathymetry. The seaward limit of deposition was determined by both the seaward decline in wave energy, which limited rate of supply from shoreward portions of the shelf, and the increasing convexity of the shelf profile, which caused bypassing of available sediment. Similarly, the convex morphology near the river mouth limits gravity-driven mid-shelf deposition despite the high inshore sediment delivery. Greatest mid-shelf deposition was consistently predicted and observed to occur north of the river mouth because the mid-shelf is concave in this region.

Moore's (1969) hypothesis that wave-supported, gravity-driven flows moved sediment across the continental shelf languished for so long primarily because of a lack of understanding of suspended-sediment stratification. Stratification limits turbulent diffusion out of the wave boundary layer, thereby allowing sediment concentration near the bed to build to extraordinary levels whenever sediment is abundant and waves are large enough to resuspend it. Under these conditions, suspensions move downslope, even when the bathymetric gradient is small. Moore's (1969) ideas were bred of compelling geophysical observations, but his proposed mechanisms of transport did not fit the understanding of boundary-layer hydrodynamics during his day. Only when direct physical observations failed to conform to accepted boundary-layer theory did it become clear that other physical processes were at work.

### Fate of missing sediment

Seabed observations indicate that only ~25% of the mud delivered by the river to the shelf accumulates in the mid-shelf flood deposit. So, while the plume and shelf boundary-layer observations on the Eel margin paint a novel and compelling picture of how sediment is delivered to the flood deposit, they leave unresolved the fate of the majority of the mud emanating from the river. A variety of studies conducted as part of the overall programme shed some light on the fate of the missing sediment.

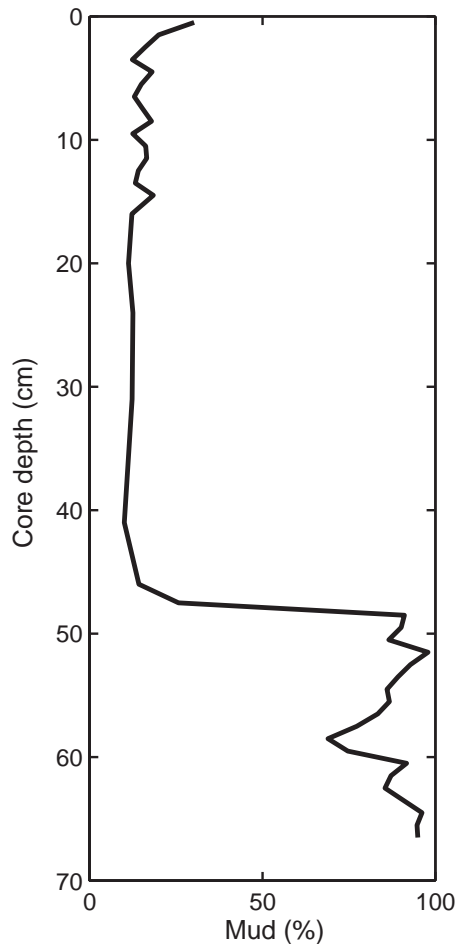
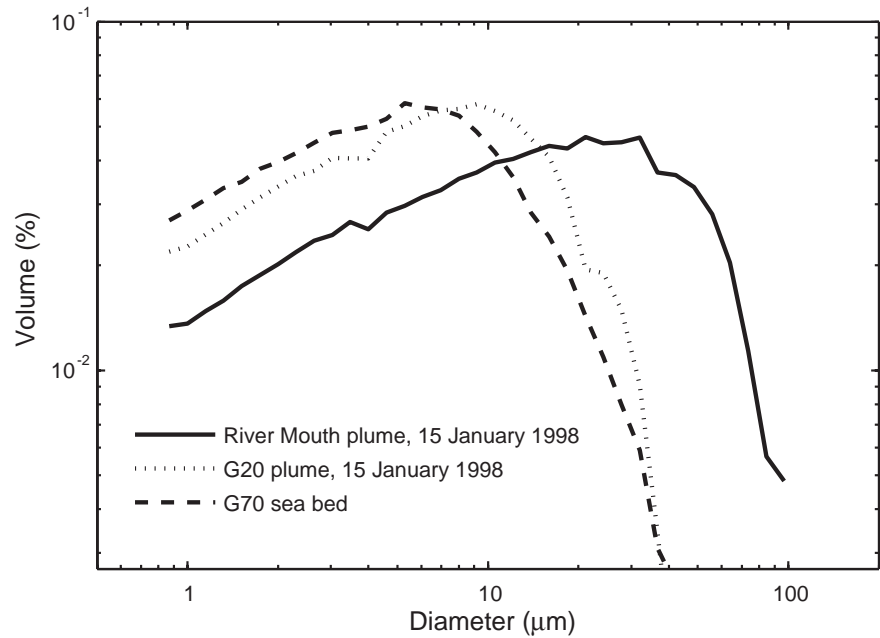
#### *Inner-shelf storage*

Inner-shelf storage may account for some of the missing sediment, but it is difficult to quantify because of the energetic nature of the environment in shallow water depths. Breaking waves make near-bed observations difficult. Extensive sediment reworking by waves complicates the interpretation of cores. Nonetheless, studies of sediment grain size in the Eel plume, and limited coring, both suggest that inner-shelf storage does trap some flood sediment.

The disaggregated inorganic grain-size distributions gathered in the plume at the river mouth and at the 20-m isobath on the G line indicate that coarse silt sank rapidly from the plume in the vicinity of the river mouth (Fig. 23). At the mouth, approximately 15–20% of the suspended load was coarser than 30  $\mu\text{m}$ , yet by the G line only about 1% of the grains in suspension were so large. This coarse silt does not appear in the flood deposit. The surficial-sediment grain-size distribution at G70 following the January 1997 flood was similar to the plume grain-size distribution at the 20-m isobath. It contained few grains coarser than 30  $\mu\text{m}$ . These observations reveal rapid dumping of coarse silt and sand near the river mouth. This material was presumably redistributed by waves in shallow water. It did not follow the same transport pathway as the finer plume sediment, which moved across shelf to the flood deposit.

Cores demonstrated that muds as well as sands can accumulate on the inner shelf. In a core from I45, a mud-rich layer was detected 45 cm below the surface (Fig. 24; Crockett & Nittrouer, 2004). Based on an analysis of  $^{137}\text{Cs}$  and  $^{210}\text{Pb}$ , the mud layer probably formed during the massive 1964

**Fig. 23** Disaggregated inorganic grain-size distributions from the Eel margin. Percentage volume concentration versus diameter is shown for the plume at the river mouth (solid line) and at G20 (dotted line) on 15 January 1998. The dashed line shows the size distribution in the January 1997 flood deposit at G70. Coarse silt and sand are lost from the plume between the river mouth and G20.



flood (Crockett & Nittrouer, 2004). The results of Scully *et al.* (2002) suggested that even during the relatively energetic January 1997 flood, more sediment was supplied to the inner shelf than could be removed by gravity-driven transport. This notion that mud can accumulate in the energetic nearshore environment of the inner Eel shelf was supported by observations of measurable  $^7\text{Be}$  in grab samples collected from 30–50-m water depths in 1997 (Sommerfield *et al.*, 1999). Crockett & Nittrouer (2004) estimated that up to 10% of the mud delivered to the shelf by the Eel may end up in the predominantly sandy deposits of the inner shelf.

The accumulation of mud in energetic nearshore environments may appear paradoxical. However, whenever supply of mud overwhelms the ability of waves, currents, or gravity to remove it, mud can deposit (McCave, 1972). Periods of large supply, i.e. floods, clearly are required on the energetic Eel shelf. Low wave energy during high discharge, although rare, would further enhance the potential for mud deposition on the inner shelf.

**Fig. 24** (left) Mud (silt and clay) percentage versus depth in core at I45. The abrupt increase in mud percentage at ~45 cm core depth is interpreted as a deposit from the 1964 flood on the Eel River. (Redrawn from Crockett & Nittrouer, 2004.)

*Along-shelf bypassing*

A significant fraction of sediment may have bypassed the Eel shelf in the along-shelf direction. Two factors favour along-shelf bypassing. First, resuspension in the surf zone reintroduces sediment into the northward flowing plume, thus retarding sedimentation losses from the plume (Curran *et al.*, 2002a). Direct evidence for this mechanism is lacking, but it does help to explain the relatively low values for effective settling velocity in the plume. Visual observations from the helicopter on one plume survey revealed a sediment-laden plume streaming past Trinidad Head at the northern limit of the Eel shelf.

The second factor that favours along-shelf bypassing is sediment stranding within the plume. Sediment aggregation rate in a suspension is a second-order function of sediment concentration. As concentration falls due to sedimentation and dilution, aggregation rate slows markedly. Eventually, aggregation time-scales grow so long that aggregation no longer affects sinking dynamics (Curran *et al.*, 2002b). The remaining fine sediment, with its low, single-particle settling velocities, stays in the plume for long periods before sinking out. The **stranded** sediment can be transported great distances (e.g. Geyer *et al.*, 2000). This process explains the common appearance on satellite images of large sediment plumes emanating from river mouths that account for only a small fraction of the sediment delivered to the coastal ocean by the river (Mertes & Warrick, 2001). The stranded sediment possesses a distinct optical signature visible to satellite sensors, yet these plumes may carry only 1–2% of the total sediment load.

Measurements from the STRATAFORM programme do not place tight constraint on the quantity of sediment exported north of the Eel shelf by the plume. Geyer *et al.* (2000) used observations at the K line to estimate that 30–40% of the Eel's load was transported more than 10 km beyond the river mouth in the along-shelf direction, but Mertes & Warrick (2001) indicated that far-field plumes contain a much smaller fraction of a river's initial sediment load. More observations are required to resolve the fate of mud that does not sink from plumes in the immediate vicinity of river mouths.

*Transport from shelf to slope*

Flood-derived sediment may have been transported beyond the shelf to the slope. Observations of water-column light attenuation and deposition rates of sediment in traps and on the seafloor suggest that sedimentation on the open slope during the study period was comparable in magnitude with inner-shelf storage, and may in fact have rivalled accumulation in the flood deposit (Alexander & Simoneau, 1999; McPhee-Shaw *et al.*, 2004).

A series of water-column transmissometer profiles was collected over the Eel shelf and slope in 1996 and 1998–99 (McPhee-Shaw *et al.*, 2004). These surveys documented the common occurrence of **intermediate nepheloid layers** (INLs), which are layers of fluid with higher sediment concentration than surrounding water, and which extend from the margin into the basin interior. Some of the observed layers originated from mid-shelf depths similar to the depth of the flood deposits. Others detached from the continental slope in water depths > 150 m, i.e. beyond the shelf break. The shelf INLs had sediment concentrations as much as  $0.012 \text{ kg m}^{-3}$  above background, and they extended as far as 25 km into the basin from their detachment points. The slope INLs carried less sediment and only extended basinward 3–8 km. The shelf INLs were prevalent during periods when waves were large and winds were favourable for downwelling. These conditions were associated with winter and spring. Slope INLs showed no marked seasonal variability, although they were most pronounced in August. These differences suggest different mechanisms of formation of INLs on the shelf and slope.

The detachment of shelf INLs over the mid-shelf mud deposit and the correlation of INLs with large waves and downwelling point to wave resuspension of recently deposited flood sediments as a likely source for shelf INLs (McPhee-Shaw *et al.*, 2004). Observations from the tripod at K60 in 1998 revealed the removal of flood sediment by wave resuspension, thereby supporting the hypothesis of wave resuspension as a source for INLs (Traykovski *et al.*, 2000). By estimating typical concentrations and spatial scales of shelf INLs, McPhee-Shaw *et al.* (2004) proposed that approximately 10% of the total annual load of the Eel could be transported from the shelf to the slope by shelf INLs.

The lack of seasonal variability in slope INLs adjacent to the highly seasonal Eel shelf suggests that slope INLs are decoupled from shelf processes (McPhee-Shaw *et al.*, 2004). Their formation is more likely to be tied to resuspension by internal tides. The stratification of the water column at the shelf edge of the Eel margin is such that over a range of depths on the upper slope, energy associated with M2 internal tides propagates upslope parallel to the seabed (Cacchione *et al.*, 2002; MCPhee-Shaw *et al.*, 2004). The propagation leads to intensification of near-bed flow, probably strong enough to cause sediment resuspension. In general, slope INLs appeared where bathymetric gradients favoured this focusing of internal-tide energy (McPhee-Shaw *et al.*, 2004). Also in these regions, seabed grain sizes are relatively coarse (Alexander & Simoneau, 1999), suggesting active winnowing of surficial sediments.

Shelf-to-slope transport of fluvial sediment helps to explain sediment-trap data on the Eel slope. From September 1995 to January 1997, a mooring carrying three sediment traps was deployed in 450 m of water on the Y line, 50 km north of the river mouth (Walsh & Nittrouer, 1999). The traps were located at depths of 60 m, 220 m and 435 m. Flux to the traps was predominately lithogenic sediment, accounting for 53%, 70% and 83% of the flux to the top, middle and bottom traps, respectively. Sediment flux was greater than on other open slopes, and it was episodic. For example, six of 33 sampling intervals accounted for more than 50% of the flux to the middle trap. Walsh & Nittrouer (1999) argued that the episodic flux implicated INLs as an important transport pathway for Eel River sediment crossing the continental shelf. The timing and magnitude for pulses of sediment flux on the slope varied with sediment resuspension by waves, river discharge and shelf circulation (Walsh & Nittrouer, 1999). These results are consistent with those from the water-column surveys of light attenuation (McPhee-Shaw *et al.*, 2004).

The appearance of  $^7\text{Be}$  in slope sediments lends credence to the hypothesis that river-derived sediment can be transported rapidly across the shelf to the upper slope of the Eel margin. Following the January 1997 flood, and at no other time during the 394-day observation period, the middle sediment trap at Y450 contained measurable  $^7\text{Be}$  (Walsh & Nittrouer, 1999). Similarly, following the January

1995 flood and again after the January 1997 event,  $^7\text{Be}$  was detected in cores collected on the upper slope (Sommerfield *et al.*, 1999). Detection of  $^7\text{Be}$  in upper slope sediments reveals rapid bypassing of the continental shelf by a significant amount of Eel sediment (Sommerfield *et al.*, 1999), because the half-life of  $^7\text{Be}$  is only 53.3 days and its source in coastal waters is primarily terrestrially derived sediments. Furthermore, the modelling results of Scully *et al.* (2003) suggested that significant gravity-driven transport of flood-derived sediment can reach the upper slope following floods that have large associated wave energy, and this transport may account for a significant fraction of the total fine sediment input.

Other radionuclides can be used to constrain whether short- and long-term loss rates of sediment from the shelf to the slope are similar. The amount of sediment bypassing the shelf to the slope over decadal time-scales was estimated by Alexander & Simoneau (1999), who used  $^{210}\text{Pb}$  and  $^{137}\text{Cs}$  to constrain sediment accumulation rates in 60 cores collected from a range of depths on the upper slope. Accumulation rates were relatively high for the open slope, ranging from 0.2 to 1.3  $\text{g cm}^{-2} \text{yr}^{-1}$ . These high accumulation rates indicate that over longer time-scales, redistribution of fluvial sediment is widespread. When integrated across the slope and through time, these accumulation rates can account for as much as 20% of the sediment discharge of the river (Alexander & Simoneau, 1999). These various slope studies on the Eel margin, despite the fact that they address sediment loss from shelf to slope on different time-scales, agree that 10–20% of the discharge reaches the slope. Together, deposits on the inner shelf, the mid-shelf, and the slope may account for approximately half of the sediment discharged by the Eel.

#### *Transport to the Eel Canyon*

Coring studies conducted in the Eel Canyon implicate down-canyon losses as a major sink for sediment delivered to the Eel shelf (Mullenbach & Nittrouer, 2000; Mullenbach *et al.*, 2004). Cores were collected from the canyon in January and March 1998. Profiles of  $^7\text{Be}$  and  $^{210}\text{Pb}$  were generated from each core. The winter of 1998 was characterized by large waves and multiple moderate discharge events starting in mid-January. January cores, which

were collected prior to the onset of flooding on the river, exhibited only slightly elevated  $^7\text{Be}$  in the top 1 cm and no detectable  $^7\text{Be}$  below. In the top 2 cm of the January cores,  $^{210}\text{Pb}$  was depleted slightly. March cores, by contrast, contained significantly elevated  $^7\text{Be}$  inventories down to 8-cm depth in core. Profiles of  $^{210}\text{Pb}$  activity were non-steady state, suggesting rapid episodic accumulation of sediment. Finally, cores collected in March contained more clay in surface sediments than did the January cores. These differences suggest that thick layers of flood sediment can form annually in the Eel Canyon. This hypothesis is supported by the modelling of Scully *et al.* (2003) that predicted a significant gravity-driven flux into the canyon following floods of the Eel River. Over  $2.0 \times 10^8$  kg of sediment was predicted to enter Eel Canyon during the January and February floods of 1998, potentially explaining the presence of  $^7\text{Be}$  observed in the cores collected in March 1998.

The inventory of  $^7\text{Be}$  decreased downward through the top 8 cm of the March cores. This distribution differed from cores taken in the flood deposit on the shelf, in which  $^7\text{Be}$  was constant to the bottom of distinct flood layers but then decreased abruptly. This pattern of  $^7\text{Be}$  in canyon cores suggests that the tops of cores taken in March comprised mixtures of older shelf sediment and recently discharged muds that were emplaced throughout the winter. The recently discharged sediment, with high  $^7\text{Be}$ , became more abundant through the course of the winter. Emplacement was likely to have been episodic and associated with periods characterized by large waves (Mullenbach & Nittrouer, 2000).

Deeper in the cores collected from the Eel Canyon head were two to three layers characterized by fine sediment and depleted  $^{210}\text{Pb}$ . These properties are consistent with rapid emplacement of fluvially derived sediment. The layers therefore probably record periods of enhanced sedimentation associated with past floods (Mullenbach & Nittrouer, 2000). Although the unsteady  $^{210}\text{Pb}$  profiles made it difficult to constrain accumulation rates, minimum rates of  $0.4 \text{ cm yr}^{-1}$  were required to explain the presence of excess  $^{210}\text{Pb}$  at the bottom of the cores. Using this value to reconstruct the accumulation rate of the fine-grained layers led to the conclusion that a large fraction of the sediment delivered by the Eel River is transported from shelf

to slope through the canyon, potentially closing the sediment budget. This intriguing result is poorly constrained due to a lack of core coverage and time control within the cores, yet it clearly implicates down-canyon transport as a major sediment sink.

Near-bed observations at the head of the Eel Canyon suggest that Moore's (1969) proposed mechanism for transport of sediment into canyons is sound. From January to April 2000 a tripod was deployed in 120 m of water in the northern thalweg of the Eel Canyon (Puig *et al.*, 2003, 2004). The tripod carried two current meters located at 30 cmab and 100 cmab, a pressure sensor, a sonic altimeter, two OBSs at the same heights as the current meters and a seabed-imaging video camera. Unfortunately, the OBSs failed, making estimation of suspended-sediment concentration difficult. To fill this void, camera opacity was used as a proxy for suspended-sediment concentration.

Tripod data showed clearly that elevated camera opacity, and by implication suspended-sediment concentration, was correlated with large waves and not with Eel River discharge (Fig. 25; Puig *et al.*, 2003, 2004). When opacity was so high as to render images black for several hours, velocity was larger near the bed, as observed with wave-supported, gravity-driven flows on the shelf (Fig. 25). Waves were implicated in the maintenance of the dense suspension by fluctuations in down-canyon current at the same frequencies as fluctuations in pressure. Puig *et al.* (2004) argued that these observations demonstrated that waves liquefied fine sediment at the canyon head and that the sediment flowed down-canyon as wave-supported, gravity-driven underflows (Lee *et al.*, this volume, pp. 213–274; Parsons *et al.*, this volume, pp. 275–337).

The crude sediment budget presented here relies on a small number of observations and uses tools with intrinsically different time-scales. It must be regarded, therefore, as highly speculative. Nonetheless, the estimates of accumulation rate in the various regions produce a relatively consistent, closed sediment budget. Inner shelf storage accounts for 10% of the annual discharge of fine sediment by the river. The mid-shelf flood deposit contains 20–25%, and the slope stores 10–20%. An unknown quantity of sediment exits the Eel margin to the north, carried by the buoyant coastal current. This loss term probably amounts to a few per cent of the Eel discharge. If along-shelf export

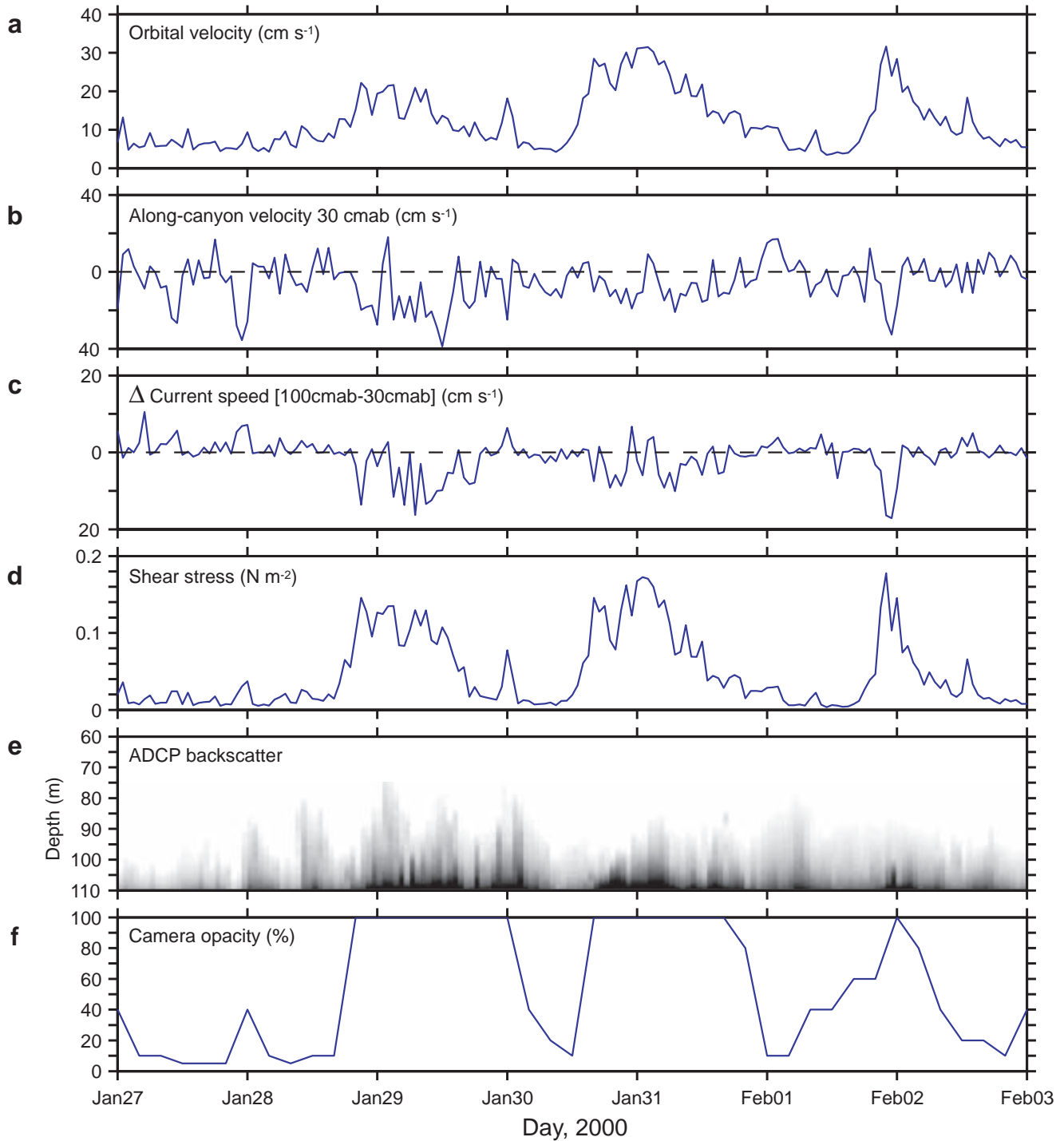


**Fig. 25** Tripod measurements from the head of the Eel Canyon in 2000. (a) Wave orbital velocity. (b) Along-canyon velocity at 30 cmab, with positive values corresponding to up-canyon flow. (c) Difference between along-canyon current velocities at 100 and 30 cmab. (d) Boundary shear stress. (e) Intensity of acoustic backscatter measured by an ADCP as a function of height above bottom. Darker greys indicate higher sediment concentration. (f) Opacity on a seabed-imaging video camera. High opacity indicates dark images caused by high suspended-sediment concentration. Three periods of elevated wave orbital velocities (a) and shear stresses (d) were accompanied by increased acoustic backscatter near the seabed (e) and periods of large camera opacity (f), reflecting increased suspended-sediment concentration. During these periods, near-bed flow was directed down the canyon (b), and flow was faster at 30 cmab than it was at 100 cmab (c). These results indicate that sediment resuspension from waves resulted in formation of gravity-driven flows. (Redrawn from Puig *et al.*, 2004.)

beyond the margin is assigned a value of 5% of the discharge, 45–55% of the Eel's load must be accounted for. This quantity is similar to the estimated storage of sediment in the Eel Canyon.

## SUMMARY AND CONCLUSION

### Summary of STRATAFORM sediment delivery

Eel margin studies that focused on delivery of flood sediment to the seabed produced a picture of shelf sediment processes remarkably consistent with the speculative conceptual model proposed by Moore (1969) in the early days of process-based investigation of continental-margin sediment transport. So, it is fitting to summarize this chapter with Moore's own words:

'Silt- and clay-sized particles introduced by streams and rivers are initially distributed by floating surface layers of fresh turbid water; this distribution is not widespread, and the lutum mostly settles to the bottom relatively near the river mouth. Subsequently or contemporaneously, during occurrence of long-period swell, the lutum is resuspended by the flattened orbital motion of the swell as it impinges on the bottom. Where this motion is long enough and where a sufficient supply of loose silts and clays exists, a turbid layer will develop over the seafloor. Turbid layers move across the seafloor as wide, relatively thin sheets under the influence of coastal current and downslope gravity flow superimposed on the to-and-fro movement of the swell. These two component forces should result in a net movement of most of the river-supplied lutum, diagonally across the shelf, nearly parallel to the coast, but with a small offshore component.'

In the next paragraph, Moore proposed that if suspensions are dense enough, then they can develop into autosuspending, channelized turbidity currents when they encounter a canyon. Otherwise,

'If the turbid layer is not of sufficient thickness, density, and duration to form a channelized, low-density turbidity current, it should after flowing into the canyon gully, or depression, lose its wave-generated orbital component of velocity and perhaps also its coastal-current component. Thus, it will flow

downslope, depositing lutum until it dissipates. This process may cause relatively rapid accumulation of fine sediment on canyon and valley walls and on the floors of the canyons as well. Where no canyon interception occurs and the turbid layer flows over the shelf edge, it will dissipate by deposition on the mainland basin slope. Because deposition is over a broader front on the open slope and is believed to accumulate slowly relatively to canyon walls, it forms a largely stable deposit not easily induced to fail by slumping.'

Although envisioned many years ago, confirmation of this conceptual model required the observational and modelling efforts described in this chapter.

### Questions for future research

Delivery of sediment to the seabed is complex, and many new questions have arisen from studies on the Eel margin. Perhaps the most important question is: 'Do wave-supported, gravity-driven flows dominate cross-shelf sediment transport in other systems?' The conditions required to form such flows are ample fine sediment, combined with large waves. Sediment must be abundant enough to induce suspended-sediment stratification. Exactly how much is required depends on the velocity shear in the water column. The Eel shelf supports this type of flow because the river produces a high yield of sediment and discharges episodically, and because waves typically accompany floods.

Aspects of the Eel arguably are unique. The sediment yield of the river is high because of the underlying, easily eroded geological substrate. Added to this property of the basin are land-use practices that favour high sediment yields. In northern California and elsewhere in western North America, excess sediment production has been linked to forestry operations (e.g. Best *et al.*, 1995). Paired basin analysis within the Redwood Creek watershed just north of the Eel Basin showed that sediment yield from logged tributaries was up to an order of magnitude greater than from nearby forested tributaries (Nolan & Janda, 1995). Extensive logging in the Eel watershed probably contributes to its high sediment load and distinguishes it from less impacted systems and from systems in the recent geological past. During the latter half

of the 20th century, precipitation in the Eel Basin increased, also increasing the sediment yield (Sommerfield *et al.*, this volume, pp. 157–212).

The close timing of peak sediment discharge and large waves also distinguishes the Eel system from other systems (Wheatcroft, 2000). The trend of the watershed parallel to the coast is a manifestation of the complex plate geometry in the region, and it is a factor in the occurrence of basin-wide intense precipitation during storms. The watershed geometry also produces short lag times between precipitation and discharge into the ocean, so sediment arrives in the coastal ocean when waves are large.

Together, these features of the Eel system and other similar systems lead to the formation of open-shelf, wave-supported, gravity-driven flows. Extreme conditions, however, may not be necessary. Moore (1969) formed his conceptual model of these flows based on observations in California's Borderland Basins to the south, where sediment yields and discharges are lower. Close timing between sediment discharge and waves may not be necessary. If sediment does not compact too rapidly, then it may reside on the seafloor for days to weeks before being entrained into wave-supported, gravity-driven flows during storms. The canyon observations of Puig *et al.* (2003, 2004) support the hypothesis that the seabed can provide enough sediment to a wave boundary-layer to fuel this type of flow. Perhaps open-shelf, wave-supported, gravity-driven flows form near many mountainous, coastal rivers that drain collisional margins. Observations that can characterize thin, near-bed flows on other shelves will reveal the generality of the fluid-mud processes at work on the Eel shelf.

A second question is: 'How is fine sediment from rivers delivered to canyon heads during sea-level highstands?' Modelling studies suggest that hyperpycnal inflows of sediment-laden river waters can deliver sediment rapidly and efficiently to canyon heads (Parsons *et al.*, this volume, pp. 275–337; Syvitski *et al.*, this volume, pp. 459–529), as do observations from the Sepik River in Papua New Guinea (Kineke *et al.*, 2000). Limited observations, however, indicate that oceanographic processes deliver sediment to the Eel Canyon head, where waves subsequently generate wave-supported, gravity-driven flows via liquefaction of recently deposited sediment (Mullenbach & Nittrouer, 2000;

Puig *et al.*, 2003, 2004). Future studies in complex canyon systems will help clarify which pathways dominate under various forcings.

A third question is: 'How does fine sediment become trapped in inner-shelf sands?' Historically, on wave-dominated coasts, muds were thought to bypass the inner shelf completely. Yet cores from the Eel shelf suggest that layers of mud can deposit and persist under energetic forcing. The mechanisms of mud burial within sandy deposits are unclear, but perhaps relate to suspended-sediment stratification and suppression of turbulence. Resolving these mechanisms as well as rates of fine-sediment accumulation on the inner shelf poses considerable challenges. Equipment placed on the inner shelf is at high risk, and establishing age control in coarse, frequently resuspended, inner-shelf sands is difficult. Nonetheless, improved understanding of this transition region is vital to building integrated models of stratigraphy on continental margins.

A final question is: 'What is the importance to overall sediment budgets of far-field suspended-sediment transport in buoyant coastal currents?' Satellites offer compelling visual documentation of this transport pathway. The plumes may be visually spectacular, but they may not be important quantitatively due to relatively low sediment concentrations within them. If they are supplied constantly with sediment, however, either by river discharge or resuspension of bottom sediments, coastal currents hold the potential, over time, to redistribute considerable quantities of sediment along the coast. As with the other questions, more observations are needed to improve understanding of this sediment-transport pathway.

In closing, the pattern of discovery regarding sediment delivery to the seabed on continental shelves is classic. Early inquiry generated competing hypotheses that motivated subsequent investigations. These investigations strongly favoured one hypothesis over the others, namely that advection by near-bed currents was the dominant cross-shelf transport mechanism for muds. The data that supported this hypothesis, however, were inadequate for examining the alternative hypothesis for cross-shelf transport proposed by Moore (Moore, 1969), because they did not characterize the region of the flow within the wave boundary layer. The diverse and sophisticated array of sensors deployed during STRATAFORM was able to characterize this

near-bed region, and in so doing exposed the dominance of wave-supported, gravity-driven flow on this open, wave-impacted shelf. These findings challenge the reigning paradigm of continental-shelf sediment transport, and undoubtedly will fuel research for years to come.

## ACKNOWLEDGEMENTS

Joe Kravitz took active interest in the work described here, from inception of the research to final publication of this volume. We recognize his contribution with simple and sincere thanks. We are all grateful to the Office of Naval Research for years of support for our research. The editors and reviewers shouldered a heavy load in producing this volume. In particular, this paper benefited from comments and criticisms from editors Chuck Nittrouer, Pat Wiberg, James Syvitski and reviewers Steve Goodbred, Lonnie Leithold, Don Wright, Harry Roberts and Nick McCave.

## NOMENCLATURE

Symbol	Definition	Dimensions
$a_f$	aggregate fraction in suspension	
$B$	integrated buoyancy anomaly	$L^2 T^{-2}$
$C_D$	drag coefficient	
$C_s$	suspended-sediment mass concentration	$M L^{-3}$
$d_{25}$	upper quartile diameter of aggregates	$L$
$d_{50}$	median diameter of aggregates	$L$
$Fr$	Froude number	
$f$	Coriolis frequency	$T^{-1}$
$g$	gravitational acceleration	$L T^{-2}$
$g'$	modified gravity	$L T^{-2}$
$h$	water depth	$L$
$h_c$	river channel depth	$L$
$h_p$	plume thickness	$L$
$Li$	internal Rossby radius of deformation	$L$
$\ell$	thickness of dense layer	$L$
$Q$	river discharge	$L^3 T^{-1}$
$Ri$	Richardson number	

$Ri_B$	bulk Richardson number	
$U_{max}$	maximum nearbed velocity	$L T^{-1}$
$U_w$	nearbed wave velocity	$L T^{-1}$
$U_g$	nearbed gravity-current velocity	$L T^{-1}$
$u$	plume speed	$L T^{-1}$
$V_c$	nearbed alongshore current velocity	$L T^{-1}$
$W_c$	river channel width	$L$
$W_p$	width of coastal current	$L$
$w_e$	effective settling velocity	$L T^{-1}$
$x_e$	e-folding distance	$L$
$\alpha$	bathymetric gradient	
$\rho$	density of basin water	$M L^{-3}$
$\rho_s$	sediment density	$M L^{-3}$
$\Delta\rho$	density contrast between plume and basin water	$M L^{-3}$
$\theta$	angle of bathymetric gradient	degrees

## REFERENCES

- Agrawal, Y.C. and Pottsmith, H.C. (1994) Laser diffraction particle sizing in STRESS. *Cont. Shelf Res.*, **14**, 1101–1121.
- Alexander, C.R. and Simoneau, A.M. (1999) Spatial variability in sedimentary processes on the Eel continental slope. *Mar. Geol.*, **154**, 243–254.
- Allredge, A.L., Granata, T.C., Goschalk, C.G. and Dickey, T.D. (1990) The physical strength of marine snow and its implications for particle disaggregation in the ocean. *Limnol. Ocean.*, **35**, 1415–1428.
- Bagnold, R.A. (1962) Auto-suspension of transported sediment; turbidity currents. *Proc. Roy. Soc., London, Ser. A*, **265**, 315–319.
- Bale, A. and Morris, A.W. (1987) *In situ* measurement of particle size in estuarine waters. *Estuarine Coast. Shelf Sci.*, **24**, 253–263.
- Bates, C.C. (1953) Rational theory of delta formation. *Bull. Am. Assoc. Petrol. Geol.*, **37**, 2119–2162.
- Berhane, I., Sternberg, R.W., Kineke, G.C., Milligan, T.G. and Kranck, K. (1997) The variability of suspended aggregates on the Amazon continental shelf. *Cont. Shelf Res.*, **17**, 267–285.
- Best, D.W., Kelsey, H.M., Hagans, D.K. and Alpert, M. (1995) Role of fluvial hillslope erosion and road construction in the sediment budget of Garrett Creek, Humboldt County, California. In: *Geomorphic Processes and Aquatic Habitat in the Redwood Creek Basin, Northwestern California* (Eds K.M. Nolan, H.M.

- Kelsey and D.C. Marron), pp. M1–M11. *U.S. Geol. Surv. Prof. Pap.*, 1454.
- Boldrin, A., Bortoluzzi, G., Frascari, F., Guerizoni, S. and Rabitti, S. (1988) Recent deposits and suspended sediments off the Po Della Pila (Po River, main mouth), Italy. *Mar. Geol.*, **79**, 159–170.
- Brown, W.M. and Ritter, J.R. (1971) Sediment transport and turbidity in the Eel River basin, California. *U.S. Geol. Surv. Wat. Supply Pap.*, **1986**, 70 pp.
- Burt, T.N. (1986) Field settling velocities of estuary muds. In: *Estuarine Cohesive Sediment Dynamics* (Ed. A.J. Mehta), pp. 126–150. Springer-Verlag, New York.
- Cacchione, D.A., Drake, D.E., Losada, M.A. and Medina, R. (1990) Bottom-boundary-layer measurements on the continental shelf off the Ebro River, Spain. *Mar. Geol.*, **95**, 179–192.
- Cacchione, D.A., Wiberg, P.L., Lynch, J., Irish, J. and Traykovski, P. (1999) Estimates of suspended-sediment flux and bedform activity on the inner portion of the Eel continental shelf. *Mar. Geol.*, **154**, 83–97.
- Cacchione, D.A., Pratson, L.F. and Ogston, A.S. (2002) The shaping of continental slopes by internal tides. *Science*, **296**, 724–727.
- Cowan, E.A. (1993) Characteristics of suspended particulate matter and sedimentation of organic carbon in Glacier Bay fjords. In: *Proceedings of the Third Glacier Bay Science Symposium, 1993* (Ed. D.R. Engstrom), pp. 24–28. National Park Service, Anchorage, Alaska.
- Cowan, E.A. and Powell, R.D. (1990) Suspended sediment transport and deposition of cyclically inter-laminated sediment in a temperate glacial fjord, Alaska, U.S.A. In: *Glacimarine Environments: Processes and Sediments* (Eds J.A. Dowdeswell and J.D. Scourse), pp. 75–89. Special Publication 53, Geological Society Publishing House, Bath.
- Crockett, J.S. and Nittrouer, C.A. (2004) The sandy inner shelf as a repository for muddy sediment: an example from Northern California. *Cont. Shelf Res.*, **24**, 55–73.
- Curran, K.J., Hill, P.S. and Milligan, T.G. (2002a) Fine-grained suspended sediment dynamics in the Eel River flood plume. *Cont. Shelf Res.*, **22**, 2537–2550.
- Curran, K.J., Hill, P.S. and Milligan, T.G. (2002b) The role of particle aggregation in size-dependent deposition of drill mud. *Cont. Shelf Res.*, **22**, 405–416.
- Curry, J.R. (1965) Late Quaternary history, continental shelves of the United States. In: *The Quaternary of the United States* (Ed. H.E. Wright Jr. and D.G. Frey), pp. 723–735. Princeton University Press, Princeton, NJ.
- Dearnaley, M.P. (1996) Direct measurements of settling velocities in the Owen Tube: a comparison with gravimetric analysis. *J. Sea Res.*, **36**, 41–47.
- Drake, D.E. (1972) Distribution and transport of suspended matter, Santa Barbara Channel, California. *Deep-sea Res.*, **18**, 763–769.
- Drake, D.E. (1976) Suspended sediment transport and mud deposition on continental shelves. In: *Marine Sediment Transport and Environmental Management* (Eds D.J. Stanley and D.J.P. Swift), pp. 127–158. John Wiley & Sons, New York.
- Drake, D.E. (1999) Temporal and spatial variability of the sediment grain-size distribution on the Eel shelf: the flood layer of 1995. *Mar. Geol.*, **154**, 169–182.
- Drake, D.E. and Cacchione, D.A. (1985) Seasonal variation in sediment transport on the Russian River shelf, California. *Cont. Shelf Res.*, **4**, 495–514.
- Drake, D.E., Kopack, R.L. and Fischer, P.J. (1972) Sediment transport on Santa Barbara-Oxnard shelf, Santa Barbara Channel, California. In: *Shelf Sediment Transport: Process and Pattern* (Eds D.J.P. Swift, D.B. Duane and O.H. Pilkey), pp. 307–332. Dowden, Hutchinson and Ross, Stroudsburg, Pennsylvania.
- Drake, D.E., Cacchione, D.A., Meunch, R.D. and Nelson, C.H. (1980) Sediment transport in Norton Sound, Alaska. *Mar. Geol.*, **36**, 97–126.
- Droppo, I.G. and Ongley, E.D. (1994) Flocculation of suspended sediment in rivers of southeastern Canada. *Water Res.*, **28**, 1799–1809.
- Dunbar, C.O. and Rodgers, J. (1957) *Principles of Stratigraphy*. John Wiley & Sons, New York, 356 pp.
- Dyer, K.R. and Manning, A.J. (1999) Observation of the size, settling velocity and effective density of flocs and their fractal dimensions. *J. Sea Res.*, **41**, 87–95.
- Dyer, K.R., Cornelisse, J., Dearnaley, M.P., et al. (1996) A comparison of *in situ* techniques for estuarine floc settling velocity measurements. *J. Sea Res.*, **36**, 15–29.
- Edzwald, J.K., Upchurch, J.B. and O'Melia, C.R. (1974) Coagulation in estuaries. *Environ. Sci. Technol.*, **8**, 58–63.
- Eisma, D. (1986) Flocculation and de-flocculation of suspended matter in estuaries. *Neth. J. Sea Res.*, **20**, 183–199.
- Eisma, D. and Kalf, J. (1984) Dispersal of Zaire River suspended matter in the estuary and the Angola Basin. *Neth. J. Sea Res.*, **17**, 385–411.
- Eisma, D., Boon, J., Groenewegen, R., Ittekkot, V., Kalf, J. and Mook, W.G. (1983) Observations on macro-aggregates, particle size and organic composition of suspended matter in the Ems estuary. *Mitt. Geol. Palaontol. Inst. Univ. Hamburg*, **55**, 295–314.
- Eisma, D., Bernard, P., Cadee, G.C., et al. (1991) Suspended-matter particle size in some West-European estuaries; Part I: particle size distribution. *Neth. J. Sea Res.*, **28**, 193–214.

- Eisma, D., Bale, A.J., Dearnaley, M.P., Fennessy, M.J., van Leussen, W., Maldiney, M.-A., Pfeiffer, A. and Wells, J.T. (1996) Intercomparison of *in situ* suspended matter (floc) size measurements. *J. Sea Res.*, **36**, 3–14.
- Emery, K.O. (1952) Continental shelf sediments off southern California. *Geol. Soc. Am. Bull.*, **63**, 1105–1108.
- Emery, K.O. (1969) The continental shelves. *Sci. Am.*, **221**, 106–122.
- Fennessy, M.J., Dyer, K.R. and Huntley, D.A. (1994) INSSEV: an instrument to measure the size and settling velocity of flocs *in situ*. *Mar. Geol.*, **117**, 107–117.
- Folk, R.L. (1977) *Petrology of Sedimentary Rocks*. Hemphill Publishing Company, Austin, Texas, 186 pp.
- Fox, J.M. (2003) *Flocculation on the Po River delta*. MSc thesis, Dalhousie University, Halifax, Nova Scotia, Canada, 74 pp.
- Fox, J.M., Hill, P.S., Milligan, T.G., Ogston, A.S. and Boldrin, A. (2004) Floc fraction in the waters of the Po River prodelta. *Cont. Shelf Res.*, **24**, 1699–1715.
- Friedrichs, C.T., Wright, L.D., Hepworth, D.A. and Kim, S.C. (2000) Bottom-boundary-layer processes associated with fine sediment accumulation in coastal seas and bays. *Cont. Shelf Res.*, **20**, 807–841.
- Garvine, R.W. (1987) Estuary plumes and fronts in shelf waters: a layer model. *J. Phys. Ocean.*, **17**, 1877–1896.
- Geyer, W.R., Beardsley, R.C., Candela, J., et al. (1996) Physical oceanography of the Amazon Shelf. *Cont. Shelf Res.*, **16**, 575–616.
- Geyer, W.R., Hill, P.S., Milligan, T.G. and Traykovski, P. (2000) The structure of the Eel River plume during floods. *Cont. Shelf Res.*, **20**, 2067–2093.
- Gibbs, R.J. (1982a) Floc breakage during HIAC light-blocking size analysis. *Environ. Sci. Technol.*, **16**, 298–299.
- Gibbs, R.J. (1982b) Floc stability during Coulter counter sizer analysis. *J. Sediment. Petrol.*, **52**, 657–660.
- Gibbs, R.J. and Konwar, L. (1983) Disruption of mineral flocs using Niskin bottles. *Environ. Sci. Technol.*, **17**, 374–375.
- Grant, W.D. and Madsen, O.S. (1986) The continental-shelf bottom boundary layer. *Ann. Rev. Fluid Mech.*, **18**, 265–305.
- Hamblin, A.P. and Walker, R.G. (1979) Storm-dominated shallow marine deposits: the Fernie-Kootenay (Jurassic) transition, southern Rocky Mountains. *Can. J. Earth Sci.*, **16**, 1673–1690.
- Hill, P.S. (1992) Reconciling aggregation theory with observed vertical fluxes following phytoplankton blooms. *J. Geophys. Res.*, **97**(C2), 2295–2308.
- Hill, P.S. (1996) Sectional and discrete representations of floc breakage in agitated suspensions, *Deep-sea Res.*, **43**(5), 679–702.
- Hill, P.S. and Nowell, A.R.M. (1995) Comparison of two models of aggregation in continental-shelf bottom boundary layers. *J. Geophys. Res.*, **100**(C11), 22749–22763.
- Hill, P.S., Syvitski, J.P., Cowan, E.A. and Powell, R.D. (1998) *In situ* observations of floc settling velocities in Glacier Bay, Alaska. *Mar. Geol.*, **145**, 85–94.
- Hill, P.S., Milligan, T.G. and Geyer, W.R. (2000) Controls on effective settling velocity in the Eel River flood plume. *Cont. Shelf Res.*, **20**, 2095–2111.
- Hoskin, C.M. and Burrell, D.C. (1972) Sediment transport and accumulation in a fjord basin, Glacier Bay, Alaska. *J. Geol.*, **80**, 539–551.
- Hunt, J.R. 1986. Particle aggregate breakup by fluid shear. In: *Estuarine Cohesive Sediment Dynamics* (Ed. A.J. Mehta), pp. 85–109. Springer-Verlag, New York.
- Johnson, B.D. and Wangersky, P.J. (1985) A recording backward scattering meter and camera system for examination of the distribution and morphology of macroaggregates. *Deep-sea Res.*, **32**, 1143–1150.
- Kineke, G.C., Sternberg, R.W., Trowbridge, J.H. and Geyer, W.R. (1996) Fluid-mud processes on the Amazon continental shelf. *Cont. Shelf Res.*, **16**, 667–696.
- Kineke, G.C., Woolfe, K.J., Kuehl, S.A., et al. (2000) Sediment export from the Sepik River, Papua New Guinea: evidence for a divergent sediment plume. *Cont. Shelf Res.*, **20**, 2239–2266.
- Kirby, R.R. and Parker, W.R. (1977) The physical characteristics and environmental significance of fine-sediment suspensions in estuaries. *Symposium on Estuaries, Geophysics and the Environment*, National Academy of Science, Washington, pp. 110–120.
- Kranck, K. (1973) Flocculation of suspended sediment in the sea. *Nature*, **246**, 348–350.
- Kranck, K. (1980) Experiments on the significance of flocculation in the settling of fine-grained sediment in still water. *Can. J. Earth Sci.*, **17**, 1517–1526.
- Kranck, K. (1981) Particulate matter grain-size characteristics and flocculation in a partially mixed estuary. *Sedimentology*, **28**, 107–114.
- Kranck, K. (1984) The role of flocculation in the filtering of particulate matter in estuaries. In: *The Estuary as a Filter* (Ed. V. Kennedy), pp. 159–175. Academic Press.
- Kranck, K. and Milligan, T.G. (1992) Characteristics of suspended particles at an 11-hour anchor station in San Francisco Bay, California. *J. Geophys. Res.*, **97**, 11373–11382.
- Kranck, K., Petticrew, E., Milligan, T.G. and Droppo, I.G. (1992) *In situ* particle size distributions resulting from flocculation of suspended sediment. In: *Nearshore and Estuarine Cohesive Sediment Transport* (Ed. A.J. Mehta), pp. 60–74. Coastal and Estuarine Studies Series, Vol. 42, American Geophysical Union, Washington, DC.

- Krone, R.B. (1962) *Flume Studies of the Transport of Sediment in Estuarial Shoaling Processes*. Hydraulic Engineering Laboratory and Sanitary Engineering Research Laboratory, University of California, Berkeley.
- Leithold, E.L. (1989) Depositional processes on an ancient and modern muddy shelf, northern California. *Sedimentology*, **36**, 179–202.
- Leithold, E.L. and Hope, R.S. (1999) Deposition and modification of a flood layer on the northern California shelf: lessons from and about the fate of terrestrial particulate organic carbon. *Mar. Geol.*, **154**, 183–195.
- Lentz, S.J. and Helfrich, K.R. (2002) Buoyant gravity currents along a sloping bottom in a rotating fluid. *J. Fluid Mech.*, **464**, 251–278.
- Marr, J.E. (1929) *Deposition of the Sedimentary Rocks*. Cambridge University Press, 245 pp.
- McCave, I.N. (1972) Transport and escape of fine-grained sediment from shelf areas. In: *Shelf Sediment Transport: Process and Pattern* (Eds D.J.P. Swift, D.B. Duane and O.H. Pilkey), pp. 225–248. Dowden, Hutchinson and Ross, Stroudsburg, PA.
- McCave, I.N. (1975) Vertical flux of particles in the ocean. *Deep-sea Res.*, **22**, 491–502.
- McCave, I.N. (1984) Size spectra and aggregation of suspended particles in the deep ocean. *Deep-sea Res.*, **31**, 329–352.
- McPhee-Shaw, E.E., Sternberg, R.W., Mullenbach, B. and Ogston, A.S. (2004) Observations of intermediate nepheloid layers on the northern California continental margin. *Cont. Shelf Res.*, **24**, 693–720.
- Mertes, L.A.K. and Warrick, J.A. (2001) Measuring flood output from 110 coastal watersheds in California with field measurements and SeaWiFS. *Geology*, **29**, 659–662.
- Migniot, C. (1968) Etude des proprietés physiques de différents sédiments très fins et de leur comportement sous des actions hydrodynamiques. *La Houille Blanche*, **23**, 591–620.
- Milligan, T.G. (1995) An examination of the settling behaviour of flocculated suspensions. *Neth. J. Sea Res.*, **33**, 163–171.
- Milligan, T.G. and Hill, P.S. (1998) A laboratory assessment of the relative importance of turbulence, particle composition and concentration in limiting maximal floc size. *J. Sea Res.*, **39**, 227–241.
- Milligan, T.G. and Kranck, K. (1991) Electro-resistance particle size analyzers. In: *Principles, Methods and Applications of Particle Size Analysis* (Ed. J.P.M. Syvitski), pp. 109–118. Cambridge University Press, New York.
- Mitchum, R.M. Jr., Vail, P.R. and Thompson III, S. (1977) Seismic stratigraphy and global changes in sea level, Part 2: the depositional sequence as the basic unit for stratigraphic analysis. In: *Seismic Stratigraphy – Applications to Hydrocarbon Exploration* (Ed. C.E. Payton), pp. 53–62. Memoirs 26, American Association of Petroleum Geologists, Tulsa, OK.
- Moore, D.G. (1969) *Reflection Profiling Studies of the California Continental Borderland: Structure and Quaternary Turbidite Basins*. *Geol. Soc. Am. Spec. Pap.*, **107**, 142 pp.
- Morehead, M.D. and Syvitski, J.P. (1999) River-plume sedimentation modeling for sequence stratigraphy: application to the Eel margin, northern California. *Mar. Geol.*, **154**, 29–41.
- Morehead, M.D., Syvitski, J.P.M., Hutton, E.W.H. and Peckham, S.D. (2003) Modeling the inter-annual and intra-annual variability in the flux of sediment in ungauged river basins. *Global Planet. Change*, **39**(1/2): 95–110.
- Mulder, T. and Syvitski, J.P.M. (1995) Turbidity currents generated at river mouths during exceptional discharges to the world oceans. *J. Geol.*, **103**, 285–299.
- Mullenbach, B.L. and Nittrouer, C.A. (2000) Rapid deposition of fluvial sediment in the Eel Canyon, northern California. *Cont. Shelf Res.*, **20**, 2191–2212.
- Mullenbach, B.L., Nittrouer, C.A., Puig, P. and Orange, D. (2004) Sediment deposition in a modern submarine canyon: Eel Canyon, northern California. *Mar. Geol.*, **211**, 101–119.
- Myrow, P.M. and Southard, J.B. (1996) Tempestite deposition. *J. Sediment. Res.*, **66**(5), 875–887.
- Nelson, B.W. (1970) Hydrography, sediment dispersal and recent historical development of the Po River delta. In: *Deltaic Sedimentation – Modern and Ancient* (Eds J.P. Morgan and R.H. Shaver), pp. 152–184. Special Publication 15, Society of Economic Paleontologists and Mineralogists, Tulsa, OK.
- Nittrouer, C.A. (1999) STRATAFORM: overview of its design and synthesis of its results. *Mar. Geol.*, **154**, 3–12.
- Nittrouer, C.A. and Sternberg, R.W. (1981) The formation of sedimentary strata in an allochthonous shelf environment: the Washington continental shelf. *Mar. Geol.*, **42**, 201–232.
- Nolan, K.M. and Janda, R.J. (1995) Impacts of logging on stream-sediment discharge in the Redwood Creek Basin, northwestern California. In: *Geomorphic Processes and Aquatic Habitat in the Redwood Creek Basin, Northwestern California* (Eds K.M. Nolan, H.M. Kelsey and D.C. Marron), pp. L1–L8. *U.S. Geol. Surv. Prof. Pap.*, **1454**.
- Nolan, K.M., Kelsey, H.M. and Marron, D.C. (1995) Summary of research in the Redwood Creek basin, 1973–1983. In: *Geomorphic Processes and Aquatic Habitat in the Redwood Creek Basin, Northwestern California* (Eds K.M. Nolan, H.M. Kelsey and D.C. Marron), pp. A1–A6. *U.S. Geol. Surv. Prof. Pap.*, **1454**.

- Nunn, P.D. (1999) *Environmental Change in the Pacific Basin*. John Wiley & Sons, Chichester, 357 pp.
- Ogston, A.S. and Sternberg, R.W. (1999) Sediment-transport events on the northern California continental shelf. *Mar. Geol.*, **154**, 69–82.
- Ogston, A.S., Cacchione, D.A., Sternberg, R.W. and Kineke, G.C. (2000) Observations of storm and river flood-driven sediment transport on the northern California continental shelf. *Cont. Shelf Res.*, **20**, 2141–2162.
- O'Melia, C.R. and Tiller, C.L. (1993) Physiochemical aggregation and deposition in aquatic environments. In: *Environmental Particles*, Vol. 2 (Eds J. Buffle and H.P. van Leeuwen), pp. 353–386. Lewis Publishers, Boca Raton, FL.
- Palanques, A. and Drake, D.E. (1990) Distribution and dispersal of suspended particulate matter on the Ebro continental shelf, northwestern Mediterranean Sea. *Mar. Geol.*, **95**, 193–206.
- Parsons, J.D., Bush, J.W.M. and Syvitski, J.P.M. (2001) Hyperpycnal plumes with small sediment concentrations. *Sedimentology*, **48**, 465–478.
- Postma, H. (1967) Sediment Transport and Sedimentation in the Estuarine Environment. In: *Estuaries* (Ed. G.H. Lauff), pp. 158–179. A.A.A.S. pub 83.
- Puig, P., Ogston, A.S., Mullenbach, B.L., Nittrouer, C.A. and Sternberg, R.W. (2003) Shelf-to-canyon sediment-transport processes on the Eel continental margin (northern California). *Mar. Geol.*, **193**, 129–149.
- Puig, P., Ogston, A.S., Mullenbach, B.L., Nittrouer, C.A., Parsons, J.D. and Sternberg, R.W. (2004) Storm-induced sediment-gravity flows at the head of the Eel submarine canyon. *J. Geophys. Res.*, **109**, C03019, doi:10.1029/2003JC001918.
- Schubel, J.R., Wilson, R.E. and Okubo, A. (1978) Vertical transport of suspended sediment in upper Chesapeake Bay. In: *Estuarine Transport Processes* (Ed. B. Kjerfve), pp. 161–175. University of South Carolina Press, Columbia, SC.
- Scrutton, P.C. and Moore, D.G. (1953) Distribution of surface turbidity off Mississippi delta. *Bull. Am. Assoc. Petrol. Geol.*, **37**, 1067–1074.
- Scully, M.E., Friedrichs, C.T. and Wright, L.D. (2002) Application of an analytical model of critically stratified gravity-driven sediment transport and deposition to observations from the Eel River continental shelf, northern California. *Cont. Shelf Res.*, **22**, 1951–1974.
- Scully, M.E., Friedrichs, C.T. and Wright, L.D. (2003) Numerical modeling of gravity-driven sediment transport and deposition on an energetic continental shelf: Eel River, northern California. *J. Geophys. Res.*, **108**, 17–1–17–14.
- Seymour, R.J. (1986) Nearshore auto-suspending turbidity flows. *Ocean Eng.*, **13**, 435–447.
- Shepard, F.P. (1932) Sediments of the continental shelves. *Geol. Soc. Am. Bull.*, **43**, 1017–1040.
- Sherwood, C.R., Butman, B., Cacchione, D.A., et al. (1994) Sediment-transport events on the northern California continental shelf during the 1990–91 STRESS experiment. *Cont. Shelf Res.*, **14**, 1063–1099.
- Smith, J.D. and Hopkins, T.S. (1972) Sediment transport on the continental shelf off of Washington and Oregon in light of recent current measurements. In: *Shelf Sediment Transport: Process and Pattern* (Eds D.J.P. Swift, D.B. Duane and O.H. Pilkey), pp. 143–180. Dowden, Hutchinson and Ross, Stroudsburg, PA.
- Sommerfield, C.K., Nittrouer, C.A. and Alexander, C.R. (1999) <sup>7</sup>Be as a tracer of flood sedimentation on the northern California continental margin. *Cont. Shelf Res.*, **19**, 335–361.
- Sternberg, R.W. and Larsen, L.H. (1976) Frequency of sediment movement on the Washington continental shelf: a note. *Mar. Geol.*, **21**, 37–47.
- Sternberg, R.W. and McManus, D.A. (1972) Implications of sediment dispersal from long-term, bottom-current measurements on the continental shelf of Washington. In: *Shelf Sediment Transport: Process and Pattern* (Eds D.J.P. Swift, D.B. Duane and O.H. Pilkey), pp. 181–194. Dowden, Hutchinson and Ross, Stroudsburg, Pennsylvania.
- Sternberg, R.W., Berhane, I. and Ogston, A.S. (1999) Measurement of size and settling velocity of suspended aggregates on the northern California continental shelf. *Mar. Geol.*, **154**, 43–53.
- Stumm, W. and Morgan, J.J. (1981) *Aquatic Chemistry*, 2nd edn. Wiley-Interscience, New York, 780 pp.
- Swift, D.J.P. (1970) Quaternary shelves and the return to grade. *Mar. Geol.*, **8**, 5–30.
- Swift, D.J.P., Duane, D.B. and Pilkey, O.H. (1972) *Shelf Sediment Transport: Process and Pattern*. Dowden, Hutchinson and Ross, Stroudsburg, PA, 656 pp.
- Syvitski, J.P.M. and Murray, J.W. (1981) Particle interaction in fjord suspended sediment. *Mar. Geol.*, **39**, 215–242.
- Syvitski, J.P.M., Asprey, K.W., Clattenburg, D.A. and Hodge, G.D. (1985) The prodelta environment of a fjord: suspended particle dynamics. *Sedimentology*, **32**, 83–107.
- Syvitski, J.P.M., Asprey, K.W. and Heffler, D.E. (1991) The Flocc Camera: a three-dimensional imaging system of suspended particulate matter. In: *Microstructure of Fine-grained Sediments* (Eds R.H. Bennett, W.R. Bryant and M.H. Hulbert), pp. 281–289. Springer-Verlag, New York.

- Syvitski, J.P.M., Asprey, K.W. and LeBlanc, K.W.G. (1995) *In situ* characteristics of particles settling within a deep-water estuary. *Deep-sea Res., II*, **42**, 223–256.
- Syvitski, J.P.M., Morehead, M.D., Bahr, D. and Mulder, T. (2000) Estimating fluvial sediment transport: the rating parameters. *Water Resour. Res.*, **366**, 2747–2760.
- ten Brinke, W.B.M. (1994) Settling velocities of mud aggregates in the Oostercherde tidal basin (the Netherlands), determined by a submersible video system. *Estuar. Coast. Shelf Sci.*, **39**, 549–564.
- Traykovski, P., Geyer, W.R., Irish, J.D. and Lynch, J.F. (2000) The role of wave-induced density-driven fluid mud flows for cross-shelf transport on the Eel River continental shelf. *Cont. Shelf Res.*, **20**, 2113–2140.
- Trowbridge, J.H. and Kineke, G.C. (1994) Structure and dynamics of fluid muds on the Amazon continental shelf. *J. Geophys. Res.*, **99**, 865–874.
- Walker, R. (1973) Mopping up the turbidite mess. In: *Evolving Concepts in Sedimentology* (Ed. R.N. Ginsburg), pp. 1–37. Studies in Geology, No. 21, Johns Hopkins University, Baltimore.
- Walsh, J.P. and Nittrouer, C.A. (1999) Observations of sediment flux to the Eel continental slope, northern California. *Mar. Geol.*, **154**, 55–68.
- Wheatcroft, R.A. (2000) Oceanic flood sedimentation: a new perspective. *Cont. Shelf Res.*, **20**, 2059–2066.
- Wheatcroft, R.A. and Borgeld, J.C. (2000) Oceanic flood deposits on the northern California shelf: large-scale distribution and small-scale physical properties. *Cont. Shelf Res.*, **20**, 2163–2190.
- Wheatcroft, R.A., Sommerfield, C.K., Drake, D.E., Borgeld, J.C. and Nittrouer, C.A. (1997) Rapid and widespread dispersal of flood sediment on the northern California margin. *Geology*, **25**, 163–166.
- Whitehouse, U.G., Jeffrey, L.M. and Debrecht, J.D. (1960) Differential settling tendencies of clay minerals in saline waters. *Proceedings of the 7th National Conference on Clays and Clay Minerals*, pp. 1–79.
- Wright, L.D. (1977) Sediment transport and deposition at river mouths: a synthesis. *Geol. Soc. Am. Bull.*, **88**, 857–868.
- Wright, L.D. and Coleman, J.M. (1974) Mississippi River mouth processes: effluent dynamics and morphologic development. *J. Geol.*, **82**, 751–778.
- Wright, L.D., Wiseman, W.J., Bornhold, B.D., *et al.* (1988) Marine dispersal and deposition of Yellow River silts by gravity-driven underflows. *Nature*, **332**, 629–632.
- Wright, L.D., Kim, S.-C. and Friedrichs, C.T. (1999) Across-shelf variations in bed roughness, bed stress and sediment suspension on the northern California continental shelf. *Mar. Geol.*, **154**, 99–115.
- Wright, L.D., Friedrichs, C.T., Kim, S.C. and Scully, M.E. (2001) Effects of ambient currents and waves on gravity-driven sediment transport on continental shelves. *Mar. Geol.*, **175**, 25–45.